



POLITECNICO DI TORINO

Master's Degree in Civil Engineering

MASTER'S DEGREE THESIS

**Sustainable Exoskeletons and Connections
Design based on a Two-Stage Optimization
Framework**

Supervisor:

Prof. Giuseppe Carlo Marano

Prof. Beatrice Faggiano

Co-supervisors:

PhD. Eng. Raffaele Cucuzza

PhD. Eng. Giacomo Iovane

Candidate:

Tomás Lazzuri

JULY 2024 - A.Y. 2023/2024

*Para mi familia,
por su inquebrantable fe en mí
y su amor incondicional.*

Acknowledgements

Con la entrega de este documento finaliza una de las etapas más desafiantes y motivadores que me tocó vivir y no me quedan más que palabras de agradecimiento a todas aquellas personas que me han acompañado en este camino.

En primer lugar este título se lo debo enteramente a mi familia, quienes confiaron siempre ciegamente en mí a pesar de lo disruptivas que sonaran siempre mis ideas. Su amor, acompañamiento y confianza motivaron siempre mi camino y es por eso que mi mamá Daniela, mi papá Gastón y mi hermana Camila, merecen y merecerán siempre mi admiración y agradecimiento. Gracias por brindarme siempre todas las herramientas, las que estuvieron a su alcance y las que no también. Por último, gracias por enseñarme siempre que en la simpleza de una persona yace toda su grandeza.

Especial mención también para mis abuelos, Mirian, Hector, Iris y Delmiro que siempre estuvieron para mí en los momentos que más los necesité y me transmitieron siempre los valores que hoy me definen como persona.

Quiero recordar en este preciado momento a todos los amigos que esta carrera me dió. Especialmente a mi dream team, quienes hicieron que todo fuera siempre más fácil y llevadero, Juan, Sebastián, Agustín, Ignacio y Valentina. Espero que la vida los llene sorpresas y puedan cumplir siempre sus objetivos.

Me queda agradecer a todas las personas que me acompañaron y escucharon en esta nueva experiencia que emprendí y se convirtieron en mi familia en estos últimos dos años. Juan, Diego, Sebastián, Candela, Carmela y Victoria, gracias por ser parte.

Por último quiero agradecer a las instituciones que me permitieron la consecución de este título. En primer lugar, mi más sincera admiración y agradecimiento hacia mi casa de estudios, la Facultad de Ciencias Exactas Físicas y Naturales de la Universidad Nacional de Córdoba, por haberme abierto sus puertas y brindado educación de primer nivel a través de sus excelentísimos profesionales. Quisiera agradecer también al Politecnico di Torino, mi segunda casa de estudios en estos últimos dos años, por recibirme de la mejor manera y permitirme culminar mis estudios en ambas universidades.

Esto también va dedicado para cada uno de los miembros de mi familia, para los que estuvieron y para los que están, gracias por su amor, gracias por su compañía.

Muchas gracias.

Abstract

Given that most of the buildings have been constructed before the implementation of rigorous seismic and environmental regulations in Europe, there is a pressing need to upgrade the existing building stock to meet the current standards. In response, new retrofitting techniques have been developed in recent years, in conjunction with new approaches that consider the proposed designs' reduction of costs and environmental impact.

Exoskeletons constitute a global retrofitting solution that is currently a hot topic among researchers and practitioners due to their effectiveness and high performance. This thesis proposes the design of these interventions for a real case study, corresponding to a building belonging to a scholastic complex located in Naples. The design company is better responsible for the project conducted a vulnerability assessment of the existing structures that compromise the complex and proposed a retrofitting intervention through the application of CFRP systems. The information provided by this company is used to enhance the work presented in this thesis.

This thesis proposes a complete exoskeleton design methodology composed of two stages. The first stage involves the design of the global exoskeleton intervention, which is performed using a displacement-based approach. Following this approach, the final design of the retrofitting system is obtained by controlling the damage state of the existing structure's elements. This criterion is introduced within the context of a real-coded optimization algorithm, which has been adapted to the investigated case study. This approach enables the identification of the optimal placement and sizing of the exoskeleton members.

To demonstrate the potential of the proposed retrofitting system, three scenarios are studied. The first scenario consists of retrofitting by CFRP system designed by the design company in charge of the project. The second and third scenarios correspond to the installation of steel and timber exoskeletons, respectively, designed in the first stage of the aforementioned methodology. Subsequently, from the bill of materials identified in this phase, a Life Cycle Assessment and a Total Cost comparison of the three alternatives is conducted.

The performed analysis demonstrated that timber exoskeletons can successfully replace steel ones. Furthermore, they constitute the most feasible solution from the evaluated scenarios, from the economic and environmental points of view.

The second stage of the proposed methodology concerns the design of the connections regarding the optimal timber exoskeleton solution considered the best structural solution both in terms of environmental and economic cost. An automatic routine is created with the aim to make the design of the connections faster lowering the number of different technical choices for structural joints. Furthermore, the design is primarily guided towards maximising standardisation while simultaneously controlling the total weight of the connections. Finally, the environmental impact and the cost incidence of the connections in the global intervention are evaluated.

From the second stage of the analysis, it can be concluded that the environmental impact of the connections is three times more significant than their contribution to the total economic cost of the retrofitting measure, when considering the overall intervention, which includes the foundation system and exoskeletons structures.

Contents

| | | |
|----------|-------------------------------------------------------------------------------|-----------|
| 1 | Introduction | 3 |
| 2 | Literature Review: Exoskeletons as a Retrofitting Approach | 7 |
| 2.1 | Seismic Retrofit with Exoskeleton | 9 |
| 2.1.1 | Application Philosophy in Civil Engineering | 9 |
| 2.1.2 | Exoskeleton Typologies | 10 |
| 2.1.3 | Design of High-Strength Exoskeletons according to NTC18 | 14 |
| 2.2 | Design Approach | 15 |
| 2.2.1 | Performance Based Design | 15 |
| 2.2.2 | Streamlining the Construction Process | 19 |
| 2.3 | Life Cycle Assessment | 21 |
| 2.3.1 | LCA in the Building Sector | 24 |
| 3 | 1st Stage: Displacement-based Design Optimisation Framework | 28 |
| 3.1 | Proposed Displacement Based Design Methodology | 30 |
| 3.2 | Optimisation Problem Statement | 32 |
| 3.2.1 | Mathematical Formulation of the Objective Function | 33 |
| 3.2.2 | Employed Algorithm | 40 |
| 3.3 | FEM Analyses | 48 |
| 3.3.1 | Response Spectrum Analysis | 48 |
| 4 | Description of the Case Study: Salvo D'Aquisto School | 50 |
| 4.1 | Structural Assesment | 52 |
| 4.1.1 | Historical Survey | 53 |
| 4.1.2 | Definition of Knowledge Levels and Confidence Factors | 55 |

| | | |
|----------|-----------------------------------------------------------------------|------------|
| 4.1.3 | Geometric and Physical Survey | 56 |
| 4.1.4 | Definition of the Mechanical Properties of Materials | 60 |
| 4.1.5 | Definition of Reference Actions | 63 |
| 4.2 | Reference Structural Model | 69 |
| 4.2.1 | Modelling Criteria | 69 |
| 4.2.2 | Load Combinations | 70 |
| 4.3 | Existing Structure's Seismic Vulnerability | 72 |
| 5 | Analysis and Interpretation of the optimization output | 77 |
| 5.1 | Scenario 1: Traditional Retrofitting Approach | 79 |
| 5.2 | Scenario 2: Steel Exoskeletons | 84 |
| 5.2.1 | Optimization Results | 86 |
| 5.2.2 | Structural Interpretation of Results | 88 |
| 5.3 | Scenario 3: Timber Exoskeletons | 97 |
| 5.3.1 | Timber Material | 98 |
| 5.3.2 | Optimization Results | 101 |
| 5.3.3 | Structural Interpretation of Results | 103 |
| 5.4 | Economic and Environmental Comparison of the Scenarios | 110 |
| 5.4.1 | Environmental Evaluation of the Alternatives | 110 |
| 5.4.2 | Cost Evaluation of the Alternatives | 117 |
| 6 | 2nd Stage: Stress-based Connection Design Framework | 123 |
| 6.1 | Pinned Connection for Timber Elements | 125 |
| 6.1.1 | Double Shear Steel-to-timber Connection | 126 |
| 6.2 | Automatic Routine for the Preliminary Design of Connections | 130 |
| 6.2.1 | Automation of Connection's Design | 130 |
| 6.2.2 | Routine Algorithm | 132 |
| 6.3 | Analysis and Interpretation of Results | 143 |
| 6.3.1 | Calibration of Penalty Function | 143 |
| 6.3.2 | Connections Layout Design | 148 |
| 6.4 | Economic Cost and Environmental Impact of the Connections | 151 |
| 7 | Conclusions and Future Developments | 156 |
| 8 | Bibliography | 162 |

Chapter 1

Introduction

In Europe [1], it is estimated that approximately 40% of the existing building stock was constructed before the 1960s without any rigorous consideration of seismic or environmental aspects. Moreover, a significant proportion of these buildings are situated in areas prone to seismic activity, which has led to an alarming situation of vulnerability. Over recent decades, there has been a concerted effort to identify viable solutions to address this issue.

To respond to the aforementioned challenges, several seismic retrofitting techniques have been developed in the last decades to provide structures with sufficient resistance to bear horizontal loads. The most prevalent and traditional solutions, including steel/concrete jacketing, FRP applications, CAM systems, and others, tend to enhance the resistance of buildings in general through the local confinement of elements [2]. This strategy results in a notable increase in resistance and ductility of the single element, which subsequently leads to the improvement of the structure's seismic response. Nevertheless, the approach of indirectly improving the behaviour of the global structure by retrofitting a single element and the lack of a clear and rigorous proposal regarding the number and type of elements that should be retrofitted, results in inefficient and costly interventions. These considerations, coupled with the invasive nature of these measures, have led to the proposal of costly solutions that even require the cessation of activities within the building, thereby increasing indirect costs. Indeed, this is one of the reasons why this kind of seismic intervention is not yet being applied on a significant scale despite the important necessity of them.

It is, therefore, crucial to enhance research into new retrofitting interventions that avoid the interruption of building activities (or reduce them) and, in addition, have a significant and direct impact on the global response of the structure under seismic loads. In this context, exoskeletons emerge as auxiliary structures designed to address these issues. The structures in question can be implemented in a wide variety of shapes, orientations (either parallel or perpendicular to facades) and materials, thus allowing for a solution that can be easily adapted to suit the specific conditions of each case study. Moreover, exoskeletons are, in general, a dry and prefabricated solution, which consequently, can be reversed and recycled. Accordingly, if their low maintenance requirements are also considered, exoskeletons fit perfectly according

to the sustainability requirements of civil engineering projects.

In some particular situations, such as when the building's damages are important, the demolition and reconstruction may become a feasible solution which allows even an efficient energy renovation of the building stock. However, the arrival to this point should be discouraged by all means possible due to the highly important financial, environmental and social cost of this alternative. Moreover, the amounts of waste produced, energy used as well as the need for new materials in the reconstruction phase [3], transform it into an unsuitable option.

In the present thesis, a particular building from a scholastic complex located in Naples is chosen as the case study for the application of an exoskeletons seismic retrofitting intervention. The structure's bearing system is made of unidirectional resisting frames and, most of the buildings have a development in height of 2 or 3 levels. A private enterprise was in charge of the seismic assessment of the whole complex and proposed a classical FRP intervention for the structural elements of the existing structure.

The present thesis has three main objectives. The first is to apply an innovative pre-dimensioning technique using a displacement-based approach introduced in the framework of a genetic optimization algorithm. This will enable the identification of the two main variables that have the greatest impact on the global response of the reinforced concrete structure and exoskeleton system, the positioning of the exoskeletons and the sizing of their members. This step constitutes the first stage of a complete two stage design methodology proposed.

In this optimization framework, various constraints are imposed over the course of the work. However, the underlying principle is to consistently minimize the weight of the final solution, which is in favour of the environmental quality of the solution. One of the most restrictive constraints imposed on the GA requires that certain inter-storey drift limits be respected. These limits are fixed and motivated by other literature studies and ensure that the structure will remain in a condition of no damage or repairable damage after the occurrence of an ultimate limit state seismic action.

The second main objective of this thesis is to perform an economic and environmen-

tal comparison of three proposed interventions proposed: the classical FRP intervention conducted by the enterprise, a high-performance steel exoskeletons retrofitting and, the installation of more sustainable timber exoskeletons. In particular, special attention is paid to the viability of implementing the last intervention and evaluating if it constitutes a competitive solution for the seismic retrofitting of existing structures.

The aforementioned environmental comparison of the proposed solutions is carried out through the introduction of the bill of materials required for each of them and as an input to the Life Cycle Assessment framework. In this way, the LCA is employed to quantify the environmental impacts associated with the alternatives and to understand which of them produces the least amount of emissions.

The final objective of the present work, which corresponds to the second stage of the proposed design methodology, is the automatization of the design of the connections for the optimal timber exoskeletons solution. In general, connections account for approximately 15% to 20% of the total budget of a project, which makes it imperative to pay special attention to them during the design phase. Given the various variables involved in the design of a connection and the number of connections per exoskeleton that may be included in the final solution, it is important to identify connections that not only minimise the use of material (and their weight) but also enhance the constructability. To achieve this goal, an algorithm that performs an automatic routine for designing the connections is written. The latter, coupled with an optimisation algorithm, allows for obtaining a design that takes into account the trade-off between standardisation and total joint weight.

Furthermore, after obtaining the optimal design of the connections through the proposed algorithm, its impact on the environmental impact (evaluated through an LCA analysis) and its incidence on the total cost of the solution is evaluated.

Chapter 2

Literature Review:

Exoskeletons as a Retrofitting

Approach

In this chapter, the main concepts derived from a comprehensive literature review performed over several papers, academic documentation and normative regulations are summarized.

Section 2.1.1 introduces the concept of exoskeletons, the philosophy behind their use and the cases in which their use is recommended.

Section 2.1.2 discusses the different types of exoskeletons. It provides an overview of the main aspects that characterise each type of exoskeleton and the advantages and disadvantages they have.

The general approach taken by designers in designing high-strength exoskeletons according to the Italian regulation NTC 18 [4] is described in Section 2.1.3.

The design approach commonly used in research is presented in Section 2.2. The concepts of performance-based design and displacement-based design are introduced, as well as the common steps taken by exoskeleton designers in the research field. It is also noted how the concepts of constructability and standardisation are aligned with circular economy goals and should be considered when designing.

Finally, the literature review concludes in Section 2.3, where the Life Cycle Assessment methodology is explained together with the reference normative that should be followed for its application. Moreover, its application to a building or a building product is discussed.

2.1 Seismic Retrofit with Exoskeleton

Exoskeletons are auxiliary structures with a two- or three-dimensional arrangement of their constituent elements, designed with the main purpose of resisting significant lateral loads. Exoskeletons represent an innovative retrofitting technique, not yet included in the international standard codes, but offering a series of advantages not only from a structural point of view, but also from an energy and architectural point of view. They represent a versatile retrofitting solution that can be adapted to a wide range of different cases where existing buildings require seismic and even energetic improvement due to the lack of awareness of these concepts in the old design codes.

2.1.1 Application Philosophy in Civil Engineering

The concept of exoskeletons draws inspiration from the field of biomimicry [5, 6], which examines the principles of nature and applies them to the development of human technologies. In certain instances, such as the case of sea creatures, turtles or snails, nature has evolved a protective structure that serves a dual purpose: to safeguard the individual while also showcasing remarkable aesthetic qualities.

The aforementioned motivational triggers render exoskeletons an interesting retrofitting intervention, as they offer a viable and effective alternative to resist lateral loads while permitting even the renewal of the architectural facades. Among the distinguishing characteristics of this retrofitting technique in comparison to the classical ones, it should be highlighted that the system can be applied from the exterior of the existing structure, obviating the necessity for internal interventions and the subsequent interruption of activities [7]. In the case of residential buildings, relocating the occupants to carry out this type of intervention represents an organisational constraint, as it would require the provision of temporary accommodation for the occupants and their furniture until the work is completed. In the case of multi-purpose buildings, interrupting activities can result in significant loss of time or may simply not be possible. Hence, the possibility the external installation of these structures, make them a feasible intervention for the described cases [8].

Exoskeletons constitute a reversible and recyclable option since they are dry and

even prefabricated solutions. As introduced in [9], the use of these alternatives is highly recommended due to their low environmental and social impact given by the important reduction in construction times, waste reduction and the reversible nature that characterise them.

The principle of these structures is to absorb the seismic loads taken by the primary building, transfer them by the link which join both structures, and finally unloading them through an independent foundation system the exoskeleton may have, protecting in this way, the original structure [10]. Furthermore, they could be seen as a “sacrificial” appendage, which will basically absorb seismic loads and unload the existing structure [11].

Nevertheless, exoskeletons cannot always be applied; although the system can easily sort out architectural constraints within the building, it struggles to overcome urban restrictions such as the free spacing required around the building perimeter. This results in a convenient retrofitting solution, particularly for isolated buildings, as remarked in [11]. Moreover, they are not a viable alternative whenever facade preservation is required, and in some particular situations, local interventions for floor, columns, or column-beam joint strengthening may be needed before their installation [10]. Lastly, due to their considerable cost owing to their high performance, the installation of exoskeletons is recommended in cases where global interventions or significant strengthening of the building is required.

2.1.2 Exoskeleton Typologies

Exoskeletons are characterised as a versatile solution, with the potential to be implemented in a variety of case studies. This Section presents the different typologies that can be chosen during the design process, as well as the particular advantages to be exploited of each.

Endo-Exoskeleton

Starting from the most general classification and regarding to the bio-mimicry language [5], these types of retrofitting solutions can be classified according to their relative positioning or, better still, their placement with respect to the existing

structure to be retrofitted in endoskeletons and exoskeletons. The first solution is one in which their constitutive elements are placed among the frames of the existing structure. In contrast, exoskeletons are positioned externally, thus avoiding the need to interrupt the activities of the building in question.

As outlined in [7], both options permit seismic upgrading of the building, via an increase in strength and stiffness. The primary factor influencing the designer's decision is the feasibility of operating from either inside or outside the building, along with the associated costs of the different scenarios. Furthermore, external factors such as urban planning considerations, architectural criteria, geometric constraints, and client preferences may also influence the selection of one of these typologies.

Shape and Orientation

Exoskeletons can be designed as either two-dimensional (e.g. shear walls) or three-dimensional (e.g. cores) structures. In the case of planar exoskeletons, they can be oriented either parallel or perpendicular to the façade. With regard to three-dimensional exoskeletons, they can be constituted as **partial systems** if placed isolately around the structure perimeter or as **spatial systems** if wrapping all around the structure perimeter [12].

In particular, perpendicular exoskeletons permit an interesting increasement of the floor area, thereby creating the possibility of introducing new spatial configurations which can be exploited for new activities (such as balconies or terraces). However, such additions should be introduced with rigid floor diaphragms in order to ensure that they can withstand the new loads. In a retrofitting system designed to enhance the seismic performance of an existing structure, the introduction of non-negligible masses will result in an increase in seismic forces and a modification of the natural periods of the structure. These factors must be carefully considered by the designer as explain in [13].

Exoskeletons oriented parallel to the building façade offer a crucial advantage in terms of the required free space in the surrounding area of the building. This makes them the only possible solution when there is not enough room to place them. Furthermore, due to the typical columns spacing in buildings and since parallel ex-

oskeletons may be linked to the structure in the beam-column joint, the installation of parallel solution involves the use of better-inclined diagonals, which facilitates the control of lateral displacements as shown in. [14]. However, these solutions cannot be placed freely in the structure perimeter due to interference with certain elements, such as the obstruction of openings or main passages, which reduces the functionality of the building.

As previously outlined, an alternative to the bi-dimensional systems is the three-dimensional system, which is more expensive but offers greater versatility. Diagrids, for instance, can be constructed in a variety of shapes and offer an interesting solution from both a structural and an architectural point of view. It is possible to create shells that may be either flat or curved, which can surround the existing structure. In addition to the aesthetic enhancement of the building, these solutions can constitute an integrated system that can even improve the energy consumption of the building. This is achieved by the system behaving as a thermal and acoustic barrier, or by including these types of insulation barriers behind the structural cover.

With regard to the previously outlined point, it is important to consider that if an improvement in energy efficiency is sought through the implementation of these alternatives, a partial system would not be an effective solution. In order to achieve this and as reviewed by [15], three-dimensional spatial systems are required, as they can provide an envelope which, in addition to having a structural function, can also enhance the energy performance of the building. Examples of these configurations of exoskeletons can be seen in the works of [16, 17].

Dissipative Capacity

With regard to the structural connection between the exoskeleton and the existing structure, it is possible to classify them into two main groups: **dissipative exoskeletons (DE)** and **high-strength exoskeletons (HS)** [18]. Both solutions are designed to achieve similar seismic performances, although they are achieved in different ways. Dissipative solutions control the response of the building by dissipating seismic energy in devices placed at the base or in localized dampers, reducing in this way acceleration and thus inertia forces on the structure [19]. In contrast,

elastic high-strength solutions achieve the required targets by adding stiff external structures connected to the existing one. This last configuration is characterised by a predominantly elastic behavior until the global collapse, consequently requiring bigger structural elements to provide those levels of stiffness.

Both alternatives present advantageous or disadvantageous characteristics, which, according to the case study and the designer's preferences, may enhance the chosen option. It is, however, important to note that dissipative solutions require a significant degree of deformation capacity in the existing structure, which, in general, is not capable of providing it. Consequently, as observed by [13], a preliminary weakening intervention is necessary to ensure the installation of the dissipative devices, which in turn induces additional costs. As discussed in [20], when the stiff solutions are preferred, it is important to note that the internal load path of the existing structure is highly modified. This may result in a concentration of loads on the elements attached to the external exoskeletons, which could motivate a local retrofitting intervention in those elements.

As outlined by [18], in comparison to high-strength elastic exoskeletons, the cross sections required for the elements when a dissipative solution is preferred are smaller. Furthermore, the damage is mainly localised in these sacrificial devices. However, it is important to note that the overall cost of the intervention should be carefully analysed, as it can be reduced by the amount of material required, but at the same time is increased by the elevated cost of these devices.

2.1.3 Design of High-Strength Exoskeletons according to NTC18

The selection of high-strength exoskeletons as a retrofitting intervention, coupled with the imposition of inter-storey drift as control parameters in a performance-based design (as proposed by [14]), results in a significant unloading of the existing structure due to the presence of the external rigid exoskeletons. Their presence, in different points of the structure's perimeter directly modify the internal force distribution, thus, exoskeletons capture high amounts of load and the existing reinforced concrete structure results unloaded at the expense, in some cases, of an increase of the global shear base.

Particular attention should be paid in the design phase when proposing this kind of intervention. The structural performance is increased by providing additional stiffness and in some cases even helps to regularize the floor plan, reducing the participation of rotational modes during seismic events [21].

Moreover, the mass of the exoskeleton has to be defined and introduced in the analysis, since its not minor contribution can lead to an inaccurate analysis of the dynamic behavior of the building [22]. Last but not least, to enhance a proper load transfer among both structures, rigid connections results a good options and the diaphragmatic behavior of the existing floor must be ensured, otherwise, they should be subjected to a local retrofitting intervention.

Regulation Guidelines for Design

A discussion of the Section 7.2.3 of the Italian regulation [4] is worthy of consideration. This Section sets out the bases required to design the structural elements subjected to seismic loads.

In this chapter, the regulation considers the differentiation between primary and secondary elements when evaluating the response of a structure to seismic loads. It states that some elements may be considered secondary, with the capacity to bear vertical loads and to follow the structure's displacements without losing bearing capacity. Furthermore, it is emphasised that these elements cannot be considered as a determining factor in the transition of the structure from an irregular to a regular

configuration, nor can they contribute to the stiffness and strength of the structure under horizontal actions to more than 15% of the primary elements' contribution. In other words, this implies that the primary elements must have at least seven times the stiffness of the secondary elements.

The requirement imposed by normative was evidently not intended for the implementation of a global retrofitting intervention such as exoskeletons. However, this differentiation plays a fundamental role in the design of these structures.

In accordance with the established norms, practitioners and designers typically analyse the existing structure as a "secondary structure", while the exoskeletons are considered the "primary structure". In this way, the proposed design is thought to result in an almost complete unloading of the existing structure. Due to the lack of knowledge on the stress distribution inside the existing structure when exoskeletons are installed, this approach is generally preferred, obtaining in this way a sufficiently safe solution. However, it should be understood that this approach limits the existing structure's contribution to the bearing of the horizontal actions. As outlined in Section 1, despite the majority of current building stock has not been designed with a proper concern for seismic action, the high number of earthquakes that have occurred in the last decades demonstrate that they have a certain strength. After demonstrating this, they may even be found to be much higher than that 15%.

2.2 Design Approach

2.2.1 Performance Based Design

The performance-based seismic design (PBSD), as indicated by [23] was first introduced in the 1990s and constitutes a tool for the design of structures by specifying a certain seismic performance that the structure must outperform under different earthquake actions. When implementing this approach, selecting an appropriate performance index is crucial for the final outcomes and conclusions drawn from the analysis, as they are highly sensitive to the proposed limits. One of the most widely implemented alternatives of this approach is the displacement-based seismic design (DBD), which was first proposed by [24]. This approach is typically employed in reinforced concrete structures and aims to limit structural damage by controlling the

displacement response. In this context, one of the principal deformation indexes, the inter-story drift ratio, is closely related to the damage state of not only non-structural but even structural components of a building. This index is in general used in the DBD, as evidenced by the work of [23].

Trough a DBD approach, several studies [23, 25, 26] were conducted to evaluate the feasibility of imposing different design targets (following the DBD) and correlating them with a particular damage index. In this manner, once a number of different performance levels, for example fully operational, operational, repairable damage or collapse prevention, have been defined, it is possible to correlate the design targets to a certain expected damage, and thus to the aforementioned performance levels. Consequently, taking into account that the defined performance levels are in accordance with an expected seismic action coming from a certain limit state and, in function of the importance of the building in consideration, it is possible to calibrate the threshold for these design targets. In the context of a DBD approach, the inter-storey drift and top floor displacement are two of the most frequently selected target indexes in research.

A further examination of this topic reveals that the correlation between structural performance objectives and drift limits has not been extensively studied and remains one of the unresolved issues in the PBD procedures, as cited in [25]. Several publications, including SEAOC (1995) and FEMA (1997), have attempted to define a set of performance objectives in terms of drift. However, it should be noted that a direct correlation between these limits and the damage to the structure is an oversimplification, as the level of damage is influenced by numerous factors that are not accounted for in this approach, including the failure mode of the elements, number of cycles and duration of the earthquake, the type of structural system (ductile moment resisting frame, non-ductile MRF, MRF with walls, etc.), the accumulation and distribution of the structural damage and even the distribution of internal forces among the elements. Despite these limitations, it is possible to define a general capacity curve that correlates structural performance with associated damaged states according to a different approaches, as outlined in reference [25] and shown in Figure 2.1.

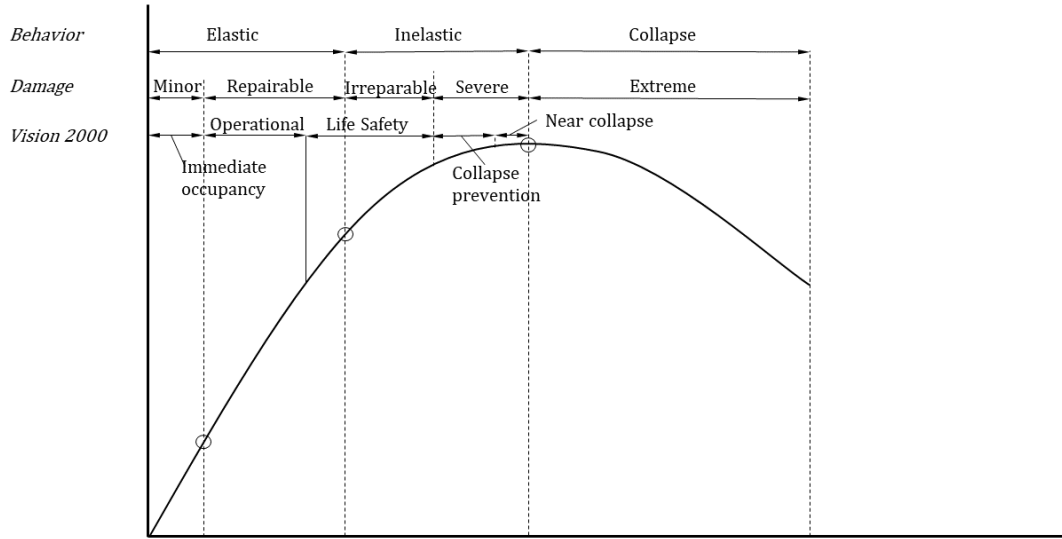


Figure 2.1: Structural performance's capacity curve, taken from [25]

There are several control parameters which can be adopted as structural boundaries in the design of exoskeletons. In scientific research the most preferred are floor displacements, inter-storey drifts, shear forces and floor accelerations [21]. In the case of seismic retrofitting of existing structures through the installation of exoskeletons designed in accordance with a DBD approach, several authors [10, 13, 21, 27] propose a common design procedure. By following a series of sequential steps, the global parameters of the exoskeletons system can be obtained. This approaches present the following common stages:

1. *Definition of control parameters*

Also known as design targets, are the parameters that represent the sought performance and which will be controlled all along the design process, respecting certain imposed limits.

2. *Multi-Degree-of-Freedom to Single-Degree-of-Freedom (MDoF to SDoF)*

At this stage, the coupled system (reinforced concrete structure + exoskeleton) is evaluated as two coupled SDoF systems through the introduction of a proposed link (rigid, spring, dissipative link, etc.). One oscillator represents the existing structure and is characterised by its structural parameters (mainly

mass and stiffness), while the other oscillator represents the exoskeleton and its design parameters will be determined in the subsequent step.

3. *Exoskeleton design parameters evaluation*

The aforementioned design parameters, as previously outlined, describe the second oscillator of the coupled system. When high-strength exoskeletons are selected, these parameters correspond to the overall mass and stiffness of the retrofitting system. In order to facilitate the generalisation of the evaluation, these parameters can be expressed in an adimensionalised form. Conversely, if dissipative exoskeletons are designed, it is of fundamental importance to consider the damping characteristics of the devices introduced.

4. *Multiple-Degree-of-Freedom (SDoF to MDoF)*

Once the design process has been completed and the criteria established by each author to be representative have been met, it is necessary to convert the design parameters of the retrofitting intervention into the properties of the individual elements that constitute each exoskeleton.

Nonetheless, this approach consisting on summarizing the complex MDoF system into a simpler SDoF system described by certain parameters, is also implemented in other research such like [28], where is clearly explained that the methodology is very sensitive to the force distribution present in the MDoF systems, and there may rise errors in the oversimplification of the system as a SDoF system. In this way, appears to need of addressing the analysis of the coupled system in its original MDOF configuration.

Accordingly, a potential field of research appears when the definition of the number, positioning, topology of the exoskeleton configuration and elements sizing of the retrofitting system is obtained, in general, based on previous experience and criteria of the designers. Different researchers criteria to define these variables, are focused on geometrical relation, global simplifications of the exoskeleton scheme (e.g. as a cantilever beam) and obtention of global top displacement using Timoshenko theory.

2.2.2 Streamlining the Construction Process

Aiming to make the existing heritage comply with the current standard code and level of safety requested by the technical regulations, a significant intervention devoted to mitigate the vulnerability under horizontal actions is required. In this context, the proposed retrofitting solutions should be technically feasible, sustainable and economically viable, and capable of being replicated in different situations [29]. The design of the intervention should therefore take account of these aspects and set out clear performance objectives and design targets as discussed in the previous Section.

In the context of the aforementioned points, the potential advantages of implementing exoskeletons suggest that they may be a suitable alternative, which can be designed according to this holistic and integrative approach.

This integral design philosophy is aimed at minimising not only the economic intervention cost but also the environmental and social impact. Consequently, it can be even argued that the simplification of the constructive process from the design phase onwards leads to the complete fulfilment of these objectives.

According to [30], the concept of constructability has been a subject of particular interest to researchers and practicing engineers since the 1980s. The term is defined as the optimal utilisation of knowledge gained from construction and empirical experience in the planning, design, purchasing and operational phases of a project, with the objective of fulfilling the project aims.

In the field of structural optimisation, optimal results are generally achieved through configurations with the minimal possible weight, which simultaneously satisfy specific conditions. Researchers agree that in order to find solutions which optimise the employment of material, this approach should be followed. However, solutions which employ the minimal possible quantity of materials are not necessarily the ones which have simultaneously the minimum cost and neither impact. In terms of circular economy goals, the standardisation of elements and constructive processes is crucial for reducing financial cost, waste of material and their associated environmental cost, as well as the duration of construction, which is directly linked to the project impact. Otherwise, an enormous increase in these indicators appears when

solutions which just minimise weight are sought.

In this way, the introduction of design approaches that focus on constructability improvement, as proposed by [31], by facilitating the standardisation of elements and the simplification of connections, enhances the constructive process while reducing the environmental impact of the project. Nevertheless, it is evident that there is a trade-off between the simplification of the construction process and material consumption. It is therefore necessary to assess the financial and environmental cost of the project in order to identify the optimal balance between these two factors.

Finally, although social cost is not always precisely identified, as introduced by [32], it is well known that the construction process of the majority of civil engineering projects has direct or indirect impacts on the daily activities of the society affected. These primarily concern an increase in environmental and noise pollution, economic losses due to delays in traffic, a decrease in the effectiveness of public services (such as public transport), and, in some cases, an increase in property taxes [33]. Consequently, the proposal of interventions aimed at enhancing constructability directly from the preliminary design phase will result in a considerable reduction in not only financial cost, environmental damage, but even social impact. This approach, when properly justified, can make an important differentiation of the project in the tender or bid evaluation phases.

Connections Design

In accordance with this philosophy, particular attention should be paid when designing the elements' connections. In general, in order to respect the performance criteria imposed, this type of intervention involves the usage of several truss structures in which there are many elements connected among them. Consequently, an important quantity of connections should be designed and subsequently installed.

A proper connection design is a key aspect to be studied, given that the connection weight can constitute between 5 and 10% of the weight of the overall intervention, while in general it can involve around 30% of the overall cost of the project.

In particular, when the number of connections cannot be further reduced or is fixed

by the global design of the structure, the only way to enhance their standardisation is by proposing similar designs in such a way that they pass the structural verifications and are not either overdimensioned. In the literature, there are not many available research studies which evaluate how, by proposing different design variables in connections, it would be possible to smartly force their standardisation. Although the connection design is dependent on the dimensions of the members to be connected and the force required to transmit between them, it is reasonable to consider how a minimal number of different connection layouts could be proposed by varying the variables typically fixed by designers during the design phase.

2.3 Life Cycle Assessment

The concept of sustainability increased their relevance over time and especially after the release of the Brundtland Report [34] by the World Commission on Environment and Development (WCED). This proposes long-term objectives for a future sustainable development that would mitigate the environmental and social impact. In this report, the authors emphasise the importance of global co-operation and outlines the three fundamental components for a sustainable development: environmental protection, economic growth and social equity.

In the context of environmental sustainability, the Life Cycle Assessment (LCA) methodology is widely used and recognised. The definition of the LCA, the outlines of its framework, the calculation rules and useful principles required for performing and LCA analysis can be found in the ISO standards 14040 [35] and 14044 [36]. On them, the LCA is defined as the *"compilation and evaluation of the inputs and outputs and the potential environmental impacts of a product system during a product's lifetime"*. In general terms, it can be stated that LCA is a type of input-output analysis, where inputs are consumed resources and the outputs are the releases to air, water, soil. Through the employment of this methodology, the environmental impact of a product or service along its entire expected life cycle can be identified, described and quantified. The underlying philosophy behind this evaluation consist on a shift of burden, so on solving a problem by not creating a different one.

According to the previously mentioned standards, the following four steps must be

respected when a LCA is implemented: goal and scope definition, inventory analysis, impact assessment and, interpretation. The framework can be clearly understood in Figure 2.2.

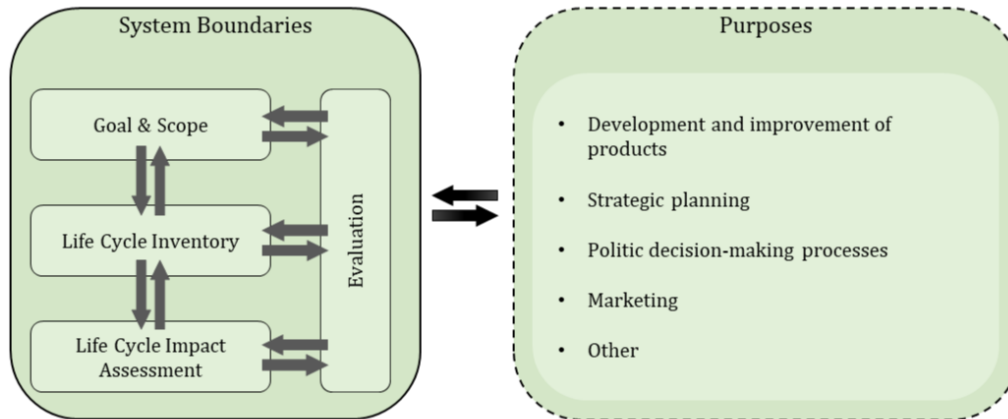


Figure 2.2: Life Cycle Assessment Framework

In the first phase of the assessment, the goal and scope of the study are defined according to what their definitions in [35]. The first element requires the definition of the aim of the study and its intended application, as well as the target group of people of the analysis. With regard to the scope, this should be clearly defined in order to demonstrate how the study's depth is in concordance with the stated purpose. When defining the scope of the study the following items must be included: definition of product system under investigation, function of the system, definition of the functional unit and reference flow, system boundaries, allocation procedures, impact assessment methodology, data requirements, estimates and assumptions for the data used, data limitations and quality requirements, type of reporting and if necessary, the critical review. Based on the goal of the analysis, the targeted audience and the product considered, the system boundaries are defined. One of the following life cycle evaluations can be chosen: "cradle to gate", "gate to gate", "cradle to grave" or "gate to grave". These essentially determine which stages of

the product's life cycle are included in the evaluation. In particular, when the term "cradle to grave" is employed, the stages of the product's life cycle are considered to include the extraction of raw materials, production, usage, end-of-life, recycling, and finally disposal. Finally, in the first stage of the analysis, it is essential to establish a functional unit. The functional unit defined in the first phase corresponds to the "*quantified function provided by the product system under investigation*", serving as the basis for the LCA study.

In the second phase, according to [35] the life cycle inventory analysis (LCI), the data for the significant inputs and outputs for each unit process among the system boundaries are gathered and connected to the functional unit. The unit process, corresponds to the smallest element considered in the LCI analysis for which input and output data are quantified. Consequently, input and output related to energy, raw materials, auxiliary inputs, products, co-products, waste and releases (to air, water and/or soil) are evaluated.

Moreover, as introduced in [35], the Life Cycle Impact Assessment (LCIA) allows to transform the waste and releases, identified in the LCI, into understandable impact indicators. These indicators permit to show how severe the contribution of each impact categories are to the environmental load according to a specified unit of measure. In Table 2.1 it can be appreciated some examples of the most recurrent indicators used in LCA as well as the impact category they correspond. In order to arrive to the final results, when performing the LCIA, it is mandatory to follow these steps: select the appropriate impact categories, classify the results and, finally, characterise them.

The *selection of the impact categories* must be in conformity with the definition of the study objective. Moreover, in [36] it is specified that the sources of the impact categories must be referenced and, it must be held a clear description of them as well as the justification of their selection. This choice must reflect the social and political relevance of the impacts. The *classification* step consists on assigning the LCI output results to the impact categories and identifying which results are present in more than one category. Finally, the *characterisation* phase involves converting the LCI results (emissions) into common units and summarizing the converted results within the various impact categories.

| Impact Category | Indicator | Unit |
|-----------------------------------------------|----------------------------------------------------------------------------------|-----------------------------------|
| Climate change - total ¹ | Global Warming Potential (GWP-total) | kg CO ₂ eq. |
| Climate change - fossil | Global Warming Potential (GWP-fossil) | kg CO ₂ eq. |
| Climate change - biogenic | Global Warming Potential (GWP-biogenic) | kg CO ₂ eq. |
| Climate change - land use and land use change | Global Warming Potential (GWP-luluc) | kg CO ₂ eq. |
| Ozone Depletion | Depletion potential of the stratospheric ozone layer (ODP) | kg CFC 11 eq. |
| Acidification | Acidification potential, Accumulated Exceedance (AP) | mol H ⁺ eq. |
| Water use | Water (user) deprivation potential, deprivation-weighted water consumption (WDP) | m ³ world eq. deprived |

Table 2.1: Core Environmental Impact Indicators (adapted from EN 15804 2022)

¹ GWP-total = GWP-fossil + GWP-biogenic + GWP-luluc.

Regarding to this last phase, as presented in Equation 2.1, characterisation factors are multiplied by the emission present in the LCI. In this way, it is possible to calculate an equivalent indicator, from now on called *environmental impact*.

$$LCI\ Output \cdot characterisation\ Factor = Environmental\ Impact \quad (2.1)$$

2.3.1 LCA in the Building Sector

Finally, as a last stage, results are interpreted. LCA is an iterative process. Therefore, at the end of the analyses, the results are reviewed and, if needed, modifications in the Goal and Scope, LCI and LCIA can be performed.

The Life Cycle Assessment technique can be applied for the products or services across the different sectors. The application of the LCA was initially developed for the assessment of simple products, but when this methodology is applied to buildings, a complex problem arises. The guidelines proposed in [35, 36] are gen-

eral considerations and when this approach is intended for buildings and building products, the evaluation should be conducted according to the specifications stated in European Standards EN 15804 (2022) [37] and EN 15978 (2011) [38]. The first document, provides the Core Product Category Rules (PCR) for the Environmental Product Declarations (EPDs) of building products or services. The second standard proposes a method for calculation the building's environmental performance and applies to both, new and existing structures.

As aforementioned, the European standard EN 15978 propose an overview of the LCA process in which the steps to follow and information required on them is specified next. In parenthesis it is indicated the information required in each step.

- Identification of assessment purpose (goal and intended use);
- Specification of assessment object (functional equivalent, reference study period, system boundary, building model - physical);
- Scenarios for the building life cycle (building model - time, life cycle stages, scenarios);
- Quantification of the building and its life cycle (net amount: material - energy - etc, gross amount, type of data);
- Selection of environmental data and other information (use of EPD's, use of other information, data quality, consistency);
- Calculation of the environmental indicators (environmental impacts, calculation method(s), aggregation);
- Reporting and communication (general information, assessment result, data sources);
- Verification

Accordingly, information on building products is of paramount importance in this procedure in order to evaluate the building level and obtain certified environmental data. For this purpose, Environmental Product Declarations (EPDs) are an useful source of information. For the object of the environmental assessment of a construc-

tion project, the system's boundaries determine the processes which will be taken into consideration on it. EN 15978 defines standard life cycle stages which includes: material production and transportation to site, construction processes, use of the product and product's end of life. Inside each phase, it is possible to identify different modules in which the environmental impact has to be quantified. The overview of these stages, demarcated by the system boundaries can be appreciated in the following figure.

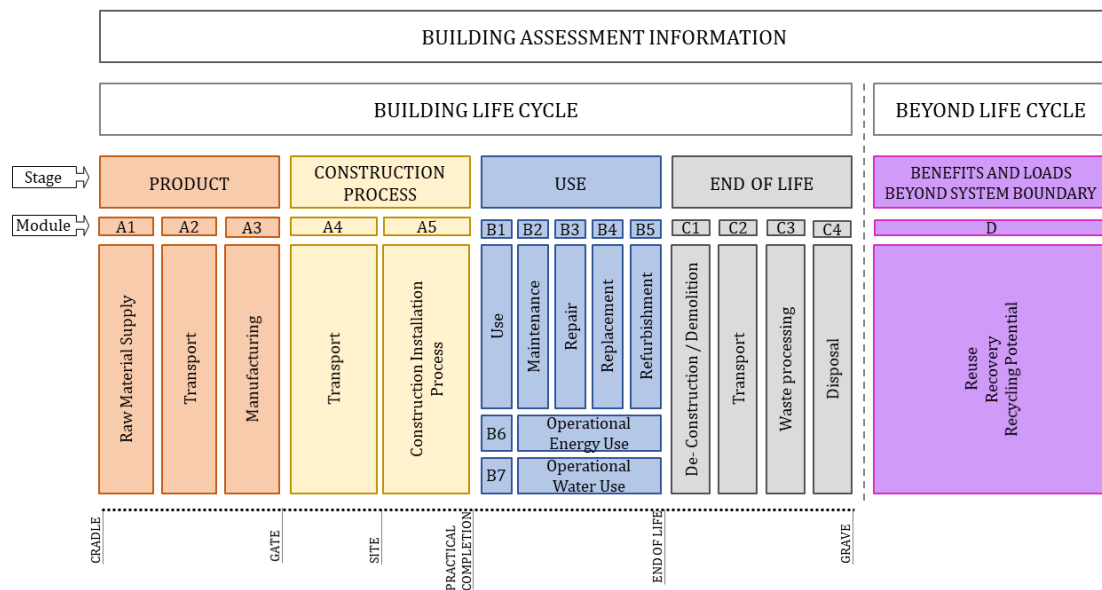


Figure 2.3: Life Cycle Assessment Framework

The *Product Stage*, evaluated for "cradle to gate" analyses, is constituted by the modules A1-A3. In it, it has to be evaluated the environmental impact due to emissions produced by raw material extraction, processing, manufacturing and transportation of materials between the mentioned processes until the product leaves the factory gates.

The *Construction Process* phase involves, in the module A4, the impact given by the released emissions during the transportation of materials or even the products to the construction site. With respect to the module A5, it is accounted for the energy usage due to activities on site (machinery use, etc.).

The *Use* stage includes the potential impact due to use (B1), maintenance (B2), local or global repairs due to unexpected events (B3), replacement of building components when their life spans are minor than the building service life (B4) and, the refurbishing of the building (B5). Moreover, on this stage it is included the operational impacts due to energy (B6) and water use (B7).

Finally, the *End of Life* stage account for the different destinies expected for the building and/or its components. In this, it is possible to identify the module C1 which refers to the deconstruction (foreseen, e.g., for steel elements) or demolition (e.g. for RC structures). The module C2 accounts for the transportation of materials from the building site to the end-of-waste state (defined in Section 7.4.5.4. of EN 15978). The collection of waste flows for its reuse, recycling and energy recovery are included in the module C3. In the module C4 are included the environmental impacts due to the pretreating of the waste and managing to the disposal site.

Additionally, beyond the building physical boundaries, other impacts can be assessed in module D. These refer to building components reuse, recycling, and recovery.

Regarding to the EPDs of the products and services involved in the LCA of a building, according to EN 15804, the environmental effects from A1 to A3, C3-C4 and D must be estimated and declared on them as a mandatory requirement. Alternative, the resting modules may be or not present in a valid Environmental Product Declaration. However, when referring to the LCA of a building, only modules cradle-to-grave analyses are mandatory, which include production stage, use stage and end-of-life without consideration of D module. The latter is declared as an additional information regarding, e.g., recyclability of construction systems.

Chapter 3

1st Stage: Displacement-based Design Optimisation Framework

This chapter presents the proposed Displacement-Based Design approach and its integration within the employed optimisation framework for the design of the exoskeleton solution. This constitutes the 1st stage of a global two-stage proposed methodology for a complete and integral preliminary design of the seismic retrofitting intervention.

At the beginning in Section 3.1, a proposed DBD methodology is presented, which can be easily introduced in the optimisation framework. The underlying philosophy of this approach is the reduction of damage to the structural elements of the existing structure.

In Section 3.2, the concept of the Genetic Algorithm is defined, and it is possible to understand how it can be used as a powerful tool to obtain a preliminary design of exoskeletons which efficiently respect the criteria established. In the same section, the mathematical formulation used in the optimisation is defined, as well as the definition of the design variables and the constraints imposed on the solutions, even for the steel or timber exoskeleton optimisation.

This section concludes with the presentation of the actual employed algorithm, allowing for a clear understanding of the workflow. Moreover, the processes of each of its constitutive phases are detailed, along with the imposed criteria or assumptions established.

The chapter concludes with an explanation of the Linear Dynamic Analysis with Response Spectrum performed in the Finite Element Model in Section 3.3.

3.1 Proposed Displacement Based Design Methodology

A different philosophy is proposed in contrast to the practice widely adopted by designers as introduced in Section 2.1.3, providing a paradigm shift in the preliminary design phase of this retrofitting intervention. A displacement-based design approach through the evaluation of the inter-storey drift is chosen, aiming to link the exoskeleton design to an elastic threshold which can ensure an acceptable damage level at the structural elements of the existing structure.

One of the advantages of this approach is the possibility of introducing a simple parameter such as the inter-storey drift as structural constraints of the optimisation problem allowing to evaluate the feasibility of the design proposed based on the control of the final structural performance of the existing structures. By doing this, the designs are focused on controlling the displacement of the existing structure under a seismic event by allowing both, the structure and existing structure to collaborate, without constraining the retrofitting solution to take more than 70% of the seismic load and exploiting even more of the capacity that the existing structure has.

By performing the safety assessment on an existing structure, dependently on the recovered information about its geometry and structural parameters, a certain degree of reliability can be achieved. However, in general, there is a lack of complete information about the actual existing building's structural behaviour and stress distribution. Moreover, when an external structure, such as an exoskeleton, is coupled to the existing one, it is very difficult to evaluate the actual level of stress that the members of the unretrofitted structure will experience. Consequently, the evaluation of a simple and measurable parameter, such as inter-storey drift, when designing the exoskeleton intervention leads to a solution that respects this controllable and reliable parameter.

In particular, a threshold of $H/600$ is imposed based on an exhaustive analysis of the scientific research when adopting displacement design targets, as presented in Section 2.2.1. By fixing this, it is possible to ensure that the structural elements are

not even damaged and remain in a fully operational condition.

Forecasting a design in which the existing structure remains in the elastic field under a ULS seismic action, might appear to be a pretentious goal. However, exoskeletons are usually preferred, due to their high performance, when important structures or infrastructures require a *safety improvement intervention* or better a *safety retrofitting intervention* (according to their definitions in Chapter C8 from *CIRCOLARE 21 gennaio 2019*). In this way, it is reasonable to expect that after an important seismic event, the intervention ensures that the structural elements will not even suffer damage.

Furthermore, in accordance with the regulation requirements, existing structures must be capable of withstanding the current standard design loads. Given that they are typically designed to resist mainly gravitational loads, the incorporation of an exoskeleton to resist horizontal loads gives rise to a complex coupled structural system. In general, non-linear analysis should be conducted to clearly understand the actual capacity of the structure reinforced with exoskeletons system. However, the introduction of an analysis of this complexity in an optimisation routine would involve an enormous computational effort. Consequently, simpler analyses such as dynamic analysis are preferred. In this direction, the inter-storey drift constraint proposed is guided to ensure that the structure subjected to Ultimate Limit State (ULS) actions will remain in the elastic field and simpler analyses are sufficiently valid.

In addition, it should be taken into account that if the designs are proposed to remain in the elastic field until failure, the contribution of the infills is still present and, the associated increase in stiffness they provide helps to respect the inter-storey drift threshold. However, since the criteria adopted by several research publications and technical regulation neglect the contribution of these elements, the model also omits the effect of infills, and thus the solutions obtained remain on the side of safety. This choice is based on the difficulty of relying on the masonry infills due to the high variability on their mechanical properties and the lack of knowledge regarding their installation and interconnection with the structural elements.

Lastly, it is remarked that the single evaluation of the inter-storey cannot account

for all the phenomena that conduct the damage of the elements, remains under evaluation for each particular case study and preferences of the designer the impose a most calibrated threshold which ensures the feasibility of the solution.

3.2 Optimisation Problem Statement

As defined in [39], "*A metaheuristic is a high-level problem-independent algorithmic framework that provides a set of guidelines or strategies to develop heuristic optimisation algorithms. The term is also used to refer to a problem-specific implementation of a heuristic optimisation algorithm according to the guidelines expressed in such a framework*". Consequently, these algorithms are usually preferred since allow its implementation without being constrained by the particular problem or even mathematical model. These high-performance algorithms are aimed at finding feasible or near-optimal solutions employing reasonable time and computational effort. This approach enables the development of robust algorithms through the integration of local and global search strategies, which introduce randomness throughout the process.

Metaheuristic algorithms are usually classified as evolutionary, physics-based, swarm-based, and bio-inspired algorithms. In this work, particular attention is paid to the first family and more specifically to the Genetic Algorithm (GA). Born in the decade of the 70s' by the hands of John Henry Holland in [40], these algorithms were inspired by biological evolution and their genetic base. Genetic Algorithms begin with an aleatory created population of individuals and evolve it through exposure to several random actions that copy the biological evolution (such as mutations and genetic recombination). According to some fixed criteria, the most outstanding individuals can survive inside the algorithm framework and those who are less competent are dismissed.

In this thesis, a real-coded Genetic Algorithm with self-calibrated strategies is implemented in such a way as to render the tool with a better adjustment to the particularities of the specific application problem.

The necessity of employing an optimisation algorithm for the design of the exoskeleton intervention arises from the findings presented in Section 2.2.1. This approach

ensures that the retrofitting intervention in a SDoF system is not oversimplified, and that the MDoF exoskeleton system is consistently evaluated. This enables the direct identification of the MDoF design parameters (such like positioning, cross sections, orientation, etc.) for each assessed configuration.

3.2.1 Mathematical Formulation of the Objective Function

The use of this optimisation tool is based on the weight minimization of the exoskeleton intervention. To give a complete definition of the problem, in the field of optimisation, three paramount components should be identified and defined: the objective function (OF), design variables (DV), and the applied constraints (C).

The mathematical formulation of the optimisation problem can be described as follows.

$$\mathbf{min} f(\mathbf{x}) = \left[N_{Ex} \cdot \rho \cdot \sum_{i=1}^{N_{El}} A_i \cdot l_i \right] \cdot \phi_1(D_i) \cdot \phi_2(S_i) \quad (3.1)$$

$$\mathbf{x} = \left[\overbrace{x_1, \dots, x_i, \dots, x_n}^{\text{Positioning DV}}, \overbrace{x_{n+1}, \dots, x_{n+j}, \dots, x_{n+m}}^{\text{Size DV}} \right]$$

subjected to :

$$x_i = \begin{cases} 0 \\ 1 \end{cases} \quad ; \quad x_{n+j}^{lower} < x_{n+j} < x_{n+j}^{upper}$$

where

- \mathbf{x} : chromosome with design variables
- N_{Ex} : total number of exoskeletons;
- N_{El} : number of elements of the single exoskeleton;
- ρ : density of steel grade S355;
- A_i : area of the i^{th} exoskeleton element;

- l_i : length of the i^{th} exoskeleton element;
- ϕ_1, ϕ_2 : penalty functions;

In accordance with the proposed design criteria presented in Section 3.1, the first design constraint is related to a maximum allowable inter-storey drift imposed. This is intended to ensure the structural integrity of the building in the elastic field and to minimize the damage to structural elements. An allowable limit drift d_{allow} is defined as the storey height divided by a factor β , which, as previously noted, should be calibrated for each specific case study. The actual inter-storey drift, denoted by δ_j , is evaluated at each pair of nodes of the structural columns of the building. After comparing the aforementioned parameters, their ratio must respect the constraint defined as $D_i < 1$.

$$D_j = \frac{\delta_j}{\delta_{allow}} < 1 \quad \forall j = 1, \dots, N_{col} \quad ; \quad \delta_{allow} = \frac{H}{\beta} \quad (3.2)$$

$$\delta_j = \sqrt{(U_{j,11} - U_{j,21})^2 + (U_{j,12} - U_{j,22})^2} \quad (3.3)$$

where

- δ_j : inter-storey evaluated at the j^{th} column;
- $U_{j,px}$: linear displacement in the x direction of the p node present in the j^{th} column;
- δ_{allow} : allowable inter-storey drift;
- N_{col} : total number of columns of the existing structure;
- H : height of the storey;
- β : allowable inter-storey drift factor;

The second design constraint corresponds to the structural verifications of the exoskeleton elements. As introduced in Section 1, two retrofitting systems are proposed, one conformed by steel elements and the other one by timber elements. The

constraint is generically defined as $S_i < 1$ for steel exoskeletons and $T_i < 1$ for timber ones.

Regarding the steel exoskeletons, all the structural verifications of their members are directly performed inside the framework of the software SAP2000 in correspondence to the Italian regulation [4]. According to what is reported in the correspondent chapter of the regulation (Section § 4.2.4), the verifications include the resistance and instability evaluation of the members subjected to axial forces, bending moment, shear forces, and combined stresses. In particular, the governing equation in most of the cases corresponds to the verification under flexure and axial compression for sections 1,2 and 3, which is recalled next.

$$S_i = \frac{N_{Ed}}{\frac{\chi_z \cdot N_{Rk}}{\gamma_{M1}}} + \sqrt{\left(k_{zy} \cdot \frac{M_y^{Ed} + N_{Ed} \cdot e N_y}{\frac{\chi_{LT} \cdot M_y^{Rk}}{\gamma_{M1}}} \right)^2 + \left(k_{zz} \cdot \frac{M_z^{Ed} + N_{Ed} \cdot e N_z}{\frac{M_z^{Rk}}{\gamma_{M1}}} \right)^2} < 1$$

On the other hand, when the configuration with timber elements is evaluated, since the structural software chosen (SAP2000) does not directly include the timber stress verification, an independent code was created in order to perform them. From the structural software, it is possible to obtain the acting forces on the exoskeleton elements under the different load combinations defined and, later, they were introduced in the framework of the new algorithm in order to perform the verifications of the timber elements.

In order to evaluate them, the *CNR DT 206-R1/2018* was used. This is an Italian official document based on the Eurocode 5, created for the project, execution, and control of the timber structures and, it is possible to find on it the structural verifications required for timber elements.

As will be detailed later, most of exoskeleton elements are mainly subjected to axial loads as a consequence of the proposed interconnection of their elements. Conversely, just a few of them are also subjected to shear and bending moments. In all cases, the elements are always subjected to forces that are parallel to the wood fibers, which is of paramount importance to keep in consideration when evaluating the resistance of the timber element.

The constraints $T_{i,j} < 1$, regarding the timber structural verification included in this project correspond to the following ones.

$$T_{i,c} = \frac{\sigma_{c,0,d}}{k_{crit,c} \cdot f_{c,0,d}} < 1 \quad (3.4)$$

$$T_{i,t} = \frac{\sigma_{t,0,d}}{f_{t,0,d}} < 1 \quad (3.5)$$

$$T_{i,t} = \begin{cases} \frac{\sigma_{t,0,d}}{f_{t,0,d}} + \frac{\sigma_{m,y,d}}{k_{crit,m} \cdot f_{m,y,d}} + k_m \cdot \frac{\sigma_{m,z,d}}{f_{m,z,d}} < 1 \\ \frac{\sigma_{t,0,d}}{f_{t,0,d}} + k_m \cdot \frac{\sigma_{m,y,d}}{k_{crit,m} \cdot f_{m,y,d}} + \frac{\sigma_{m,z,d}}{f_{m,z,d}} < 1 \end{cases} \quad (3.6)$$

$$T_{i,cr} = \begin{cases} \left(\frac{\sigma_{c,0,d}}{f_{c,0,d}} \right)^2 + \frac{\sigma_{m,y,d}}{f_{m,y,d}} + k_m \cdot \frac{\sigma_{m,z,d}}{f_{m,z,d}} < 1 \\ \left(\frac{\sigma_{c,0,d}}{f_{c,0,d}} \right)^2 + k_m \cdot \frac{\sigma_{m,y,d}}{f_{m,y,d}} + \frac{\sigma_{m,z,d}}{f_{m,z,d}} < 1 \end{cases} \quad (3.7)$$

$$T_{i,cs} = \begin{cases} \frac{\sigma_{c,0,d}}{k_{crti,c,y} \cdot f_{c,0,d}} + \frac{\sigma_{m,y,d}}{k_{crti,m,y} \cdot f_{m,y,d}} + k_m \frac{\sigma_{m,z,d}}{f_{m,z,d}} < 1 \\ \frac{\sigma_{c,0,d}}{k_{crti,c,y} \cdot f_{c,0,d}} + k_m \frac{\sigma_{m,y,d}}{k_{crti,m,y} \cdot f_{m,y,d}} + \frac{\sigma_{m,z,d}}{f_{m,z,d}} < 1 \\ \frac{\sigma_{c,0,d}}{k_{crti,c,z} \cdot f_{c,0,d}} + k_m \frac{\sigma_{m,y,d}}{k_{crti,m,y} \cdot f_{m,y,d}} + \frac{\sigma_{m,z,d}}{f_{m,z,d}} < 1 \\ \frac{\sigma_{c,0,d}}{k_{crti,c,z} \cdot f_{c,0,d}} + \frac{\sigma_{m,y,d}}{k_{crti,m,y} \cdot f_{m,y,d}} + k_m \frac{\sigma_{m,z,d}}{f_{m,z,d}} < 1 \end{cases} \quad (3.8)$$

$$T_{i,s} = \frac{\tau_d}{f_{v,d}} < 1 \quad (3.9)$$

where

- $T_{i,c}$: DCR related to simple compression verification (resistance and instability);
- $T_{i,t}$: DCR related to simple tension verification (resistance);
- $T_{i,cr}$: DCR related to combined compression and bending verification (resistance);
- $T_{i,cs}$: DCR related to combined compression and bending verification (instability);
- $T_{i,s}$: DCR related to shear verification (resistance);

Equations (3.4) and (3.5) are evaluated for the elements which are subjected exclusively to axial forces, while equations from (3.6) to (3.9) are evaluated for elements subjected to combined axial and flexural actions.

To include in the OF evaluation the different constraints defined in both exoskeleton typologies, a penalty system was employed.

$$\begin{aligned}\phi_1 &= \sum_{i=1}^{N_{col}} D_j^{unf} \\ \phi_{2,S} &= \sum_{j=1}^{N_{Ex}} \sum_{i=1}^{N_{El}} S_{i,j}^{unf} \\ \phi_{2,T} &= \sum_{j=1}^{N_{Ex}} \sum_{i=1}^{N_{El}} T_{i,j}^{unf}\end{aligned}$$

In order to evaluate the first penalty (ϕ_1), the inter-storey drift evaluated at each pair of nodes of the structure's columns (δ_j) for the different seismic combinations defined, is calculated. Later, the drift ratios (D_j) are obtained by dividing each value of δ_j by the imposed allowable inter-storey drift (δ_{allow}). Finally, ϕ_1 is the sum of the drift ratios which present values bigger than 1 (where $\delta_j > \delta_{allow}$), named D_j^{unf} . In such a way, both the number and severity of the violations are being considered.

The second penalty (ϕ_2) is related to the second design constraint and, thus is referred to the structural verifications. Given that systems constructed from two distinct materials are evaluated, the penalty is then obtained as $\phi_{2,S}$ for the steel exoskeletons, while as $\phi_{2,T}$ for the timber ones. Following the same reasoning, the demand-capacity ratios (DCR) of each exoskeleton element (S_i or T_i) can be computed in order to evaluate the constraint. Subsequently, by summing all the DCR that are greater than one, called S_i^{unf} or T_i^{unf} , it is possible to calculate the penalty for each different solution.

Each penalty $\phi_{2,S}$ and $\phi_{2,T}$ as well as the demand-capacity ratios S_i and T_i , are calculated and applied independently in the correspondent optimisation analysis performed.

Design Variables

$$\mathbf{x} = \left[\overbrace{x_1, \dots, x_i, \dots, x_n}^{\text{Positioning DV}}, \overbrace{x_{n+1}, \dots, x_{n+j}, \dots, x_{n+m}}^{\text{Size DV}} \right] \quad (3.10)$$

In this study, positioning and size optimisations have been made, which can be reflected in the design variables chosen. The single exoskeleton consists of a truss structure positioned perpendicular to the building façade, whose configuration remains unchanged.

The variables from x_1 to x_n are related to the positioning of the single exoskeleton. Previously, must be selected which are the possible insertion points for the single exoskeletons in the perimeter of the building and consequently, the number of potential positions n where they can be installed. In this case, these points are defined by the presence of external columns, and there, exoskeletons are placed perpendicularly to the facade. These design variables are binary variables in which, if $x_i = 1$, a single exoskeleton is installed in the i^{th} position, while if $x_i = 0$, no exoskeleton is placed in that position. Moreover, it is possible to evaluate the amount of exoskeletons present in the considered configuration since, $\sum_{i=1}^n x_i = N_{Ex}$.

Instead, the variables from x_{n+1} to x_{n+m} correspond to the sizes of the exoskeleton's elements. In particular, circular hollow and rectangular cross-sections, as indicated

in Sections 5.2 and 5.3, were chosen respectively for the steel and timber systems assessed. After defining a table with the different cross-sections proposed to the algorithm, they could be selected through an identifier index. In this way, these are discrete variables representing the position of the chosen cross-section in the table. In addition, the table is sorted according to the cross-sectional area of each option, in such a way that becomes easy to understand that lower index correspond to smaller areas. The variable x_{n+j} is limited among x_{n+j}^{lower} and x_{n+j}^{upper} , respectively the lower and upper bound of the table.

A total of 17 design variables are defined for this particular case study. The binary positioning variables are shown in Figure 3.1, while the discrete sizing variables and the exoskeleton topology are shown in Figure 3.2.

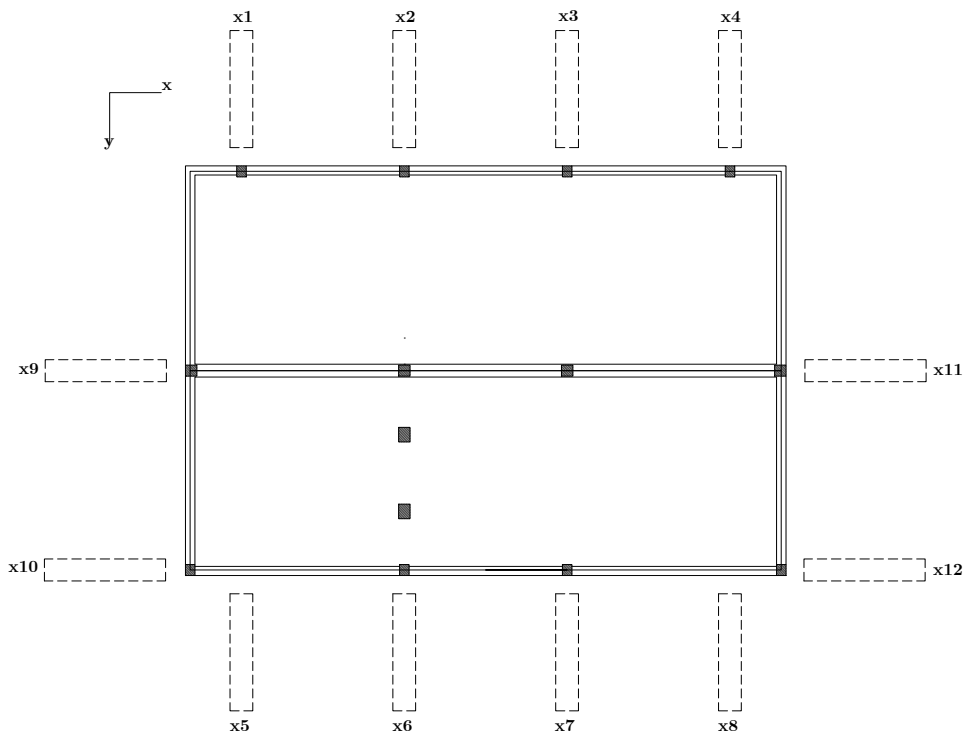


Figure 3.1: Allowable Exoskeleton's Placement Position

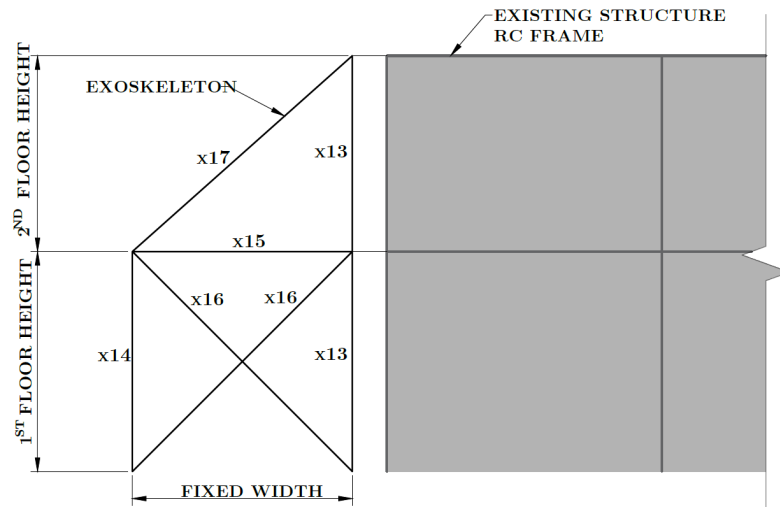


Figure 3.2: Schematic Representation of the Single Exoskeleton's Topology

3.2.2 Employed Algorithm

The genetic optimisation algorithm employed for this thesis is summarised in Figure 3.3. From an initial population initialization until the achievement of a final end criterion, the iterative algorithm allows the identification of an optimal solution according to the specified objective function.

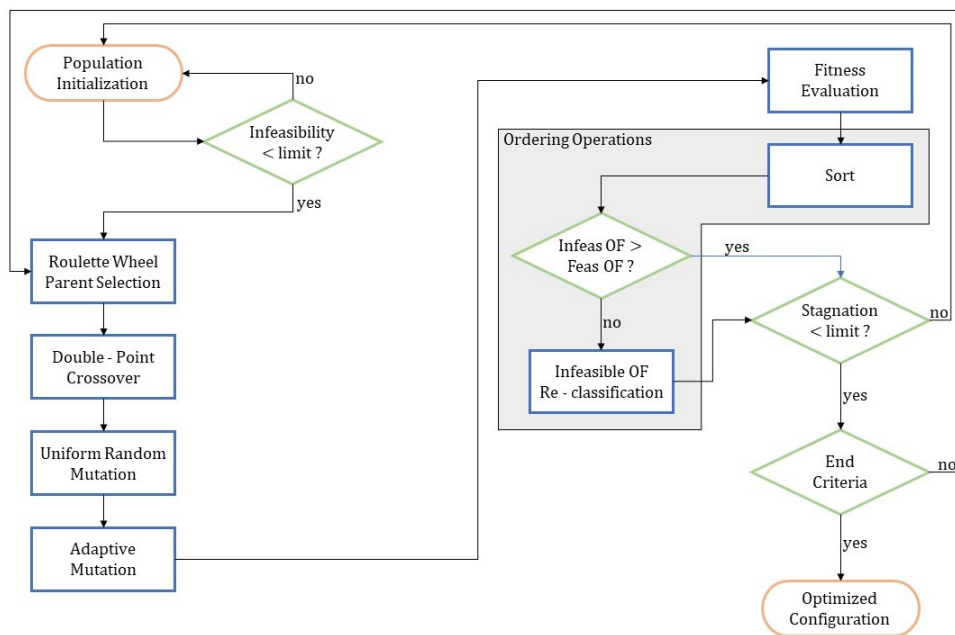


Figure 3.3: Flowchart of the employed Genetic Algorithm taken from [20]

Population Initialization

The first step in any genetic optimisation framework consists of the creation of an initial population constituted by a user-defined number of individuals (*popsiz*e). Each of these constitutes a potential solution to the problem and, thus in this case, represents a singular configuration of exoskeletons surrounding the existing building. The design variables, previously defined as the positioning of the single exoskeleton and the cross-section of their constitutive elements, are gathered in a vector called "chromosome" shown in Equation 3.10. In this way, each single member of the initialized population is represented by its own chromosome where the information of their design variables is stored.

The initial population is generated through a random process, meaning that the design variables of each chromosome are chosen in an aleatory way, and hence each individual proposed is randomly designed.

After this definition, for each population member, it has to be calculated their associated OF value as defined in the right member of Equation 3.1. In order to achieve this, the information present within the chromosome is transformed and interpreted through the use of a MATLAB code. The OAPI tools provided by CSI enable the direct modelling of retrofitting solutions from the code in the structural software SAP2000. Once the model has been created and the structural analysis has been set, it is possible to obtain information about the displacements of the existing structure and the DCR of the exoskeleton elements. This enables the calculation of the individual's OF.

In order to guide the algorithm to converge to a near-optimal solution, the initial population must have at least a 10% (user-defined) of its members verifying both displacement and structural constraints as explained in Section 3.2.1. In order to evaluate this, an in-feasibility check of the whole population is performed and if this threshold is not respected, a new random population is regenerated until there are sufficient feasible solutions.

Roulette Wheel Parent Selection

Hereafter, the iterative and evolutive process begins. In the field of Genetic Programming, there are several techniques for the selection of the individuals prone to be combined and give birth to new individuals in the further iterations of the process. These individuals, commonly called as "parents", are selected through a Roulette Wheel technique. This last assigns to the individuals a certain probability to be chosen in function of their fitness, thus the individuals with lower OF will have greater probabilities of being chosen. The use of this reasoning is based on the Darwinian genetic evolution, in which is demonstrated that the best individuals present higher probabilities to reproduce and survive.

In the proposed algorithm, the probability of being chosen is assigned to each individual in accordance with their positioning in the population list. Those at the top of the list have greater probabilities of being selected, and in general, these are the individuals with the lowest values of OF. However, as explained in the *Ordering Operation* phase, apart from their fitness, there are other criteria to order the population.

Double - Point Crossover

After the *Parent Selection* step, new individuals can be derived, the "children". As already introduced, these individuals' chromosome is obtained as a combination of the parents' allowing the appearance of better individuals with lower OF evolving in this way the population iteration by iteration. In the genetic optimisation framework, this operation is known as *Crossover*.

At each cycle, a specified number of children ($numch$) can be generated from each pair of chosen parents. In this work, it is fixed that the number of children must be equal to the number of parents, then $numch = popsize$. Several ways can be proposed to perform this combination of chromosomes, particularly, and due to its tested efficiency, a Double-Point crossover is employed. This technique consists of randomly defining two division points (r_1 and r_2) on the parents' chromosome, in such a way that the beginning and the end of the vectors cannot be trimmed. Once these points are aleatorily chosen, both parents' chromosomes are divided into 3 por-

tions, and by respecting the relative position of the design variables, it is possible to give birth to the two new children. The first child is constituted by the first and last part of the first parent, while by the second parent's middle part; consequently, the second child is formed by the first and last part of the second parent, and the middle part of the first parent. The chromosome combination through the Double-Point technique is represented below.

$$parent^1 = [x_1^1, x_2^1, x_3^1 \mid x_4^1, x_5^1, x_6^1, x_7^1, x_8^1 \mid x_9^1, x_{10}^1]$$

$$parent^2 = [x_1^2, x_2^2, x_3^2 \mid x_4^2, x_5^2, x_6^2, x_7^2, x_8^2 \mid x_9^2, x_{10}^2]$$

$$children^1 = [x_1^1, x_2^1, x_3^1, x_4^2, x_5^2, x_6^2, x_7^2, x_8^2, x_9^1, x_{10}^1]$$

$$children^2 = [x_1^2, x_2^2, x_3^2, x_4^1, x_5^1, x_6^1, x_7^1, x_8^1, x_9^2, x_{10}^2]$$

The creation of children allows the appearance of new and potentially feasible solutions that keep the characteristics of their parents, allowing the algorithm in this way to research new options which can be better than the previously evaluated ones. It can be verified that, from this point onwards, the total population is constituted by a number of individuals equal to $popsiz e + numch$, which in this work it is also equal to 2 times $popsiz e$.

Uniform Random Mutation

After a certain number of iterations, since children are mostly generated as a combination of the best individuals, the new populations may eventually present potential solutions with strong similarities among them. Accordingly, this is useful since allows the algorithm to rapidly converge towards a solution but, at the same time, it may involve to be in presence of a "local optimal". In this situation, the best individuals have similar chromosomes, and it is difficult for the algorithm to find potential solutions far from the already evaluated ones.

With the aim of giving the algorithm the capability of further exploration of solutions, the *Mutation* technique is employed. In the present work, the mutation is allowed to be performed variable by variable of the chromosome of each child created. Randomly, the algorithm can choose whether to perform or not the mutation of the evaluated variable in function of a small probability of occurrence previously fixed.

Since there are 2 types of variables, in case the variable is binary, the mutation consists of changing its value to the opposite one. Conversely, when evaluating the discrete variables representing the cross-section of the element, the mutation consists of aleatory picking a different one from the cross-section list provided respecting its upper and lower bounds.

Adaptive Mutation

It was evidenced that in advanced iterations, some population members present the same exact chromosome. On one side, this repetition of the solution remarks its potential, but on the other side, reduces the exploration of the algorithm by analyzing an actual minor number of different options per iteration.

This modified mutation is forced to be applied to those repeated individuals, in which, for each group of replicated individuals just one remains unchanged while the rest are subjected to a slight mutation.

$$individual_i = [\overbrace{x_1^i, x_2^i, \dots, x_n^i}^1, \overbrace{x_{n+1}^i}^2, \overbrace{x_{n+2}^i}^3, \dots, \overbrace{x_{n+m}^i}^{m+1}]$$

The chromosomes exposed to this process are divided into $m + 1$ parts and the modification is performed on just one of them. Randomly the part to be mutated is selected, and in case the binary part of the chromosome is chosen, it is completely regenerated in order to obtain a different configuration of exoskeletons but with the same total number. In case any other part of the chromosome is selected to be mutated, since they represents a cross-section, another one is chosen in the proximity of its current position in the list.

As can be appreciated, this technique better than an improvement on the exploration contributes to an increase in the exploitation of the solutions since results in configurations that are similar to the best solutions which iteration by iteration, become recurrent.

Fitness Evaluation

As previously explained in the *Parent Selection* step, the *Fitness Evaluation* involves the calculation of the OF for every single individual present in the population.

As the parents are already analyzed, after inserting children into the population, they are subjected to the structural analysis in SAP2000 performed thanks to the OAPI tools. In Section 3.3 further insights are detailed regarding the structural analysis performed and, in the Chapter 5 it is presented the specific description of the analysis performed for the case study in consideration.

The resulting values of total weight, inter-storey drift, demand-capacity ratio, and OF are saved for each configuration.

Ordering Operations

Before proceeding to the next iteration, sorting, classification, and selection operations must be carried out to order the entire resulting population; the next cycle is provided with an evolved population containing useful individuals.

Once the total population ($posize + numch$) has been sorted from minor to major OF, a classification of the population is carried out according to two criteria. The first criterion is to divide the population into two categories: feasible and infeasible members. The second criterion is to place individuals with unique OF over individuals with repeated OF. This last approach increases the probability of being selected for individuals with unique OF in the *Parent Selection* phase. Consequently, 4 groups of individuals can be identified within the population, the feasible with unique OF, the feasible with repeated OF, the infeasible with unique OF, and the infeasible with repeated OF.

After this sorting and population classification, the feasible individuals with unique OF individuals are introduced at the top of the next iteration population and will therefore present the higher probabilities to be selected in the *Parent Selection* phase. Nevertheless, to exploit new solutions and improve the research capacity of the algorithm, it is useful to keep a certain percentage of the population occupied by infeasible members. In this way, in the present work, it is fixed that the 10% of the new population should be filled with infeasible elements and the remaining 90% with feasible ones (*numfeas*).

The latter is the ideal configuration of the population to be introduced in the further iteration, but this is not always possible. If one of these selected groups of individuals does not have enough members to complete the required set, the group must be filled with individuals from another category. For example, if there is a small number of feasible individuals, the rest must be taken from the infeasible group. Moreover, if there are not enough infeasible elements, the next iteration population must be filled with more than a 90% of feasible elements. This selection can be better understood in the following figure.

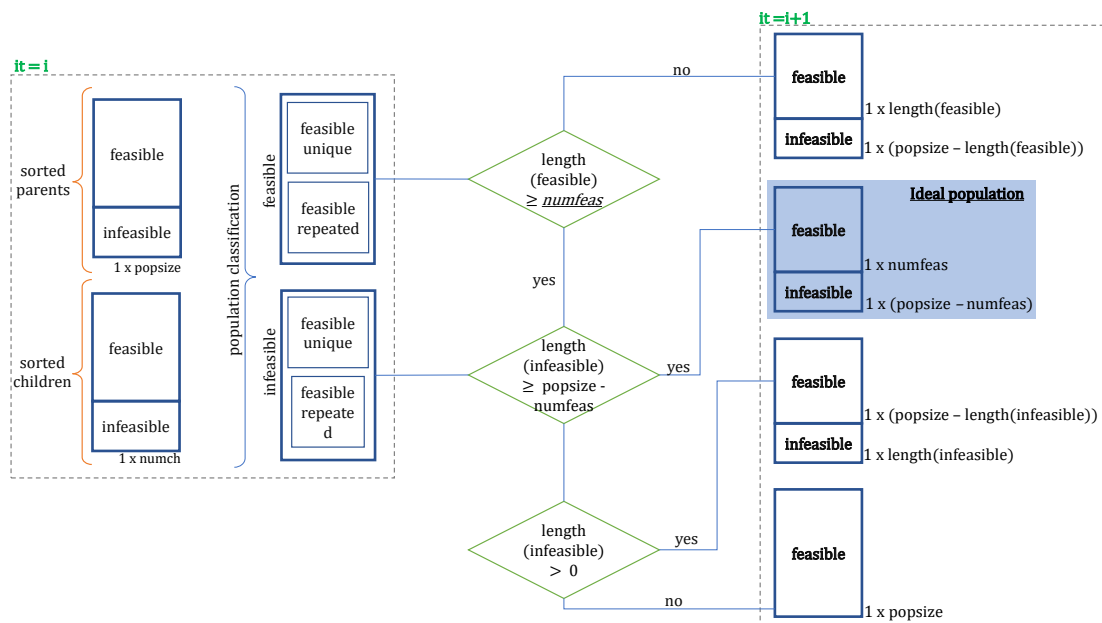


Figure 3.4: Next iteration population assembly strategy

It is possible to appreciate how, independently from the configuration of the newly

evolved population in the next iteration, always the number of individuals present in the population is the same (*popsize*).

Stagnation Check

Stagnation is a situation in which the algorithm finds a local optimal solution, resulting in minimal or no improvement in the solutions over generations. This situation typically arises when the algorithm's best solutions become highly similar, such that the majority of the generated children possess similar chromosomes to the existing solutions. Consequently, it becomes challenging for the algorithm to explore solutions that deviate from these existing solutions.

If the aforementioned scenario occurs, it is crucial to define a criterion for identifying this and providing the algorithm with the ability to address this issue. A potential solution is to reinitialize a significant proportion of the population while preserving a minimal percentage of the most successful solutions. By implementing this approach, it is possible to enhance the algorithm's exploration and increase the possibility of identifying a globally optimal solution.

The proposed algorithm incorporates a stagnation check, whereby, if after 15 iterations it is recognized that the best solution has not been overcome, the entire population, except for the three best solutions, is randomly reinitialized in the same manner as in the *Population Initialization* phase. By keeping the three best individuals, it is possible to retain the useful solutions that the algorithm has identified until the iteration in which the population is reset.

Stopping Criteria

Once the population has been assembled, a new iteration begins from the Parent Selection step. In this subsequent iteration, the members of the newly created population become parents. This iterative process is repeated until a finalization criterion is verified, after which the optimisation process is concluded. The aforementioned criteria can be defined in several ways. For instance, it may be specified that an individual with an OF lower than a certain value must be found. Alternatively, a

solution may be sought that complies with a certain number of constraints, or even the number of iterations may be limited to reduce the required computational effort. In this work, the optimisation end criterion corresponds to the arrival of a maximum number of iterations previously defined.

3.3 FEM Analyses

3.3.1 Response Spectrum Analysis

In the context of seismic design, the Response Spectrum Analysis is the reference method for determining the seismic effects produced on a structure. This analysis is a linear dynamic analysis, employing a linear-elastic model of the structure and a dynamic response spectrum prescribed by regulation.

To perform this analysis, SAP2000 by CSI software is employed. The company offers OAPI tools to link its products to programming languages. This enables the MATLAB software to be linked to the FEM software, allowing the modelling of the structure and retrofitting system, as well as the setting and running of the desired analysis.

A linear dynamic analysis can be performed rapidly through the use of a FEM software to predict the members' displacements, internal forces and reactions. This method assumes that the structural behaviour will remain within the linear elastic field, which is an assumption that fits the considered case study. Accordingly, the computational effort required for a linear analysis of this kind is much lower than that required for a non-linear methodology. This is because the stiffness matrix of the structure remains invariant in the former case and there is no need for its iterative recalculation.

The linear dynamic analysis consists mainly of three steps. Firstly, a modal analysis must be conducted in order to obtain the vibration modal shapes of the structure as well as their frequencies. Secondly, a design response spectrum has to be defined, from which the effects of seismic actions for each single mode can be obtained. Finally, the effects obtained must be combined. All of this procedure is automatically performed within the SAP2000 framework.

In order to determine the vibrations modes of the structure, it is of paramount importance to properly model the structure. Based on technical drawings, is possible to model with a certain level of accuracy the existing structure geometry and materials definition, as well as exoskeleton ones. In this way, the software can calculate and assembly the structure stiffness and mass matrix, which are introduced as an input in the modal analysis.

Once the modal characteristics of the structure have been obtained, it is possible to decouple the coupled equation of motion of the modelled multi-degree-of-freedom system (MDoS) into independent single-degree-of-freedom systems (SDoS) equations. These latter are essentially the equation of motion of the single modes, including their associated modal mass and stiffness, and hence their natural period. Once the design response spectrum has been defined, it is possible to easily solve the independent equations and, consequently, calculate the maximum expected response of the SDoF. In other words, the single mode contribution to the total response of the structure can be obtained.

These effects, since they are obtained from a response spectrum, do not occur simultaneously in time and need to be statistically combined. In this work, the modal combination is performed through the Complete Quadratic Combination method, CQC, which considers the interaction of modes with similar frequencies. It is assumed that a sufficient number of modes have been included, such that the total participating mass is superior to 85% as indicated in Section 7.3.3.1 of [4].

Once the combined modal effects have been evaluated, it is possible to assess the forces acting on the exoskeleton elements for each seismic load combination and perform the necessary structural verifications. With regard to the proposed DBD approach, it is also possible to calculate the inter-storey drift from the nodal displacements.

Chapter 4

Description of the Case Study: Salvo D'Aquisto School

The case study selected for this thesis corresponds to a scholastic complex located in the Italian city of Naples. The complex is composed by seven individual buildings, each with a different functional purpose. The buildings' resisting structure is provided mainly by reinforced concrete (RC) unidirectional frames.

Due to the concurrent development of this thesis and the project, there is currently no complete information available regarding the entire complex. Consequently, in this work, just one of the seven constitutive buildings is analysed and will actually correspond to the evaluated case study.

A vulnerability assessment of the entire complex was performed by a private enterprise, as well as the proposal of an intervention with FRP layers for the seismic updating of the buildings. On the other side, in the present work, are proposed retrofitting solutions through the employment of steel and timber exoskeletons according to the methodology introduced in Section 3.1.

In this chapter the most important steps of the assessment regarding to the selected building are presented, from the historical analysis review to the final structural reference model.

4.1 Structural Assesment

The structural assessment corresponds to a decision-making process aimed at removing any doubts respecting the existing building's current condition and future structural performance. Through it, it is possible to identify and propose effective interventions to fulfil the basic requirements of the buildings and update them regarding the current standard codes.

Since the building evaluated in the case study is located in the Italian territory, results are convenient to refer to the Italian normative. The safety assessment and retrofitting of existing structures can be performed by following the guidelines proposed in Chapter 8 of [4] and Chapter 8 of *CIRCOLARE 21 gennaio 2019*. The aforementioned chapters establish the general criteria that should be employed for the safety assessment, design, execution and testing of interventions on existing buildings.

The safety assessment as well as the planning of the interventions, must take into account important aspects regarding the construction. Should reflect the state of knowledge at the time of the realization of the building; identify the defects not only in design but also in construction; evaluate whether it has been subjected to actions, even exceptional, whose effects are not completely manifested; and find if there is present any kind of degradation or significant changes in the structural elements respect to the original situation.

The feasibility of representing the actual behaviour of the existing structure that the structural model provides strongly depends on the available documentation and on the quality and extension of investigations performed. In function of how deep has been investigated the geometry and construction details, the mechanical properties of materials and soils, as well as the acting permanent loads, the more precise and trustworthy the information obtained is. The use of different analysis and verification methods also depends on the completeness and reliability of the information.

In order to consider the quality of information introduced in the structural models, "confidence factors" are provided. These are coefficients employed in safety checks that modify the capacity parameters in function of the level of knowledge (KL).

The higher KL the better the obtained information and the smaller the confidence factors employed.

In a more precise way, it can be stated that the safety assessment of an existing structure is a quantitative procedure. This is aimed at determining the extent of the actions that the existing structure is able to bear with the minimum safety level required by regulation. The output of this analysis allows to evaluate whether the construction can remain without any intervention or if it is required an increase in structural safety through retrofitting interventions.

To arrive at a model with a certain quality some previous steps must be followed. These involve a historical/critical analysis, geometric and physical survey, definition of mechanical properties of materials, definition of knowledge level and confidence factors, and definition of the reference actions. The information collected from these phases regarding the analyzed case study is presented in the next section.

4.1.1 Historical Survey

The analysis begins with the investigation of the available documentation regarding the origins of the building. Design drawings and reports at the initial construction and at any subsequent intervention are of particular interest.

As already introduced, the scholastic complex named Scuola Salvo D'Aquisto is located on the municipality of Naples. Its constitute buildings are constructed on a mainly flat terrain and the the access is both pedestrian and vehicular. The construction period of the structure is estimated to have commenced between 1961 and 1975, based on the findings of the registry survey. The complex has been intended for scholastic use from its inception. It is connected to the exterior ground by a set of recently constructed above-ground staircases, which were constructed from metalwork to ensure evacuation in case of fire or exceptional events.

The spatial configuration of the scholastic complex is characterised by the presence of six structural bodies, which are hereinafter referred to as A, B, C, D, E and F, while G is a connecting portico. The load-bearing structure of all the bodies within the scholastic complex consists of unidirectional reinforced concrete frames in addition to the perimeter ones. This distribution can be appreciated in Figure 4.1. The total

volume of the buildings conforming to the school complex is approximately 17,550 cubic metres.

Furthermore, a brief description of each body is presented. However, the main focus of this thesis is Building E, which is used as a case study for the development of the proposed research.

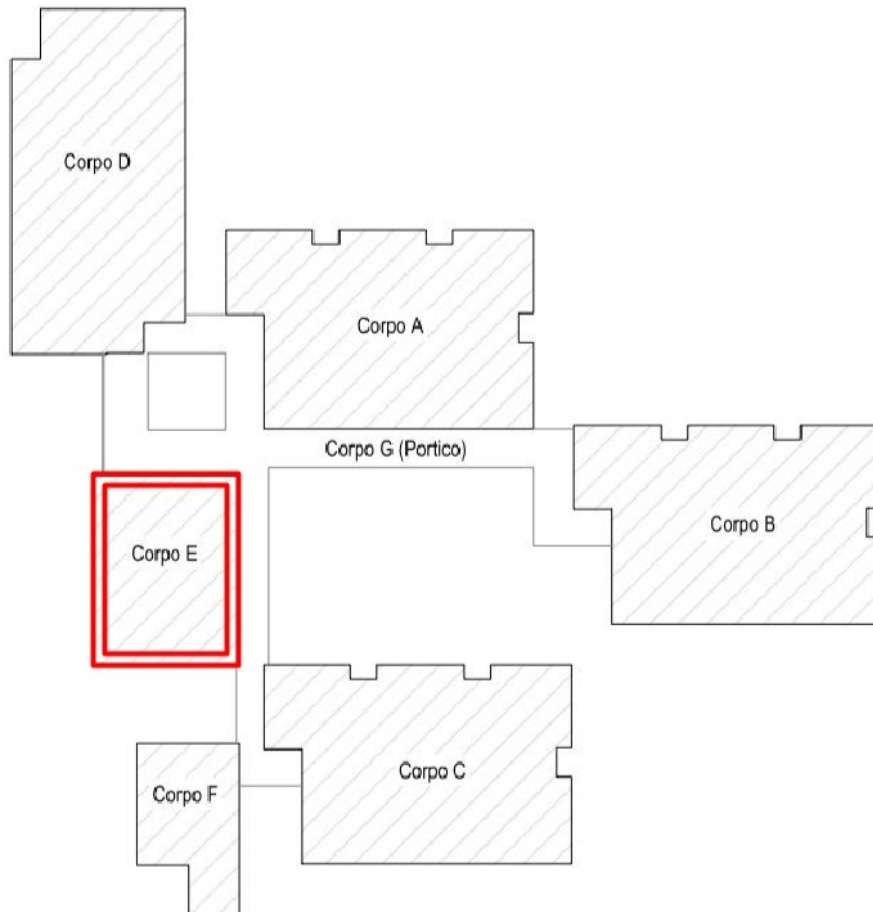


Figure 4.1: Planimetric Scheme of Structural Bodies Distribution

A preliminary survey revealed that each building is characterised by the presence of an in-plane rigid diaphragm, as well as in the roofing level. Additionally, the presence of masonry without any prevention of brittle out-of-plane failure was observed. Next, a brief description of each structural body is presented.

The pavilion bodies A, B, and C collectively constitute the buildings where classroom teaching activities take place. They share a common construction type, with frames

oriented in a single direction in addition to the perimeter frames. In particular, these buildings have three floors connected by an internal staircase.

Body D encompasses the gym area and the changing rooms. This structural building is characterised by the presence of two floors. The first is the basement, while the second is the raised ground floor with a gable roof. In particular, the upper floor is characterised by differing heights depending on the area in question.

The administrative offices, located in Body E, constitute the main entrance of the school and extend over three levels. The first level has a height of 2.00m, the second level has a height of 3.50m, while the third level, whose floor constitutes the gable roof, has a height ranging from 2.80m to 3.90m.

The structure designated as Body F is the building used as the accommodation for the caretaker. It contains a single floor that serves as the gable roof of the building.

Body G comprises a portico with a reinforced concrete load-bearing structure. It serves as a connection between the other previously described buildings and is constituted by a single perimeter frame. The roofing structure is supported by the aforementioned frame and by the frames of the adjacent structural bodies on the same side.

Furthermore, it is relevant to highlight that the original project documentation was sought through consultation of various sources with access to records on the building in question. Despite this, however, documents related to the original structural project were not found. Site surveys and historical-archival research have allowed for the architectural survey of the building. The acquired documentation has provided valuable support in defining the preliminary investigation plan and has been subject to verification during on-site surveys.

4.1.2 Definition of Knowledge Levels and Confidence Factors

Based on the insights carried out in the knowledge process, "knowledge levels" are defined by normative in order to describe how deep is the understanding of the structure's actual situation and behaviour. These constitute 3 different levels: knowledge levels 1, 2 and 3; which refer to the parameters involved in the model

as well as the related confidence factor to be used in safety checks. Moreover, the regulation also specifies which type of analysis can be employed according to the knowledge level reached, in order to ensure that more sophisticated analysis can be applied just if has been reached a sufficient understanding of the existing building.

Regarding the actual case study, the investigation project aims to achieve a **knowledge level 2** (KL2) through a campaign of on-site and laboratory tests, including destructive, semi-destructive and, non-destructive types. The associated **confidence factor** to this level is **1.2**. Furthermore, for the structures studied, the most representative elements at different levels and on each floor were examined in order to gain a better understanding of the structural system.

4.1.3 Geometric and Physical Survey

The geometric and/or structural survey must refer to the overall geometry, both of the structure and structural elements. The survey must identify the resistant organism of the building and should be addressed to the identification of damage, crack patterns and damage mechanisms.

As previously stated, the information gathered solely regarding **Building E** will be exhibited. Table 4.1 presents the information regarding the size of the building. The load-bearing structure consists of unidirectional reinforced concrete frames in

| Level | Surface [m^2] | Height [m] | Volume [m^3] |
|-----------------------|-------------------|----------------|------------------|
| Underground | 173 | 2.00 | 346 |
| Ground-floor | 173 | 3.50 | 606 |
| 1 st floor | 173 | 3.90 | 675 |

Table 4.1: Building E Dimensions

addition to the perimeter frames. The slabs are composed of hollow clay blocks and have an overall height of 25 cm including the screed and the topping slab. The roof is a non-outward thrusting heavy type, while the foundations are of the shallow type.

The individual structural bodies are isolated, yet the presence of the reinforced concrete portico, which serves as an external corridor linking the buildings, effectively

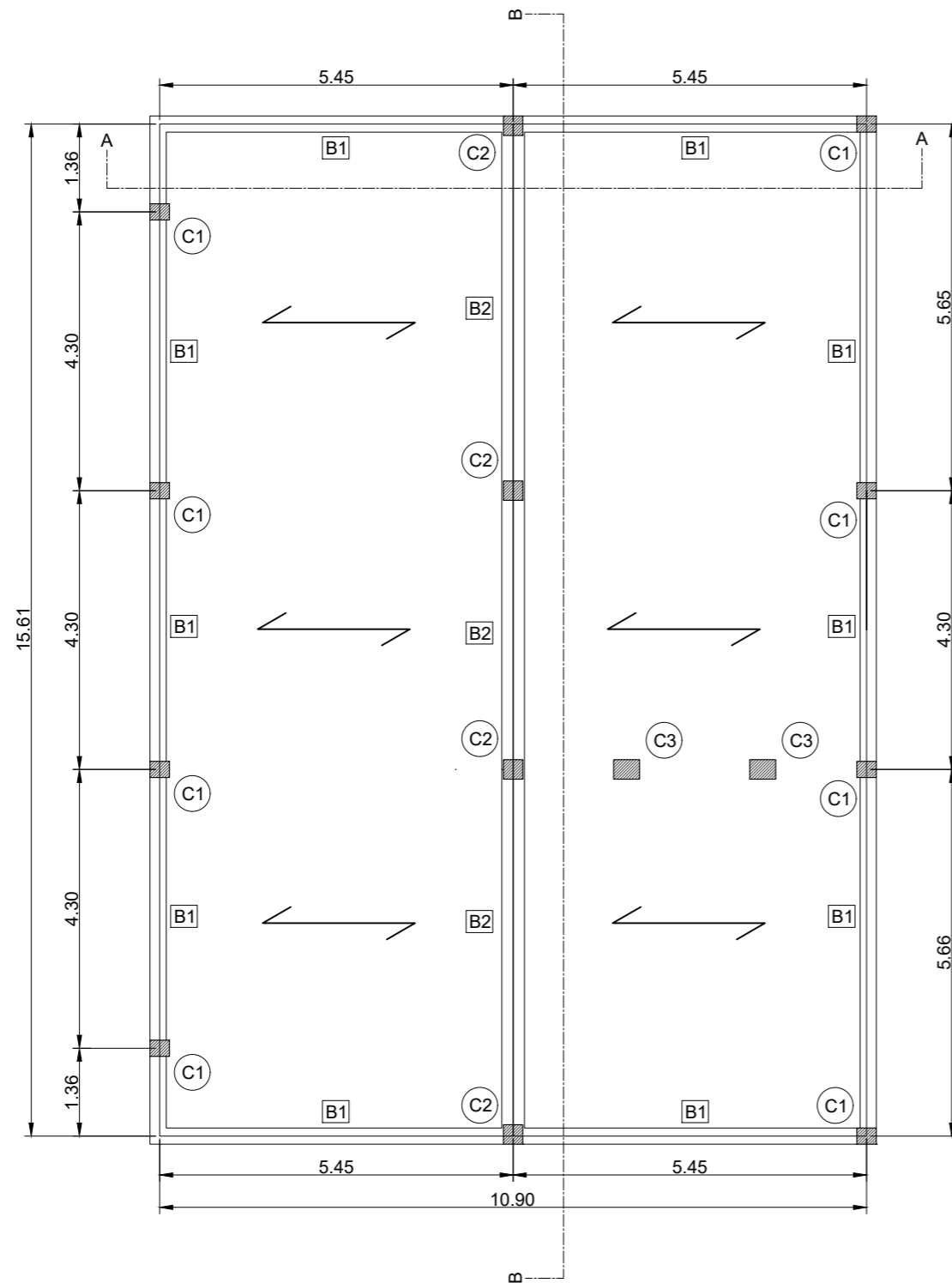
creates a structural connection among them. However, since they have an independent foundation system and the stiffness of the portico is considerably smaller than that of the buildings, the analysis of each building, including body E, can be held independently.

Regarding the building under study, during the surveys carried out, widespread degradation was observed in both the beams and columns located in the basement levels as well as on the ground floor slab's intrados. The lack of maintenance and inadequate protection against weather elements has resulted in the oxidation of the reinforcements, which has led to the spalling of a significant portion of the concrete cover and a notable reduction in the resistant sections of both the concrete and the reinforcements.

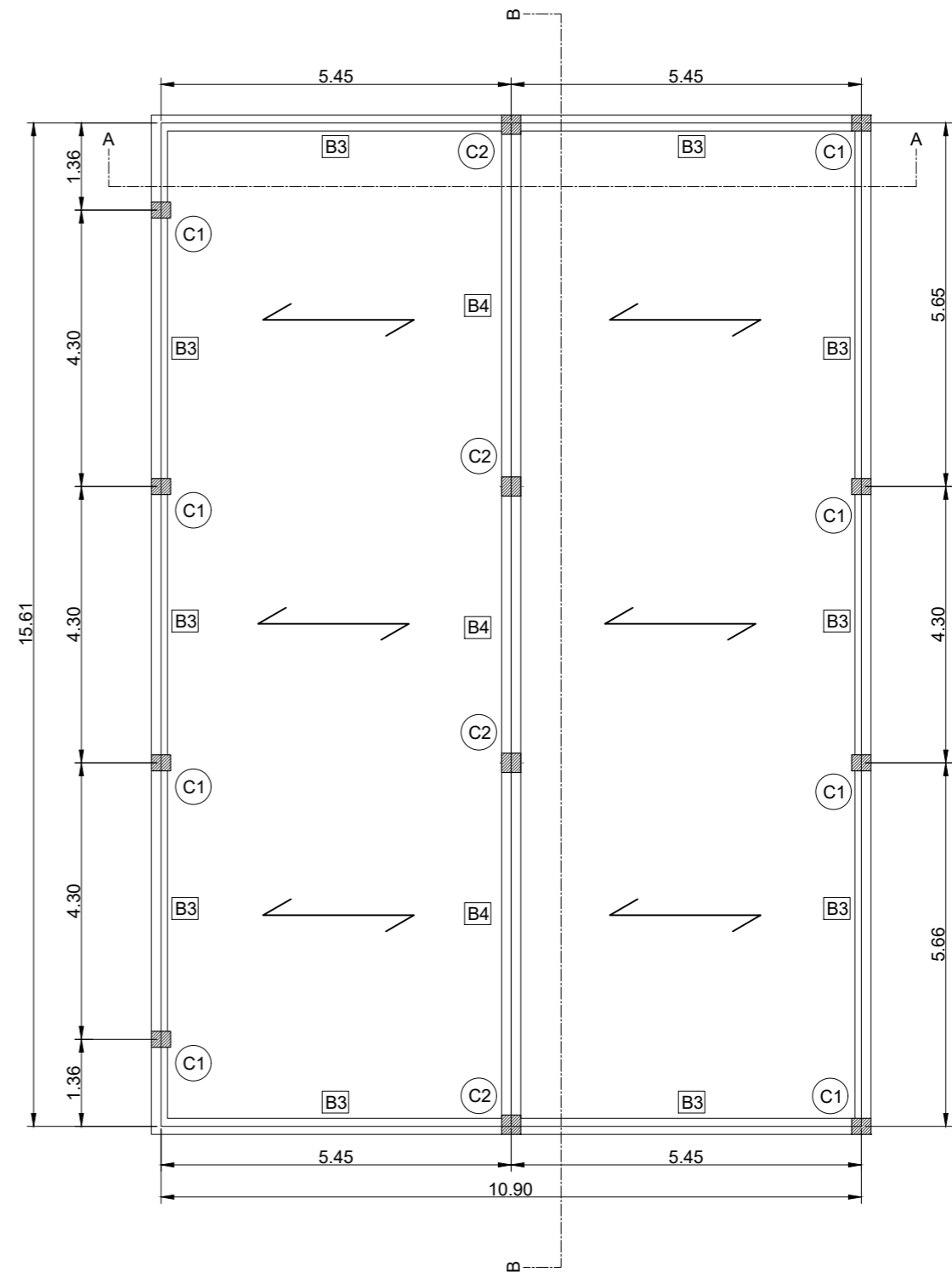
With respect to the geometry of the structure, it is known based on the survey conducted during the inspections and the available drawings. The data collected on the dimensions of the structural elements, along with the details concerning the structural specifics, allow for the development of a structural model suitable for a linear analysis.

As the construction details of the project were not available, an **extended on-site survey** was carried out to develop a proper structural model. The data collected includes information on more than 35% of the load-bearing elements, regarding the actual geometry and dimension of elements as well as the reinforcement present on them.

All the geometric information obtained from the performed surveys is presented in the technical drawings present in the *Plane 1* and *Plane 2*.



FIRST FLOOR STRUCTURE
SCALE: 1/100



ROOF STRUCTURE
SCALE: 1/100

| CROSS SECTIONS | | | |
|----------------|--------|-------|-------|
| ELEMENT | SIMBOL | b [m] | h [m] |
| COLUMN 1 | C1 | 25 | 30 |
| COLUMN 2 | C2 | 30 | 30 |
| COLUMN 3 | C3 | 30 | 40 |
| BEAM 1 | B1 | 25 | 60 |
| BEAM 2 | B2 | 35 | 60 |
| BEAM 3 | B3 | 25 | 50 |
| BEAM 4 | B4 | 30 | 50 |

CROSS SECTIONS TABLE
SCALE: ~



MASTER THESIS

PLAN: 1 - EXISTING STRUCTURE STRUCTURAL PLAN

INSTITUTION: POLITECNICO DI TORINO

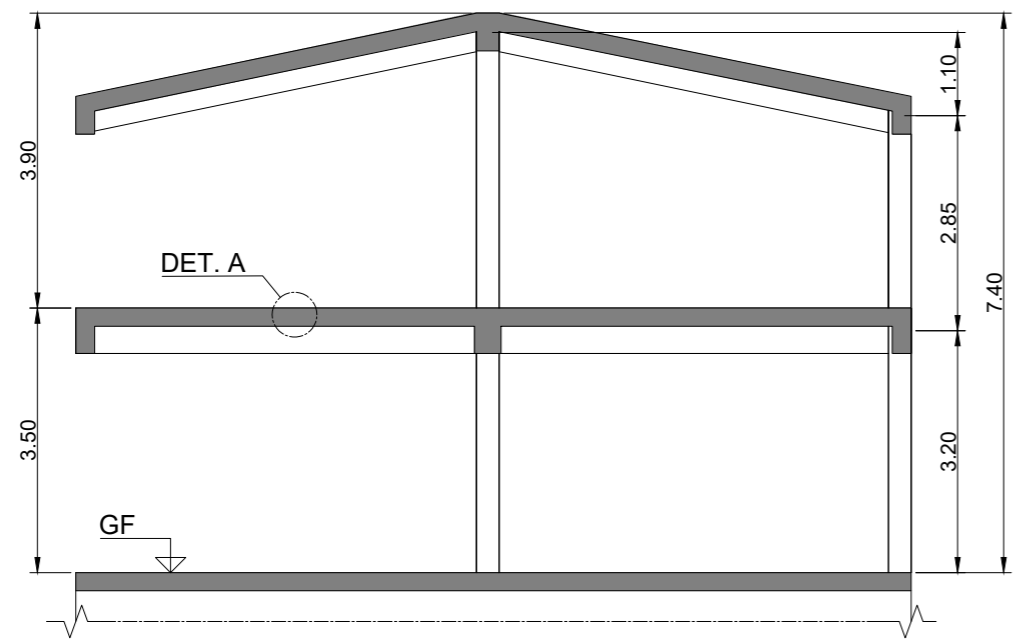
AUTHOR: TOMÁS LAZZURI

SCALE: AS SPECIFIED DATE: 19/07/2024

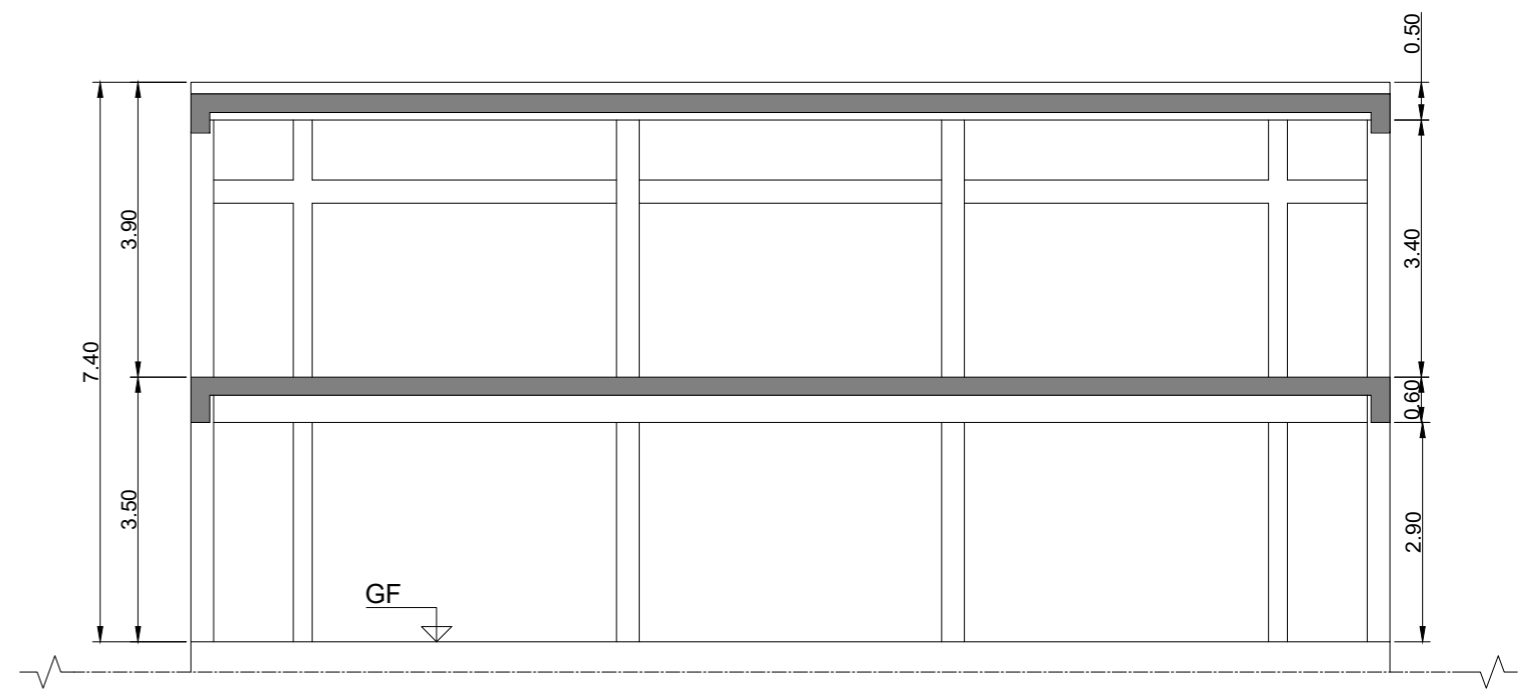
VERSION: V.1

PLAN: PLAN VIEW

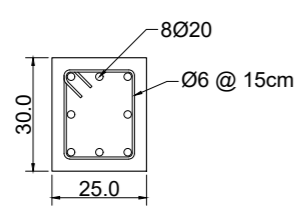
Nº: 1



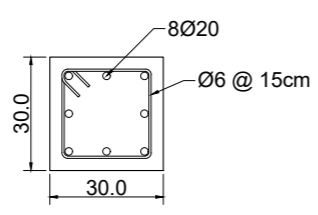
SECTION A-A
SCALE: 1/100



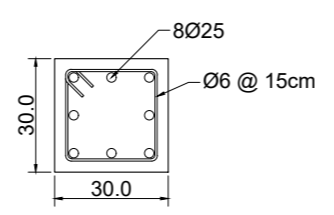
SECTION B-B
SCALE: 1/100



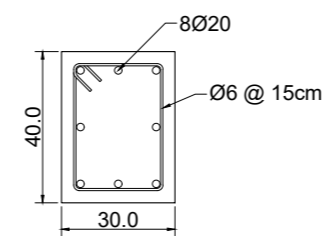
COLUMN C1
SCALE: 1/20



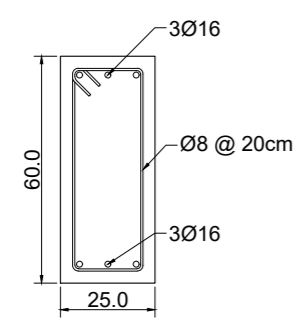
COLUMN C2
SCALE: 1/20



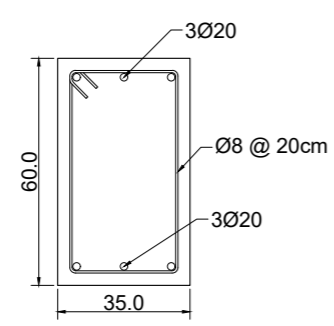
COLUMN C2 (GF LEVEL)
SCALE: 1/20



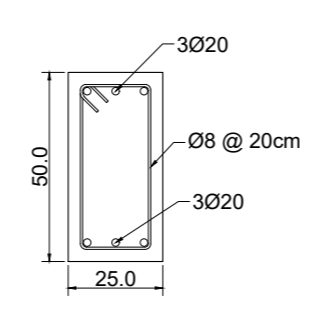
COLUMN C3
SCALE: 1/20



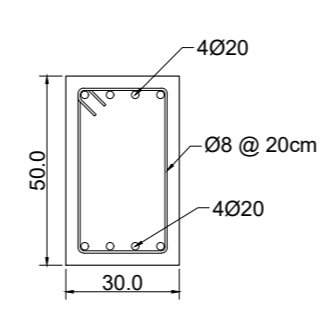
BEAM B1
SCALE: 1/20



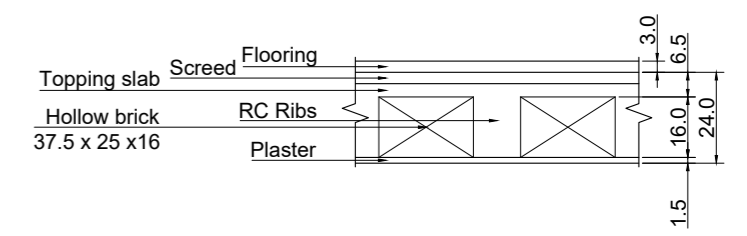
BEAM B2
SCALE: 1/20



BEAM B3
SCALE: 1/20



BEAM B4
SCALE: 1/20



DET. A : SLAB DETAIL
SCALE: 1/20



MASTER THESIS

PLAN:2 - EXISTING STRUCTURE STRUCTURAL PLAN - DETAILS

INSTITUTION: POLITECNICO DI TORINO

AUTHOR: TOMÁS LAZZURI

SCALE: AS SPECIFIED DATE: 19/07/2024 VERSION: V.1

PLAN: SECTIONS & DETAILS

Nº: 1

4.1.4 Definition of the Mechanical Properties of Materials

A structural model that accurately describes the condition and behaviour of the existing structure requires a meticulous evaluation of the mechanical properties of the on-site materials. As stipulated in Section 8.5.3. of [4], to gain a comprehensive understanding of the material's properties and their degradation, it is essential to utilise existing documentation, conduct visual inspections and perform experimental investigations. The number and typology of tests are determined on a case-by-case basis by the designer, following the recommendations outlined in the technical code. The design values of the mechanical properties of the materials are evaluated based on the investigations and tests conducted on the structure, without consideration of the classes specified in the standards for new structures.

In consideration of the knowledge level (KL2) sought in the investigation and testing campaign, and to obtain the values to be used in the safety static and seismic checks, **extended material testing** has been performed.

For the achieved knowledge level, the associated confidence factor which must be employed in the safety checks is $FC = 1.2$.

The material strengths to be employed in the capacity formulas of the elements are obtained by dividing the mean in-situ strengths by the confidence factors and partial safety factors, as indicated in Equation 4.1.

$$f_d = \frac{f_m}{FC \cdot \gamma_m} \quad (4.1)$$

In this study case, a ductile crisis mechanism of the elements is considered, consequently, the security factor applied is equal to 1.

Concrete

The mechanical properties of the structural concrete were determined by averaging the results of compression tests performed on cores taken from beams and columns.

The compressive strength measured on the cores f_{cm} is influenced by many factors that make it different from what would be measured on an equivalent standard

specimen. Among these factors appear the different methods of preparation and curing, the position of the sampling within the structural element, the presence of included reinforcements, etc.

The effect of the aforementioned factors generally tends to underestimate the strength compared to that of equivalent standard specimens. To correct this, corrective coefficients can be used. The in-situ strength is assessed using the formula proposed by Holos. This formula allows the effects of coring to be taken into account through empirical coefficients.

A statistical study was conducted to evaluate the dispersion of the results and the homogeneity of the obtained data; specifically, the following statistical expressions were calculated: arithmetic mean, standard deviation and variance. It is common practice to discard initial values if the variance exceeds its maximum value. Also, the coefficient of variation (CV) has been calculated, which represents a dimensionless measure of dispersion and provides the precision of a measurement. This index is calculated as the ratio between the standard deviation and the arithmetic mean. For the case under consideration, a CV value of 0.22 has been set as the acceptability limit.

After selecting the values for f_{cm} which allows to respect the statistic threshold of $CV = 0.22$, shown in Table 4.2, the arithmetic mean can be calculated. The calculation reported by the enterprise takes into account the cores drilled from the different floors of the different buildings. However, since this thesis only analyses building E, it was decided to only use the values pertaining to the actual case study. Furthermore, the resistance was differentiated between the samples obtained from beams and from columns.

Finally, the arithmetic mean of the values of building E is calculated. Through the application of Equation 4.1, the compressive strength of the concrete for the beams and columns employed for the model are presented in Table 4.3.

| Element | Level | Building | $f_{cm}[MPa]$ |
|----------------|--------------------|-----------------|---------------|
| Column | Underground | C | 35.38 |
| Column | Underground | D | 19.03 |
| Column | Underground | D | 15.23 |
| Column | Underground | E | 15.33 |
| Column | Ground | A | 28.25 |
| Column | Ground | B | 28.53 |
| Column | Ground | C | 17.73 |
| Column | Ground | C | 28.16 |
| Column | Ground | D | 27.88 |
| Column | Ground | D | 19.03 |
| Column | Ground | E | 19.33 |
| Column | First floor | A | 32.53 |
| Column | First floor | B | 36.17 |
| Column | First floor | C | 14.73 |
| Column | First floor | E | 22.24 |
| Beam | Underground | B | 24.99 |
| Beam | Underground | C | 31.57 |
| Beam | Underground | C | 25.55 |
| Beam | Underground | D | 34.67 |
| Beam | Underground | D | 33.78 |
| Beam | Ground | A | 29.83 |
| Beam | Ground | B | 29.28 |
| Beam | Ground | D | 21.47 |
| Beam | Ground | D | 26.76 |
| Beam | Ground | E | 15.84 |
| Beam | First floor | A | 24.71 |
| Beam | First floor | B | 29.28 |
| Beam | First floor | C | 29.65 |
| Beam | First floor | E | 15.91 |

Table 4.2: Extracted core's compressive strength

| Element | $f_{cd} [MPa]$ |
|----------------|----------------|
| Columns | 15.81 |
| Beams | 17.32 |

Table 4.3: Concrete design compressive strength

Reinforcement's Steel

Samples were taken from various elements of the buildings comprising the scholar complex. These were subjected to geometric measurements, weighed, and rectified at a laboratory authorised to perform tests on construction materials. As it was not possible to extract several samples, a limited number of reinforcement bars were inspected. A tension test was performed on these bars, enabling the yield stress and tension strength of the reinforcing steel to be determined. The mean value of the aforementioned parameters was calculated, and the design parameters to be introduced in the model were calculated using the Equation 4.1. These are shown in Table 4.4.

| $f_y[MPa]$ | $f_t[MPa]$ | $f_{yd}[MPa]$ | $f_{td}[MPa]$ |
|------------|------------|---------------|---------------|
| 337.57 | 499.10 | 281.27 | 415.92 |

Table 4.4: Reinforcement Steel Parameters

4.1.5 Definition of Reference Actions

The reference values of the actions and their combinations to be considered in the calculation, both for the safety assessment and for the design of the interventions, are those defined by the employed standard [4] for new buildings. For permanent loads, an accurate geometric-structural and material survey may allow to adopt modified partial coefficients, assigning explicitly motivated values to γ_G . The design values of the other actions (wind, snow, etc.) will be those foreseen by this standard.

Based on the survey conducted on structural and non-structural elements, the element's weights used in safety checks under static and seismic loads have been deduced.

Gravitational Loads - Structural Elements (g_{k1})

Regarding to the self-weight of the structural elements (beams and columns), these were calculated automatically by the structural software employed. Based on the unitary weight specified for the material (25 kN/m^3), the software can determine

the weight of the elements as well as the internal forces derived from it. According to the employed standard, these loads are included in g_{k1} , corresponding to the weight of the structural elements.

Gravitational Loads - Slabs (g_{k1} & g_{k2})

Due to their important thickness, the slabs were conveniently modelled as infinitely rigid diaphragms in order to account for their high in-plane stiffness. Regarding to their weight, it was calculated in function of the scheme shown in the structural details of the shown technical drawings.

Since the slab's structure corresponds to a ribbed one-way type, its self-weight as well as the overloads it has to transmit, are modelled as linear loads directly applied on the beams which are in charge of carrying the slab under consideration.

According to [4], g_{k1} corresponds to the weight of the structural elements, while g_{k2} corresponds to the weight of the non-structural elements. The values considered for these loads are shown in Table 4.5.

| Description | Thickness [m] | Width [m] | Length [m] | Unit Weight [kN/m ³] | Load [kN/m ²] |
|--------------|------------------|--------------|---------------|-------------------------------------|------------------------------|
| Topping slab | 0.035 | 0.500 | 1.000 | 24 | 0.84 |
| Ribs | 0.160 | 0.125 | 1.000 | 25 | 1.00 |
| Blocks | 0.160 | 0.375 | 1.000 | 6 | 0.72 |
| Screed | 0.030 | 0.500 | 1.000 | 21 | 0.63 |
| Plaster | 0.015 | 0.500 | 1.000 | 18 | 0.27 |
| Flooring | 0.030 | 0.500 | 1.000 | 20 | 0.60 |
| | | | | g_{k1} | 2.56 |
| | | | | g_{k2}^1 | 0.9 - 2.3 |

Table 4.5: Self-weight 1st floor and roof slab

¹ g_{k2} 1st floor: $1.5 \text{ kN/m}^2 + 0.8 \text{ kN/m}^2$ (partition walls according to Section 3.1.3 of [4]).

¹ g_{k2} roof: 0.9 kN/m^2 (does not include flooring).

Gravitational Loads - Stairs (g_{k1} & g_{k2})

The same indication made for the slab is also valid for the modelling of the loads carried by the stairs. In particular, a cantilever staircase was constructed, thus the loads due to the self-weight of materials are applied directly to the cantilever beam of the stair. The torsional moment transmitted to this beam is small and can be neglected. Furthermore, the weight of an intermediate landing of the stair, which is structurally a one-way slab, is also calculated.

Variable Loads - Slabs & Stairs (q_{k1})

The loads or overloads applied to the slabs are determined in accordance with Section 3.1.4 of [4]. As the building constitutes a component of a scholastic complex, its category, as defined in Table 3.1.II of [4], is C. Additionally, the category H, which stands for the roofing structure's overloads, must be considered. The resulting data is presented in Table 4.6.

| Category | Description | q_{k1} [kN/m ²] |
|----------|-------------------------------------------------------------------------------------------------------------------|----------------------------------|
| C | Cat. C1 Areas with tables, such as schools, cafes, restaurants, banquet halls, reading rooms, and reception rooms | 3.00 |
| C | Common stairs | 4.00 |
| H | Cat. H Accessible roofs for maintenance and repair only | 0.50 |

Table 4.6: Overload on slabs and stairs

Snow Loads (q_{k2})

The snow loads are applied to the slabs of the roof, and thus, according to the manner of modelling them, these are borne by the beams present in the roof. These loads are determined in accordance with Section 3.4 of [4] by employing the Equation 4.2.

$$q_{k2} = q_s = q_{sk} \cdot \mu_i \cdot C_E \cdot C_t \quad (4.2)$$

where:

- q_{sk} : reference value of the ground snow load;
- μ_i : shape coefficient of the roof;
- C_E : exposure coefficient;
- C_t : thermal coefficient;

The expressions, figures and tables to evaluate the previous variables can be found in the sections 3.4.2, 3.4.3, 3.4.4 and 3.4.5 respectively, of the aforementioned normative. However, the values employed in this case are show in Table 4.7.

| Zone | a_s^1 [m] | q_{sk} [kN/m ²] | α_i^2 [°] | μ_i [-] | C_E [-] | C_t [-] | q_{k2} [kN/m ²] |
|--------------|----------------|----------------------------------|---------------------|----------------|--------------|--------------|----------------------------------|
| III - Naples | 125 | 1.5 | 11.11 | 0.8 | 1 | 1 | 1.2 |

Table 4.7: Snow loads on roof slab

¹ a_s : reference height for determining q_{sk} in zone III (Naples).

² α_i : roof inclination angle.

Wind Loads (q_{k3})

In order to consider the wind loads, the Chapter 3.3 of [4] is recalled. For the sake of simplicity, it is assumed that the wind load affects only the longest façade. It is further assumed that the load is transmitted from the façade to the beams and then to the perimetral columns present in the longest façade. In particular, the wind loads are determined as a static equivalent load, as specified in Section 3.3.3 of the normative, and shown in Equation 4.3.

$$q_{k3} = p = q_r \cdot c_e \cdot c_p \cdot c_d \quad (4.3)$$

where:

- q_r : reference kinetic pressure;
- c_e : exposure coefficient;
- c_p : pressure coefficient (global);

- c_d : dynamic coefficient;

The expressions, figures and tables to evaluate the previous variables can be precised in the sections 3.3.6, 3.3.7, 3.3.8 and 3.3.9 respectively, of the aforementioned normative. However, the values employed in this case are show in Table 4.8. It is considered the pressure loads in windward walls and roof as well as the suction pressure in leeward wall and roof. It is considered the possibility of pressure and suction loads in the windward roof as its inclination angle is among 5° and 45° .

| Point of application | q_r [N/m ²] | c_e [-] | c_p [-] | c_d [-] | q_{k3} [kN/m ²] |
|--------------------------|------------------------------|--------------|--------------|--------------|----------------------------------|
| Windward wall | 456.29 | 1.95 | 0.80 | 1 | 0.71 |
| Leeward wall | 456.29 | 1.95 | -0.90 | 1 | -0.80 |
| Windward roof (suction) | 456.29 | 1.95 | -0.65 | 1 | -0.58 |
| Windward roof (pressure) | 456.29 | 1.95 | 0.15 | 1 | 0.14 |
| Leeward roof | 456.29 | 1.95 | -0.60 | 1 | -0.53 |

Table 4.8: Wind loads on longest facade

Seismic Action

The seismic action is determined according to Section 3.2 of [4]. According to it: *"The design seismic actions, which are used to assess compliance with the various considered limit states, are defined based on the "basic seismic hazard" of the construction site. They depend on the morphological and stratigraphic characteristics that determine the local seismic response."*

As a Response Spectrum analysis it is employed for the seismic evaluation of the structure, an spectral shape which describes the design seismic input must be defined. This last, depends on the limit state considered in the analysis. In particular, the safety checks as well as the design of the interventions, are assessed according to the ultimate limit state, which in case of seismic actions, corresponds to the life safety limit state (SLV).

Furthermore, due to the lack of information regarding to the construction details, and given that the building in question was designed without consideration of seismic criteria, the elastic response spectrum is employed. In other words, a conservative

approach is adopted by employing of a behavior (q) factor equal to 1.

Hence, the design elastic response spectrum of Figure 4.2 is defined according to the parameters shown in Table 4.9.

| Parameter | Value |
|-----------------------|------------------|
| V_N | 50 <i>years</i> |
| Usage Class | III |
| C_U | 1.5 |
| V_R | 75 |
| P_{VR} (SLV) | 10% |
| T_R (SLV) | 712 <i>years</i> |
| Zone | Naples, Campagna |
| Latitude | 14.2536 |
| Longitude | 40.8874 |
| a_g | 0.187 <i>g</i> |
| F_0 | 2.424 |
| T_0 | 0.347 <i>s</i> |
| Subsoil category | C |
| Topographic condition | T1 |

Table 4.9: Elastic Response Spectrum Parameters

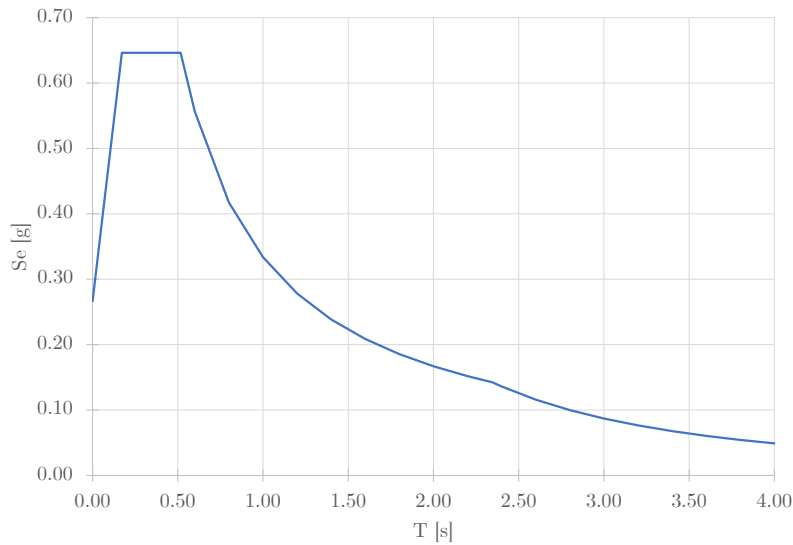


Figure 4.2: Elastic Response Spectrum

4.2 Reference Structural Model

4.2.1 Modelling Criteria

During the modeling phase, it is necessary to transfer the knowledge gathered from investigations into a structural model that is as close to physical reality as possible. This step is one of the most delicate ones in the process leading to the definition of seismic risk because translating reality into a model always involves some simplifications. The building in question has been modeled to be consistent with the findings of the investigation phase; the resistant sections are those provided by the geometric survey, excluding the plaster; the material properties are inferred from visual inspections and in situ investigations, as previously described. Regarding the existing floors, they have been modelled as infinitely rigid.

The body G (portico), although it constitutes a structural connection between all the buildings, assumes a secondary behavior due to its modest stiffness compared to the one of the other buildings. In this way, the analyzed building (E), can be modelled as an isolated structure.

It is also necessary to carefully analyze the presence of the basement, characterized by the presence of tuff block masonry infill walls approximately 50 cm thick, extending along the perimeter of the buildings. The configuration in question results in a horizontal stiffness of the basement level that is significantly greater than that of the above-ground floors. It is therefore reasonable to assume that a fixed support is provided at ground level, or at the level of the basement ceiling. From the study of numerous analogous cases addressed in the literature, where the behavior of structures with and without a rigid basement was compared, no substantial differences in terms of actions on the above-ground structures were found. The only notable difference is a slight variation in displacements, which are negligible for the purposes of seismic vulnerability verifications. Therefore, the simplifying assumption of omitting the basement from the structural model is acceptable, since the underground construction acts as a rigid block that oscillates solidly with the ground during an earthquake. Moreover, this allows for the reduction of seismic actions by neglecting the masses of the basement.

In Figure 4.3, it is reported the structural model created for this thesis in SAP2000.

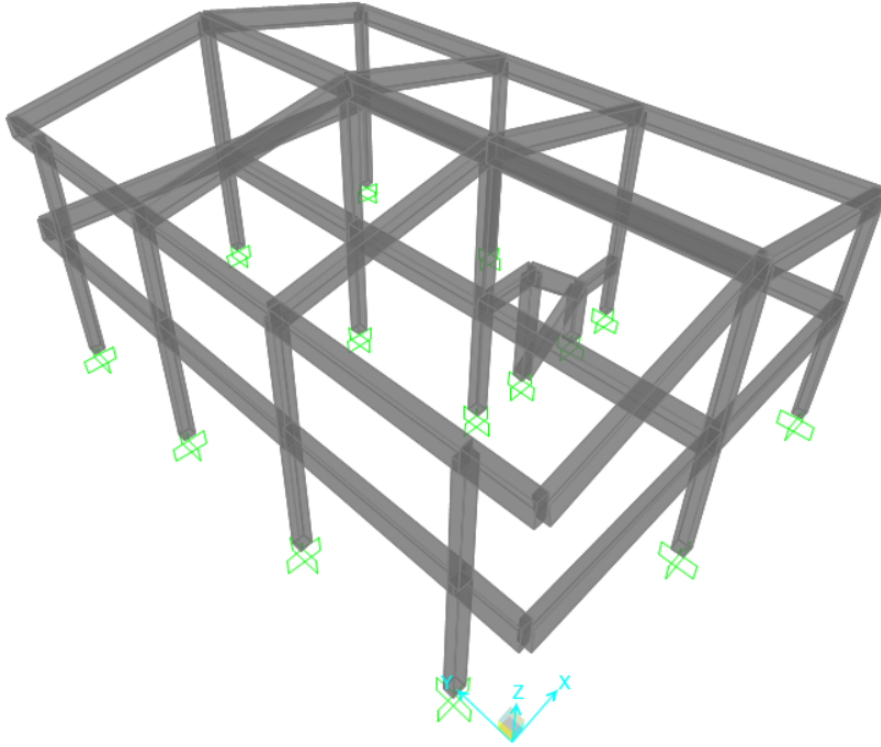


Figure 4.3: Axonometric view of the structural model

4.2.2 Load Combinations

In function of the loads indicated in Section 4.1.5, in order to perform the correspondent ultimate limit state safety checks, the following load combinations indicated in Section 2.5.3 of [4] are considered.

$$\begin{cases} \gamma_{G1} \cdot G_{k1} + \gamma_{G2} \cdot G_{k2} + \gamma_{Q1} \cdot Q_{k1} + \gamma_{Q2} \cdot \psi_{02} \cdot Q_{k2} + \gamma_{Q3} \cdot \psi_{03} \cdot Q_{k3} \\ \gamma_{G1} \cdot G_{k1} + \gamma_{G2} \cdot G_{k2} + \gamma_{Q2} \cdot Q_{k2} + \gamma_{Q1} \cdot \psi_{01} \cdot Q_{k1} + \gamma_{Q3} \cdot \psi_{03} \cdot Q_{k3} \\ \gamma_{G1} \cdot G_{k1} + \gamma_{G2} \cdot G_{k2} + \gamma_{Q3} \cdot Q_{k3} + \gamma_{Q2} \cdot \psi_{02} \cdot Q_{k2} + \gamma_{Q1} \cdot \psi_{01} \cdot Q_{k1} \end{cases} \quad (4.4)$$

$$\begin{cases} \pm E_x \pm 0.3 \cdot E_y + G_1 + G_2 + \psi_{21} \cdot Q_{k1} \\ \pm 0.3 \cdot E_x \pm E_y + G_1 + G_2 + \psi_{21} \cdot Q_{k1} \end{cases} \quad (4.5)$$

where,

- G_{k1} = structural elements self-weight (permanent);
- G_{k2} = non-structural elements self-weight (permanent);
- Q_{k1} = overloads (variable);
- Q_{k2} = snow load (variable);
- Q_{k3} = wind load (variable);
- γ_j = Partial coefficients for actions or for the effect of actions in limit state verifications;
- ψ_j = factor for combination value of a variable action;
- E = seismic action;

Equations 4.4 correspond to the fundamental load combination for structural verifications (STR), in which different variable loads are considered acting simultaneously with the permanent loads. Equations 4.5, correspond to the seismic combinations in SLV with the seismic action acting 100% in one direction and 30% in the other one.

The partial coefficients and combination factors employed in this work for the aforementioned load combinations, are shown in Table 4.10.

| Partial Coefficient / Combination Factor | Value |
|-------------------------------------------------|--------------|
| γ_{G1} (Unfavorable) | 1.3 |
| γ_{G2} (Unfavorable) | 1.5 |
| γ_{Qi} (Unfavorable) | 1.5 |
| ψ_{01} (CAT.C) | 0.7 |
| ψ_{01} (CAT.H) | 0.0 |
| ψ_{02} (level < 1000 h.a.m.s.l) | 0.5 |
| ψ_{03} | 0.6 |
| ψ_{21} (CAT.C) | 0.6 |
| ψ_{21} (CAT.H) | 0.0 |
| ψ_{22} (level < 1000 h.a.m.s.l) | 0.0 |
| ψ_{23} | 0.0 |

Table 4.10: Partial Coefficients and Combination Factors employed

4.3 Existing Structure's Seismic Vulnerability

The seismic vulnerability of the existing structure was initially evaluated by the enterprise responsible for the project. Initially, static checks were carried out on the components of the building's structure, with the parameter $\zeta_{V,i}$ calculated. This represents the ratio between the maximum value of the variable vertical overload that the construction can withstand and the value of the variable overload that would be used in the design of a new construction. The outcomes of this analysis are presented in Table 4.11, where it can be seen that the existing structure is not vulnerable under static loads.

| $\zeta_{V,i}$ shear | $\zeta_{V,i}$ flexural |
|---------------------|------------------------|
| 3.05 | 1.11 |

Table 4.11: Static Vulnerability Indexes

The seismic risk indexes for the different collapse mechanisms were evaluated through a pushover analysis in both main directions. To illustrate, for the ductile failure mechanism with seismic action mainly acting on the y direction, the results obtained are shown by the ADSR spectrum in Figure 4.4 and the compromised elements are the darker ones in Figure 4.5.

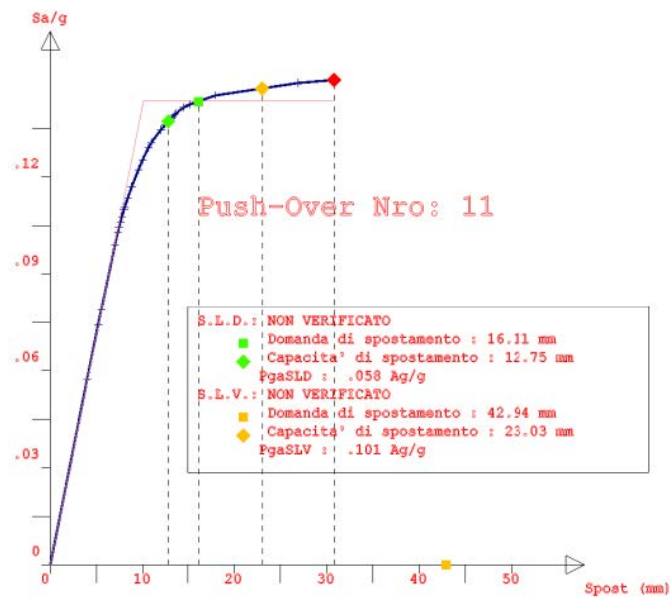


Figure 4.4: Unretrofit building ADRS: (+)Fy (-)0,3Fx (+)Ecc.5% taken from technical report provided by the design company of the project

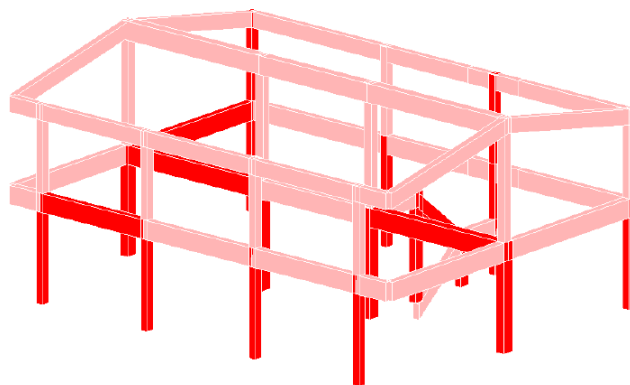


Figure 4.5: Collapse mechanism: (+)Fy (-)0,3Fx (+)Ecc.5% taken from technical report provided by the design company of the project

The most compromising seismic risk index identified in the analysis is related to the seismic action acting in the y direction, with a value of $\zeta_E = 0.54$. The results indicate that the building's ductile resources are limited and insufficient, which is re-designed according to regulations that did not have strong seismic guidelines at the time.

In this work, the vulnerability of the structure under seismic loads, as introduced in Section 3.3, is assessed instead with a response spectrum (linear-dynamic) analysis held on the reference model described in Section 4.2. This allows for a direct interpretation of the improvements achieved by the proposed exoskeleton intervention, as the results are compared using the same type of analysis.

Following the regulations, the seismic vulnerability index or seismic risk index, denoted by ζ_E , is defined as the ratio between the maximum seismic action that a structure can withstand and the maximum seismic action that would be employed in the design of a new construction. In practical terms, this ratio is obtained by dividing the $PGA_{capacity}$ by the PGA_{demand} , which corresponds to the ratio of two peak ground accelerations. The denominator corresponds to the demand on the structure obtained from the elastic response spectrum presented in Figure 4.2. The numerator can be obtained from the response spectrum which gives rise to the global collapse of the structure. Therefore, if the building is vulnerable under seismic loads since it cannot resist the actions derived from the elastic spectrum, the $PGA_{capacity}$ can be evaluated as the maximum PGA of a scaled spectrum that the structure can resist.

In order to identify the value of $PGA_{capacity}$, a scaling of the response spectrum for more recurrent return periods is performed by the Equation 4.6 presented in the auxiliary text of NTC 18 [41].

$$\log p = \log p_1 + \log \frac{p_2}{p_1} \cdot \log \frac{T_R}{T_{R1}} \cdot \log \frac{T_{R2}}{T_{R1}}^{-1} \quad (4.6)$$

In this previous equation, the parameter p represents the generic seismic parameter a_g , F_o or T_c^* . If a new seismic action is evaluated with a PGA (a_g) obtained as a percentage of the one present in the elastic response spectrum, it is possible to find the new spectrum return period T_R by employing the previous equation. Later, with the same equation, the rest of the parameters are obtained and this allows to reconstruct the shape of the scaled response spectrum which has a smaller PGA. Several response spectrums were evaluated until the one which describes the imminent global collapse of the structure was found. This last presents a PGA of 35% of the elastic response spectrum ones. Consequently, the seismic risk index

derived from the linear dynamic analysis, obtained as $PGA_{capacity} / PGA_{demand}$, is $\zeta_E = 0.35$.

Accordingly, given that the seismic vulnerability evaluated in the structural model created in this work is obtained through linear dynamic analysis, it was anticipated that the values obtained would be relatively minor in comparison to those obtained through a non-linear analysis. In light of this, it can be stated that both results are reasonably close and that both situations can be compared.

Furthermore, the linear dynamic analysis enables the calculation of the DCR of the different elements. For the sake of simplicity, the improvement in the structural behaviour is assessed by comparing these values before and after the proposed intervention with exoskeletons.

The vulnerability of the structure under static loads is evaluated by considering the fundamental combination according to [4], as presented in Equation 4.4. The results can be appreciated in Figure 4.6, from which it is clear that the modelled existing structure is not vulnerable under static loads since all the elements pass the safety checks. The most compromised elements are the central beams with DCR equal to 0.92.

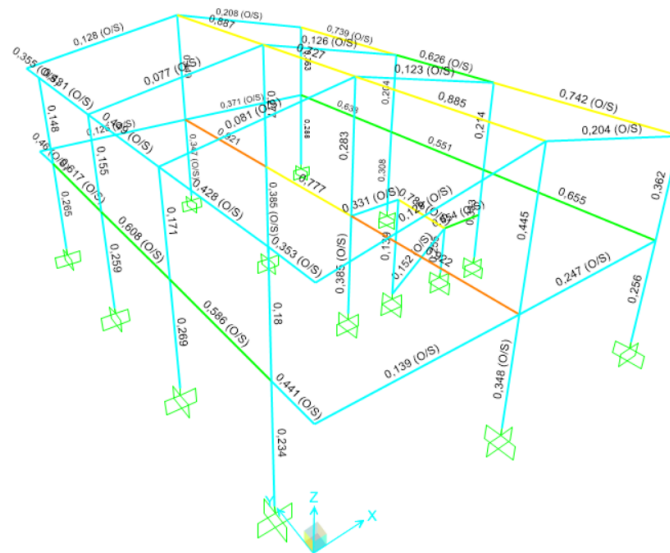


Figure 4.6: DCR under Static Loads

Conversely, when the DCR of the existing structural elements subjected to the

seismic combinations presented in Equation 4.5 (considering the elastic response spectrum) is evaluated, a highly compromising situation emerges. The results are presented in Figure 4.7, from which it is evident that virtually no element passes the safety checks.

Table 4.12 presents the average and maximum DCR values for each group of elements. This allows for an understanding of the severity and number of failing elements, as well as the location of the most critical elements. The ground floor columns are the most severely compromised elements, exhibiting the highest average and maximum DCR values, reaching almost 3. Moreover, the columns of the first floor are similarly severely compromised, exhibiting a high degree of non-compliance with safety checks. Additionally, it is possible to identify that some beams present in both slabs do not pass the structural verifications.

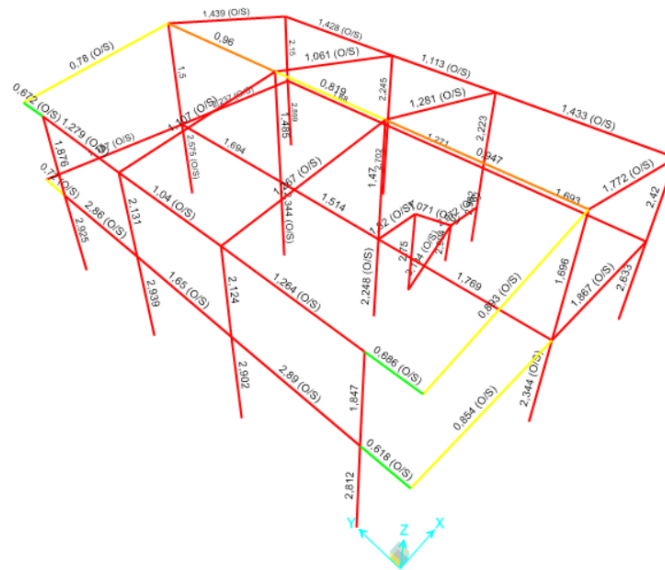


Figure 4.7: DCR under Seismic Loads

| Elements | DCR_{AVG} | DCR_{MAX} |
|-------------------------------|-------------|-------------|
| GF Columns | 2.59 | 2.98 |
| 1 ST Floor Columns | 1.79 | 2.42 |
| GF Beams | 0.89 | 2.89 |
| Roof Columns | 0.69 | 1.77 |

Table 4.12: Average and maximum DCR

Chapter 5

Analysis and Interpretation of the optimization output

The retrofitting intervention for the seismic upgrading of the existing structure is selected based on a comparative analysis of three proposed interventions. This chapter presents the analysis conducted and the results obtained for each scenario assessed.

The first scenario comprises the precise intervention proposed by the enterprise responsible for the project, which entails the installation of CFRP systems on specific nodes and columns of the building.

The second scenario implies the installation of steel exoskeletons. These structures are designed according to the methodology proposed in this thesis and described in Chapter 3. Several optimization runs are performed until the most feasible configuration is identified.

In the final scenario, the feasibility of designing exoskeletons made of a more sustainable material, timber, is evaluated. The final configuration is obtained and designed in the same way as the previous alternative. However, an additional effort is required for the calculation of the structural penalty function, since it was necessary to write an independent code which allows for the calculation of the safety checks of the members.

At the end of the chapter, the environmental cost is calculated through a life cycle assessment procedure, which considers the product, use, and end-of-life stages. This allows for the determination of the most sustainable alternative in terms of environmental impact.

Furthermore, the economic cost of each scenario is calculated. In order to perform a congruent economic evaluation and determine the most convenient solution, the list of prices from the region in which the building is located, Campania, is considered.

5.1 Scenario 1: Traditional Retrofitting Approach

The first scenario corresponds to the intervention proposed by the enterprise in order to overcome the poor lateral loads resistance of the existing structure presents.

It is proposed a **safety retrofitting intervention** aiming to achieve the required safety levels for newly constructed buildings as specified in Section 8.4.3 of [4]. For this category of interventions, safety assessment is mandatory and aims to determine whether the structure, following the intervention, is capable of withstanding the combinations of design actions with the safety level required by the [4].

With regard to the requirements of the regulation, for retrofitting interventions against seismic actions, the unit value of the parameter ζ_E is generally required. In the case of simple changes of class and/or use that result in an increase in vertical loads on the foundations of more than 10%, a minimum value of ζ_E of 0.8 is permitted.

The proposed intervention consists in the local improvement of some column-beam nodes and columns through the installation of carbon fibre-reinforced plastic (CFRP) systems. The application of these systems allows for the enhancement of column confinement, thereby increasing their ductility and strength. Furthermore, when applied in nodes, they permit the admission of significantly higher loads, as they assume a substantial portion of the action present in the node.

The CFRP systems employed for the comparison analysis performed from now on, are the **MAPEWRAP C QUADRI-AX SYSTEM** and **MAPEWRAP C UNI-AX** commercialised by the enterprise Mapei S.p.A. The first system is indicated for the plating of beam-column joints for their improvement and performance enhancement under seismic, dynamic, and impulsive stresses. The second system instead, it is indicated for the repair and structural reinforcement of undersized or damaged reinforced concrete elements providing an extra flexural reinforcement, shear reinforcement, compression confinement, and flexural compression reinforcement, allowing the seismic upgrading or improvement of structures.

The CFRP systems are composed by the previously mentioned fibres and a system of resins which should be carefully applied for their correct installation. The types of

required resins for both systems are largely analogous. Hereafter, resin 1 refers to the product *MAPEWRAP PRIMER 1* [42], resin 2 to *MAPEWRAP 11* [42] and, resin 3 to *MAPEWRAP 31* [43]. Moreover, the steps required for the installation of both fibre systems are also predominantly equal and these are summarised next:

- Prepare as indicated in the catalogue the resin 1, 2 and 3;
- Clean and prepare the concrete surface of application;
- Apply a 1st uniform coat of resin 1 with a brush or roller;
- On the concrete surface previously treated with resin 1 and while it is still "fresh," apply a layer approximately 1 mm thick of resin 2 with a notched trowel. Then, smooth the surface with a flat trowel to completely eliminate any small irregularities on the substrate. Additionally, use the same product to fill and round off the corners to create a cove with a radius of curvature of at least 2 cm;
- Apply uniformly, with a brush or roller, on the still "fresh" resin 1, a first layer approximately 0.5 mm thick of resin 3.
- On the fresh layer of resin 3, immediately lay the CFRP fabric, ensuring it is stretched without leaving any wrinkles. Press it multiple times using a roller to allow the adhesive to penetrate through the fabric fibres fully;
- Apply a 2st uniform coat of resin 3 on the fabric. To eliminate any air bubbles trapped during previous operations, roll the roller over the impregnated fabric again;
- Finally, on the still "fresh" resin, spread dry quartz sand with a particle size ranging between 1.2 and 1.9 mm.

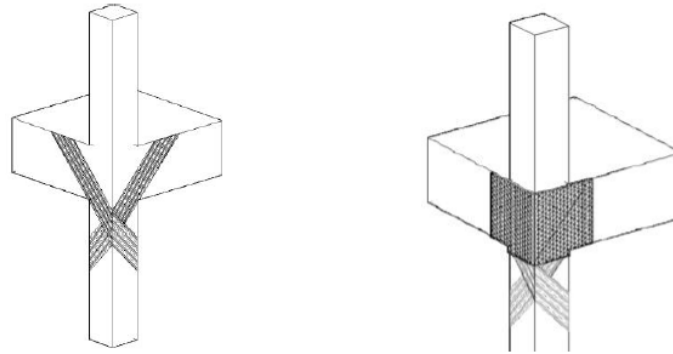


Figure 5.1: Typical CFRP intervention for unconfined nodes

In the case of nodes, the fibres should be installed with a certain inclination and final covering as indicated in Figure 5.1. Regarding its application for the confinement of columns, it can be applied in a continuous or stripped manner, depending on the results obtained from the calculation.

The main characteristics of these specific products are presented in Table 5.1.

| Property | MAPEWRAP C QUADRI-AX SYSTEM | MAPEWRAP C UNI-AX |
|-------------------------------|--------------------------------|-----------------------------------------------------------|
| Type of fibre | high-strength carbon fibre | high-strength and high-elastic modulus carbon fibre |
| Aspect | quadriaxial balanced fabric | unidirectional fabric |
| Equivalent thickness t_{eq} | 0.053 mm | 0.219 mm |
| Grammage | 380 g/m ² | 400 g/m ² |
| Consume resin 1 | 275 g/m ² | 275 g/m ² |
| Consume resin 2 | 1550 g/m ² | 1550 g/m ² |
| Consume resin 3 | 2050 g/m ² | 1300 g/m ² |

Table 5.1: CFRP System's Properties

Figure 5.2 illustrates the columns in which the upper nodes are reinforced with the aforementioned technique. Figure 5.3, on the other hand, depicts the columns in which the complete confinement method is employed.

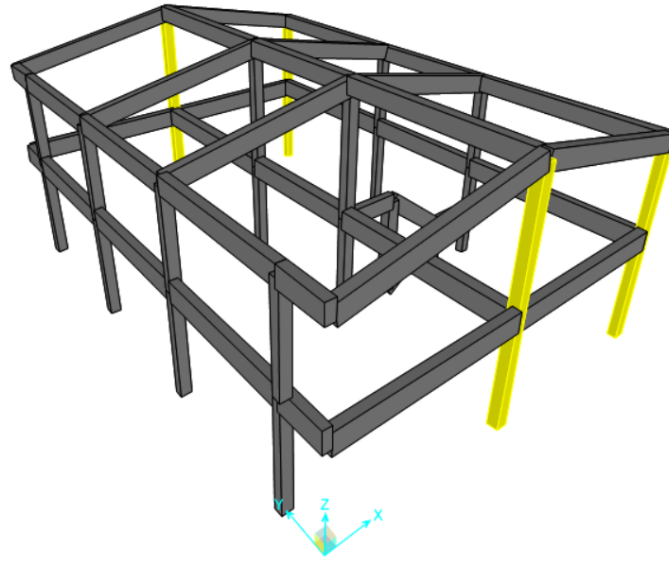


Figure 5.2: Upper nodes retrofitted with CFRP

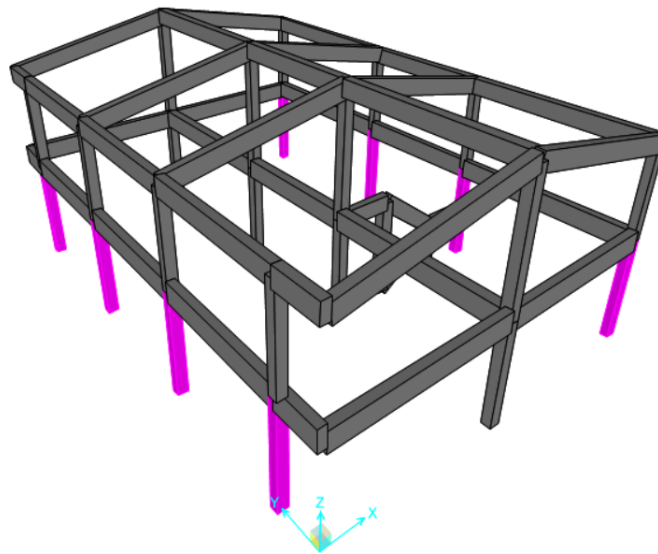


Figure 5.3: Columns retrofitted with CRFP

This intervention is proposed by the enterprise on the basis of the seismic vulnerability assessment results presented in Section 4.3. By installing the CFRP in the indicated beam-columns nodes and confining the indicated columns, there is an upgrade on the seismic response of the building. After the intervention, the minimum seismic risk indexes are the ones presented in Table 5.2. Consequently, since the minimum ζ_E among all the failure mechanisms evaluated in their analysis, results

to be over 0.8 in the limit states assessed, there is a clear improvement in the seismic response of the building.

| Limit State | Retrofitted ζ_E |
|--------------------|-----------------------------------------|
| SLD | 1.081 |
| SLV | 0.908 |

Table 5.2: Minimum Seismic Risk Indexes after Intervention

5.2 Scenario 2: Steel Exoskeletons

The scenario discussed in this section corresponds to the retrofitting of the existing structure by the installation of external steel exoskeletons. The intervention is designed using the displacement-based optimization method introduced in Chapter 3.

Using the algorithm described in Section 3.2, different exoskeleton configurations were evaluated until the one that gave the best results was obtained. The best solution, as already explained, is the one that minimises the proposed objective function. In this way, the inter-storey drift threshold proposed in the displacement-based methodology, as well as the structural safety checks of the exoskeleton members, are respected, while the total weight of the intervention is minimised.

Regarding to the setting of the employed optimization algorithm, Table 5.3 shows the main used employed in the algorithm configuration.

| Parameter | Value |
|-------------------------------|--------------|
| Number of runs | 5 |
| Number of individuals per run | 200 |
| Number of iterations | 100 |
| Stagnation check iteration | 15 |

Table 5.3: Optimization Algorithm Parameters

Regarding the material, due to its high performance, structural steel S355 is used for the exoskeleton's members. Concerning the type of structural profiles, circular hot-formed hollow sections are employed. These profiles are characterized by their outer diameter, \varnothing , and their wall thickness, t_f . Moreover, the cross-section list provided to the optimisation algorithm for the selection of each discrete variable, contains a total of 36 different options ranging from an external diameter of 101.6 *mm* to 711 *mm*.

The typical exoskeleton topology is repeated in the different positions where it can be placed. Figure 5.4 presents the typical exoskeleton configuration as well as the designation of its members.

Furthermore, in Figure 5.5, it is also possible to appreciate the positioning of the hinges modelled for the single steel exoskeleton. The selection of these hinges was made to guarantee the desired truss behaviour of the retrofitting structure. This choice allows for the appearance of mainly axial loads on the exoskeleton's members, while simultaneously avoiding the transfer of significant loads to the existing structure to which they are connected. Finally, the release of the hinges has been properly chosen in order to avoid kinematisms or local labilities of the structural members.

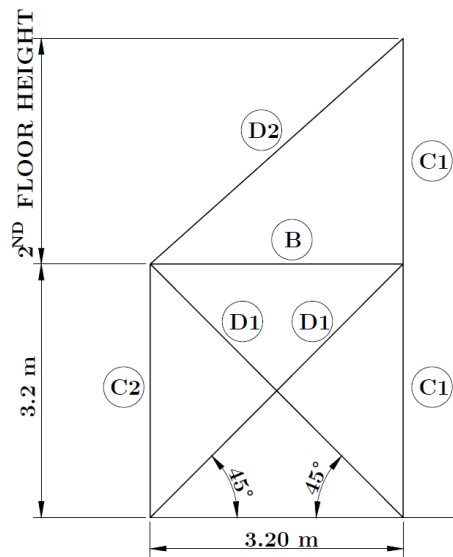


Figure 5.4: Exoskeleton's Topology and Member Designation

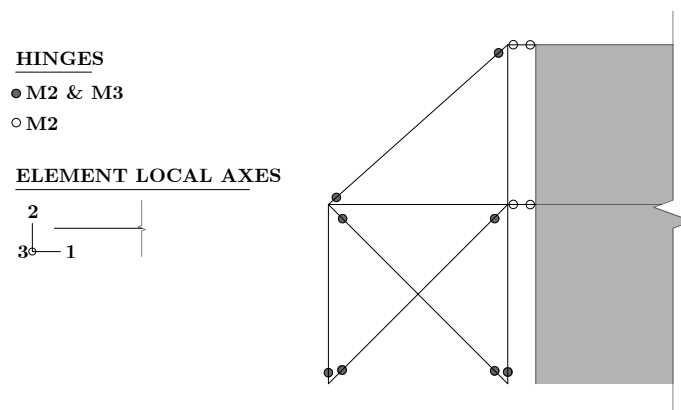


Figure 5.5: Hinges properties in the modelling of the Steel Exoskeleton

5.2.1 Optimization Results

Once all the optimization analyses have been performed, the optimal exoskeleton solution is found. The main parameters describing this solution are presented in Table 5.4. In the last Table, ID Ratio represents the inter-storey drift ratio obtained as the ratio between the maximum value and the allowable value of 5.33 mm ($H/600$). On the other hand, D/C Ratio corresponds to the maximum demand capacity ratio related to the safety checks obtained as output from the structural software.

| Parameter | Value |
|------------------------|---------------------------------------------------|
| Chromosome | [1 0 0 0 0 0 0 1 1 0 1 0 11 11 4 3 6] |
| Number of Exoskeletons | 4 |
| Seismic mass | 5.86 <i>ton</i> |
| Top displacement | 10 <i>mm</i> |
| Maximum ID Ratio | 0.9651 |
| Average ID Ratio | 0.9009 |
| Maximum D/C Ratio | 0.9558 |
| Average D/C Ratio | 0.5815 |

Table 5.4: Summary of Optimization Results

From Table 5.4, it is possible to understand how the solution found by the algorithm is mainly focused on controlling the displacements since the maximum ID Ratio is almost near 1 (limit value) and the average of all the assessed values are even very proximate to the maximum value. About the D/C, the most stressed element is operating at near capacity, which demonstrates how it is possible to optimise the material in some elements. Nevertheless, the average D/C values are considerably below the maximum value, indicating that the majority of elements operate at approximately 60% of their capacity. This is a reasonable outcome, given that an over-dimensioning of the elements is necessary to provide sufficient lateral stiffness to control the displacements.

As it can be seen in Figure 5.6, the algorithm carried out an adequate evolution during the 100 iterations in which the optimal chosen solution was found. The objective function decreases regularly and rapidly until iteration 32, after which the algorithm manages to refine the solution even more by finding one with even less

weight. The algorithm reaches the stagnation of the solution at iteration 51, which could be interpreted as an expected situation due to the simplicity of the case study and the large population proposed.

Furthermore, in the graphs below it is possible to see how, when the algorithm finds solutions with a lower weight, this automatically compromises the stresses on the elements. When the solutions are close to the optimum, there is a small trade-off between displacements and stresses.

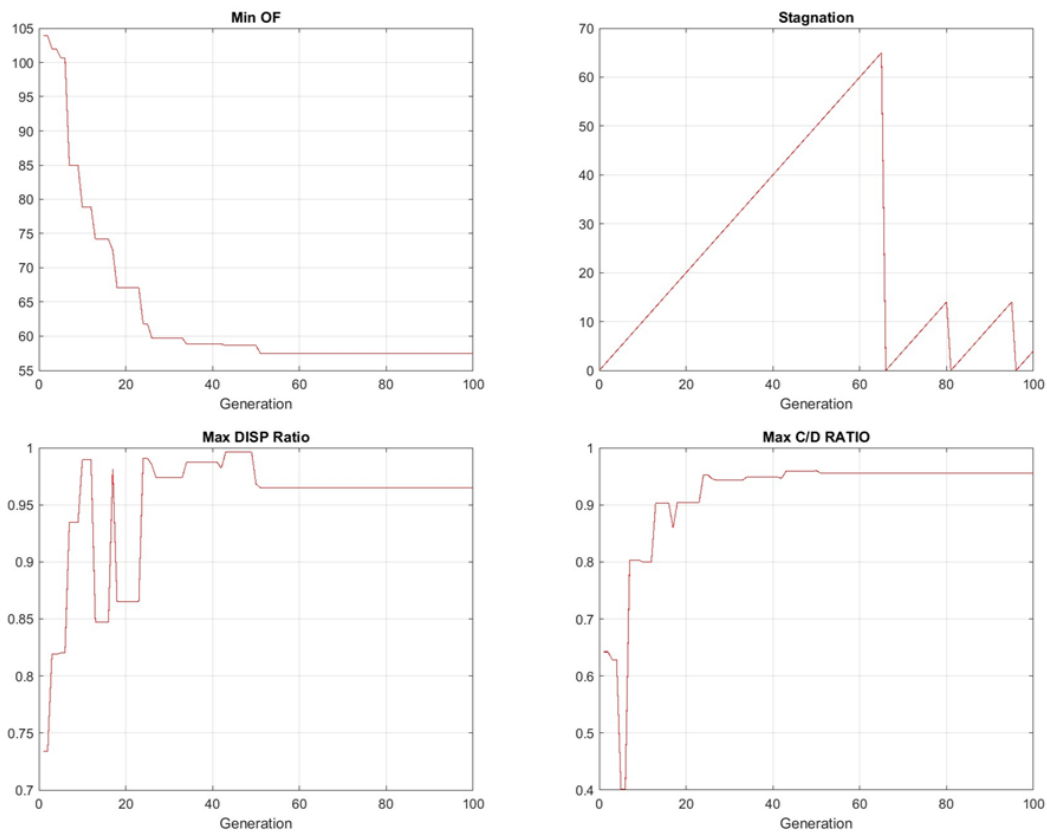


Figure 5.6: (1) Evolution of the Objective Function (2) Stagnation of the solution (3) Inter-Storey Drift Ratio (4) Demand-Capacity Ratio of the Exoskeletons

5.2.2 Structural Interpretation of Results

Exoskeleton's Design

The resulting solution presents the exoskeletons placed according to the scheme of Figure 5.8 and the steel circular hollow cross-sections of the typical exoskeletons are the ones shown in Table 5.5.

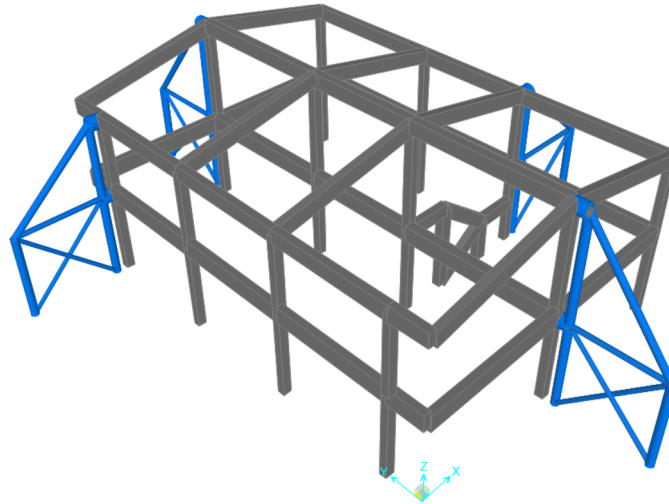


Figure 5.7: Axonometric View of the Steel Exoskeleton Intervention

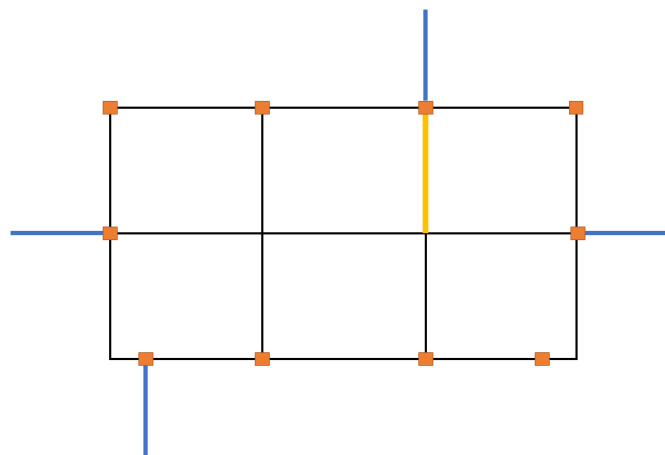


Figure 5.8: Schematic Top View of the Steel Exoskeleton's Positioning

| Element | \emptyset [mm] | t_f [mm] |
|----------------|---------------------------------------|---------------------------------|
| C1 | 273.0 | 14.2 |
| C2 | 273.0 | 14.2 |
| B | 168.0 | 8.0 |
| D1 | 140.0 | 8.0 |
| D2 | 219.0 | 10.0 |

Table 5.5: Steel Exoskeleton's Cross-sections

The positioning of the exoskeletons was found to be reasonable. Concerning the exoskeletons positioned in the most rigid direction, namely the longitudinal one, it was anticipated that they would be situated within the central columns. This configuration would prevent the centre of stiffness from translating in the transverse direction, which would otherwise result in undesired torsional actions. The placement of the exoskeletons in this configuration maintains the symmetry for the central longitudinal axis.

The configuration of the exoskeletons aligned with the transverse direction permits a shift in the centre of stiffness to a position that is more proximate to the centre of mass. The presence of the stairs initially disrupts the symmetry of the frames, resulting in a torsional behaviour. The proposed positioning of the exoskeletons aims to mitigate this effect.

Structural Effects of the Intervention: Base Shear

Given that the selected typology of intervention corresponds to a high-strength exoskeleton designed to control inter-storey drifts, it can be reasonably assumed that an important unloading ratio of the existing structure will be achieved after its application. The load carried by the not retrofitted existing structure and by the system structure plus exoskeleton is evaluated through the inspection of the base shear carried by them, considering the seismic combinations employed. Figure 5.9 illustrates the base shear experienced by these systems, while Table 5.6 presents the structure unloading ratio and the percentage of load carried by the existing structure per the two main directions of the building. The unloading ratio is defined by the

Equation 5.1.

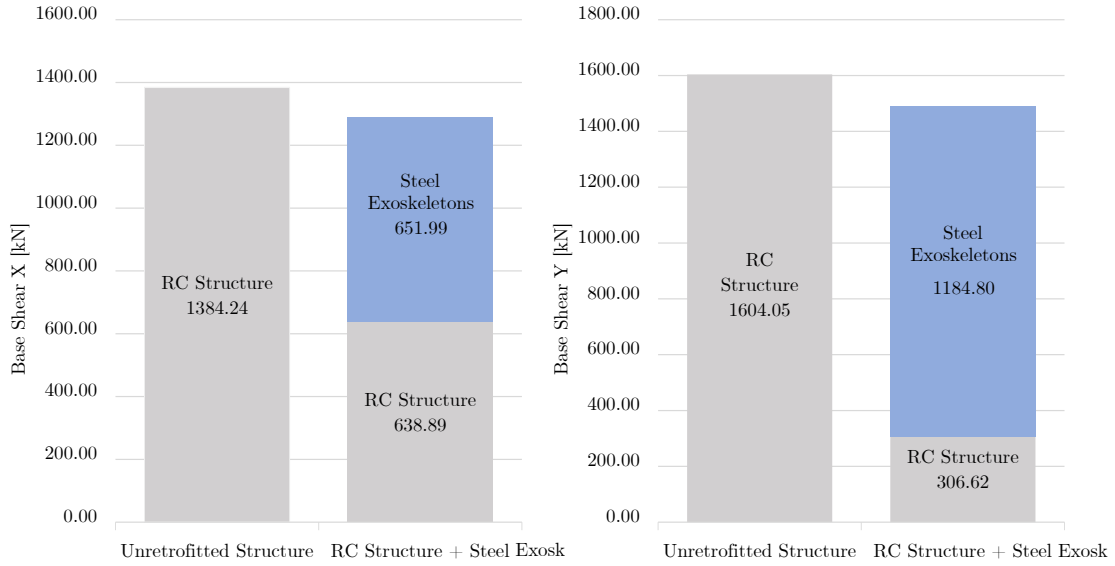


Figure 5.9: Base shear of the systems

| Base Shear | Unloading Ratio [%] | Carrying Load [%] |
|------------|------------------------|----------------------|
| $V_{r,x}$ | -53.85 | 49.49 |
| $V_{r,y}$ | -80.88 | 20.56 |

Table 5.6: Existing Structure Unloading Ratio & Carrying Load

$$UnloadingRatio = \frac{V_r - V_0}{V_0} \cdot 100[\%] \quad (5.1)$$

where:

- V_0 = base shear taken by existing structure before intervention [kN];
- V_r = base shear taken by existing structure after exoskeleton intervention [kN];

As illustrated in Figure 5.9 and Table 5.6, the primary unloading of the structure is predominantly concentrated in the longitudinal direction. The elements installed in this direction appear to be more rigid with respect to the existing structure stiffness,

allowing for a higher unloading ratio of the structure. This is evidenced by the fact that the existing structure just takes 21% of the base shear in that direction.

Concerning the transverse direction, a minor unloading ratio is observed in the exoskeleton intervention, which is consistent with expectations given the slight reduction in size of the exoskeletons in that direction. In this case, the structure takes approximately 50% of the base shear.

Given that the concept of stiffness is directly related to the loads carried by structures, it is worthwhile to recall the approach followed by many engineers for the design of exoskeletons, as introduced in Section 2.1.3, in which the existing structure as a secondary structure. Following guidelines presented by [4], secondary elements must be capable of withstanding less than 15% of the horizontal actions. This frequently employed approach significantly constrains the capacity of the existing structure to accommodate a greater proportion of the seismic action. However, as evidenced by the preceding results in both directions, the existing structure is capable of bearing more than 15% of the load, while the viability and safety of the proposed retrofitting intervention is still ensured.

Structural Effects of the Intervention: Modal Analysis

To provide a complete understanding of the seismic response of the building, it is necessary to evaluate the modal parameters. In the employed structural software, a modal analysis is performed. The software orders the modes in such a way that those with higher periods are placed at the top of the list. Table 5.7, presents the software output in terms of modal period and modal modal participating mass ratio for the two translational x and y, and the rotational degree of freedom.

It can be stated that the fundamental modes, which contribute the most to the base shear and total response of the building, are those with an important associated modal mass. Consequently, international regulations require that the number of considered modes for the evaluation of the structure response through a linear dynamic analysis should be such that the total participating modal mass for each direction must be over 80%–85%.

Regarding the non-retrofitted structure, it is possible to identify a mode of almost pure translational nature (mode 1) in the most rigid direction, longitudinal. Mode 2 is primarily a torsional mode, though it also exhibits a notable influence from the translational components. Mode 3 plays an important role in the transverse translation, yet it is also subject to significant torsional coupling. Mode 6 is another important translational mode that must be considered to account for more than 80% of the participating mass in the transverse direction. It can be observed that the majority of the modes present coupled translational and torsional components, and uncoupled modes are not identified.

The installation of exoskeletons results in a notable enhancement of the seismic response, as evidenced by the observed changes in modal parameters. Two pure translational and rotational modes can be identified, which are designated as modes 1 and 2, respectively. Mode 3 is an uncoupled translational mode that is sufficient for accounting for the total participating modal mass in the x direction. However, to comply with the regulatory requirements, mode 8 is also highlighted as a significant mode, as it contributes to reaching the threshold of 80% modal mass in the x direction. The introduction of exoskeletons has resulted in a notable shift in the centre of stiffness, positioning it close to the centre of mass of the structure on each floor. This has led to the appearance of uncoupled modes in all directions.

The presence of uncoupled modes is always desired since they simplify the analysis of the structure, providing a more predictable, reliable, and precise understanding of its response to an earthquake. Conversely, coupled modes introduce additional forces and moments that are difficult to predict or control. These added actions can result in unwanted effects, such as force concentrations and excessive deformations in localized areas.

| Unretrofitted Structure | | | | | | | |
|--------------------------------|---------------|-----------------------|-----------------------|-----------------------|------------------------------|------------------------------|------------------------------|
| MODE | Period [s] | U _x [%] | U _y [%] | R _z [%] | \sum U _x [%] | \sum U _y [%] | \sum R _z [%] |
| 1 | 0.44 | 0.03 | 0.76 | 0.15 | 0.03 | 0.76 | 0.15 |
| 2 | 0.43 | 0.13 | 0.16 | 0.62 | 0.16 | 0.93 | 0.77 |
| 3 | 0.30 | 0.42 | 0.00 | 0.14 | 0.58 | 0.93 | 0.91 |
| 6 | 0.11 | 0.39 | 0.00 | 0.04 | 0.97 | 0.93 | 0.95 |
| Retrofitted System | | | | | | | |
| MODE | Period [s] | U _x [%] | U _y [%] | R _z [%] | \sum U _x [%] | \sum U _y [%] | \sum R _z [%] |
| 1 | 0.23 | 0.01 | 0.00 | 0.88 | 0.01 | 0.00 | 0.88 |
| 2 | 0.21 | 0.00 | 0.87 | 0.00 | 0.01 | 0.87 | 0.88 |
| 3 | 0.17 | 0.72 | 0.00 | 0.04 | 0.73 | 0.87 | 0.92 |
| 8 | 0.10 | 0.08 | 0.00 | 0.07 | 0.81 | 0.87 | 0.99 |

Table 5.7: Fundamental Vibration Modes

Structural Effects of the Intervention: Demand Capacity Ratios

About the seismic vulnerability of the structure, it is recalled what was previously evaluated in Section 4.3. The demand capacity ratios (DCR) of the elements demonstrate a high level of risk for the existing structure subjected to the seismic combination of loads, as presented in Table 4.12. Figure 5.10 presents the significant improvement in the most vulnerable DCRs of each element of the RC structure. Table 5.8 displays the maximum and average values of DCR for the seismic combinations considered.

Nevertheless, some minor elements appear to be over-stressed, particularly those present in the staircase. The stair's main beams were modelled to account for the stiffness they provide to the global response; however, the safety checks of their elements are not considered in this analysis, given the significant uncertainty regarding their reinforcement configuration.

Furthermore, the staircase configuration is not suitable for the seismic design of a structure. Therefore, it would be preferable to demolish and reconstruct it with an appropriate design. However, this intervention should be conducted independently

from the proposed interventions in this thesis, as it is beyond the scope of the comparison of the three proposed scenarios. Consequently, the safety checks of the elements pertinent to the structure are neglected in this analysis.

Regarding to the rest of the elements, a concentration of forces is identified in the columns attached to the exoskeletons. That is why one of the columns presents shear over-stress and there is even one single beam which is over-stressed.

The compromised column is the one present on the ground floor, which connects the stairs with one external exoskeleton. As might be expected, these two rigid planes attract high shear forces, which are in great part taken by the reinforced concrete column. As previously mentioned, the stairs should be demolished and reconstructed to have a proper seismic design which helps to solve these sorts of problems.

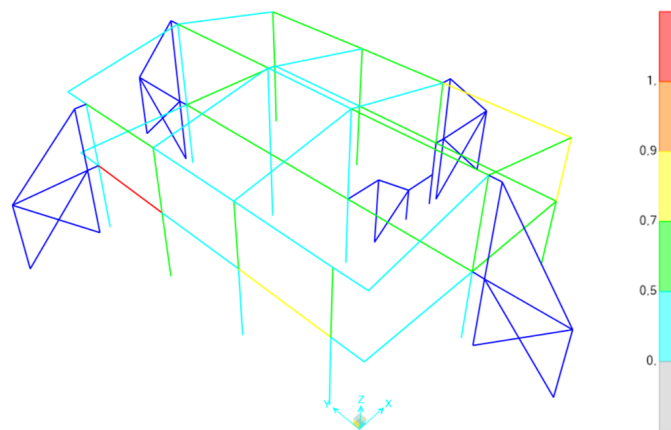


Figure 5.10: DCR of RC Elements Post-intervention

| Elements | DCR_{AVG} | DCR_{MAX} |
|-------------------------------|-------------|-------------|
| GF Columns | 0.47 | 0.54 |
| 1 ST Floor Columns | 0.44 | 0.87 |
| GF Beams | 0.31 | 1.13 |
| Roof Columns | 0.28 | 0.71 |

Table 5.8: Average and Maximum DCR Post-intervention

| | | % Non-verif. elements | Max DCR col | Max DCR beam |
|---------------------------|------------------------------|--------------------------|----------------|-----------------|
| Steel Exoskeletons | Before retrofitting | 82.76 | 2.98 | 2.89 |
| | Orthogonal exosk.: S1 | 3.45 | 0.87 | 1.13 |

Table 5.9: Results of the structural verifications of the existing buildings, in terms of percentage of non-verified elements and Demand-Capacity ratios of the most critical column and beam, before and after the retrofit, for each Scenario (S#)

Proposed Foundation System

In order to obtain a complete preliminary solution for this intervention regarding to its environmental and economic cost, it is necessary to design a new foundation system for the exoskeleton's structures. Due to the lack of information about the soil's mechanical properties, some assumptions are made. Nevertheless, the data employed and calculations performed are subject to adjustment in future executive designs.

Concerning the exoskeleton connection type with the existing structure and, after the evaluation of the effects resulting from the load combinations employed, the most compromising situation is identified. The exoskeleton foundation should be capable of bearing a tensile load of **907.94 kN** for the internal column, while simultaneously a compression load of **889.46 kN** for the external column.

It is proposed that a foundation system comprising four micro-piles with an inter-axis of 1m, joined by a top pile cap (not calculated) per exoskeleton column, be constructed. The micro-piles are aligned vertically through rotary drilling or rotary percussion and filled by the low-pressure injection of a cement mortar mixture with a dosage of 600 *kg* of cement per cubic meter of mix. The proposed piles have an external diameter of 200 *mm* and a total length of 11 *m*. The main characteristics of the elementary pile are outlined in Table 5.10.

A preliminary calculation is conducted from a safety standpoint, wherein the bearing capacity for lateral shaft friction is considered while the bearing capacity at the tip is neglected. The soil in question is classified as type C according to [4], which corresponds to moderately dense sand. A variable NSPT value for the soil

| Parameter | Value |
|--------------------|--------------------------|
| Diameter | 200 [mm] |
| Injection factor | 1.15 |
| Circumference | 722 [mm] |
| Length | 11000 [mm] |
| Cross-section area | 31400 [mm ²] |
| Pile stress | 8 [MPa] |

Table 5.10: Main Micropile's Characteristics

is hypothesised, ranging from 7 (at -1 m from the ground level) to 18 (at -12 m from the ground level), which are considered to be reasonable values for the type of soil evaluated. The shaft capacity is calculated according to the "Bustamante and Doix" method [44]. The calculation is summarized in Table 5.11, which shows that the single micropile has a capacity of 258 kN. Therefore, the proposed system of four micropiles per exoskeleton column is capable of bearing the acting loads.

| Reference Positions | Level [m] | Vertical Pressure [kN/m ²] | NSPT [-] | Bustamante [MPa] | Shaft Capacity [kN] |
|------------------------|--------------|-------------------------------------------|-------------|---------------------|------------------------|
| Ground level | 0 | 0 | - | - | - |
| Pile cap | -1 | 19 | 7 | 0.04 | - |
| | -2 | 38 | 8 | 0.04 | 29 |
| | -3 | 57 | 9 | 0.05 | 32 |
| | -4 | 76 | 10 | 0.05 | 36 |
| | -5 | 95 | 11 | 0.06 | 40 |
| | -6 | 114 | 12 | 0.06 | 43 |
| | -7 | 133 | 13 | 0.07 | 47 |
| | -8 | 152 | 14 | 0.07 | 51 |
| | -9 | 171 | 15 | 0.08 | 54 |
| | -10 | 190 | 16 | 0.08 | 58 |
| Pile tip | -11 | 209 | 17 | 0.09 | 61 |
| | -12 | 228 | 18 | 0.09 | 65 |
| | | | | Total | 258 |

Table 5.11: Single Micropile Shaft Capacity according to Bustamante's approach

5.3 Scenario 3: Timber Exoskeletons

The last proposed intervention is an alternative to the second scenario, in other words, this section evaluates the feasibility of implementing timber exoskeletons, which are designed with the same displacement-based philosophy through the employment of the optimization algorithm.

It is of interest to evaluate the performance of this alternative, given that it involves the use of a more sustainable material, which has different properties in comparison with a high-performance material such as structural steel. This approach allows to prove the potentiality of timber to effectively reproduce the same, or unless similar, structural performance when employed in exoskeleton structures. Moreover, this approach is fully aligned with the sustainability sought in any civil engineering project, as the use of this material actively contributes to the decarbonisation of the building sector.

As is well-known, the low stiffness of the material constitutes one of the main limitations when trying to apply it. Nevertheless, the employment of solid cross-sections with timber elements and the demonstrated high strength-to-weight ratio of the material indicates that the overall performance of timber exoskeletons in controlling lateral displacements is expected to be comparable with that of steel exoskeletons. Furthermore, the timber elements which constitute the exoskeletons are not slender in nature. Consequently, the buckling problems which give rise to the sudden failure of the hollow steel members proposed in the previous scenario do not occur with the timber elements.

Once more, the algorithm presented in Section 3.2 is employed, and the same displacement-based methodology is followed. However, an additional effort was required when adapting the optimization framework to this alternative. The structural software employed, SAP2000, does not integrate in its domain the structural safety checks for timber elements. Consequently, it was necessary to create an independent MATLAB code, which, through the OAPI tools provided by CSI, takes the forces acting on the exoskeleton's elements and performs the structural verifications on each of them. This allows for the evaluation of the associated structural penalty of each assessed individual within the optimization framework. sessed individual.

Concerning the configuration of the algorithm, the same parameters presented in Table 5.3 for the steel exoskeleton case are fixed.

Furthermore, the timber exoskeleton has the same topology as the one already presented for the steel ones. However, since the connections between the members of both systems are different, in Figure 5.11 it is presented the modelled hinges for the timber exoskeletons which ensure the truss behavior of the structure.

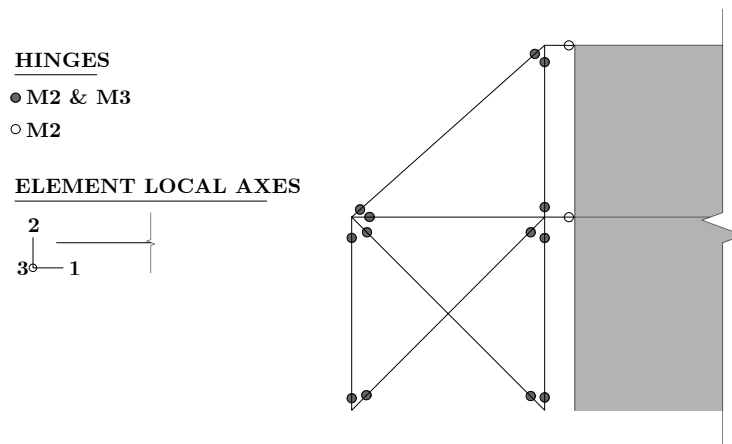


Figure 5.11: Hinges properties in the modelling of the Timber Exoskeleton

5.3.1 Timber Material

The timber material employed for the exoskeleton's elements corresponds to glued laminated timber (glulam), which constitutes one of the oldest and most widely used engineered modified wood products. Glulam elements consist of successive disposed laminations (at least four) bonded together with high-performance adhesives. The employed boards are all oriented with their main fibre direction aligned with the axial direction of the glulam element.

In this instance, 40 mm tall laminations were selected. The aforementioned laminations were employed to generate a varied catalogue of rectangular cross-sections, which included even options comprising half of the laminations. Accordingly, two catalogues were created and introduced as input into the optimisation algorithm,

one for the horizontal beam elements and the other for the resting ones. Each catalogue contains 30 options ranging from 440 cm^2 to 3600 cm^2 , whereby each discrete design variable is permitted to assume one of the independent cross-sections present on the lists.

The selected resistance class corresponds to a **GL28h**, which indicates the use of homogeneous laminations with a bending parallel to grain strength of 28 MPa . The strength and stiffness properties, as well as the density of the employed material, are presented in Table 5.12.

| Property | Value |
|-------------|----------------------|
| $f_{m,k}$ | 28 MPa |
| $f_{t,0,k}$ | 22.3 MPa |
| $f_{c,0,k}$ | 28 MPa |
| f_{vk} | 3.5 MPa |
| $E_{0,05}$ | 10500 MPa |
| $E_{90,05}$ | 250 MPa |
| G_{05} | 540 MPa |
| $r_{o,k}$ | 425 kg/m^3 |

Table 5.12: Optimization Algorithm Parameters

Furthermore, to evaluate the safety checks, it is necessary to define the corresponding service class and load duration classes of the case under analysis.

Timber experiences a significant loss of strength when a load is applied over an extended period of time. To account for this aspect, load duration classes have been defined in international regulations, providing a simple design procedure. The influence of the duration of a load on the strength capacity of the timber element is considered through the employment of a factor k_{mod} , which is also a function of a considered service class. In essence, this coefficient represents a reduction factor for the characteristic strength of the timber material. Moreover, k_{mod} considers the effect of moisture content in timber and its temporal variation, which plays a crucial role in the strength and stiffness properties of the elements. To integrate these effects into the design process, EN 1995 defines three service classes based on the anticipated level of moisture during the lifetime of the timber element.

Accordingly, in this case study, the employment of glulam for the exoskeleton's elements is supposed to be placed outside the building. Following the guidelines of EUROCODE 5, the service class for this situation corresponds to a **class 3**. The aforementioned condition pertains to environments in which the structural elements are directly exposed to wetting or immersion, and in which the average equilibrium moisture content of the wood is generally greater than 20% or such humidity is exceeded for long periods.

Furthermore, about the seismic combinations employed, the most critical type of load is the earthquake's action, which, according to Section 2.3.1.2 of the aforementioned normative, corresponds to an instantaneous load-duration class. Consequently, for the considered service class and load duration class, the corresponding k_{mod} factor is equal to **0.9**.

In addition to considering the factor k_{mod} , the partial factor γ_m must be considered in safety checks. This factor is employed to account for uncertainty in the resistance model used for design, as well as the unfavourable effects of geometrical deviations of materials. Accordingly, characteristic strength values are divided by γ_m to obtain the design strength of the material.

In this instance, Table 2.3 of EUROCODE 5 indicates that a partial factor γ_m of **1.0** can be employed for safety checks. This decision is made on the basis that the exoskeletons are designed to withstand seismic load combinations, which can be considered as accidental combinations from a conservative perspective.

Finally, the design strength parameters employed in safety checks for the calculation of the individual's corresponding structural penalty, are obtained as indicated by Equation 5.2

$$f_d = \frac{f_k \cdot k_{mod}}{\gamma_m} \quad (5.2)$$

After all these considerations, the optimization analyses are performed according to the settings already presented in Table 5.3.

5.3.2 Optimization Results

In the same as it was done for steel exoskeletons after all the optimization analyses have been concluded, the best of the optimal solutions is chosen. Table 5.13 presents the main parameters which describe the adopted solution.

| Parameter | Value |
|------------------------|----------------------------------------------------|
| Chromosome | [0 0 0 1 0 1 0 0 1 0 1 0 15 25 3 4 13] |
| Number of Exoskeletons | 4 |
| Seismic mass | 5.83 <i>ton</i> |
| Top displacement | 10 <i>mm</i> |
| Maximum ID Ratio | 0.9998 |
| Average ID Ratio | 0.9025 |
| Maximum D/C Ratio | 0.5634 |
| Average D/C Ratio | 0.2122 |

Table 5.13: Summary of Optimization Results

Table 5.13, provides further evidence that the algorithm is guided to find solutions that control mainly displacements. This is evident from the fact that the maximum ID Ratio and their average value are close to 1. The D/C of the most stressed element is reported, which indicates that in this case, it is operating at half of its capacity. The average D/C values are even lower, suggesting that the majority of elements operate at approximately 20% of their capacity. It can be seen that timber elements, due to their lower intrinsic stiffness compared to steel elements, require an even higher degree of oversizing to provide an efficient solution for controlling lateral displacements and respecting the inter-storey drift threshold proposed.

Figure 5.12 illustrates the evolution of the algorithm over the 100 iterations performed in the run in which the optimal configuration was identified. The objective function exhibits a similar pattern of decrease until iteration 30. However, in this case, a much more gradual transition can be observed, which is mainly because the cross-sections proposed for timber elements cover a much wider range of options than the commercial steel cross-section. Consequently, this effect can be identified here since more intermediate feasible solutions can be found, and a gradual transition of the OF is described. From iteration 30 on, the algorithm performs a little

refinement of the final solution, finding another lighter option. The final plateau is reached at iteration 68, at which point no further improvements could be identified.

The graphs at the bottom illustrate the trade-off between displacements and stresses. The identification of a solution with a lower maximum displacement ratio implies an increase in the stresses of its elements. In contrast to the steel case, the evolution of the maximum D/C ratio for truss elements (those subjected to only axial load) and beam elements (those subjected to axial load and bending moments) is plotted in the last graph.

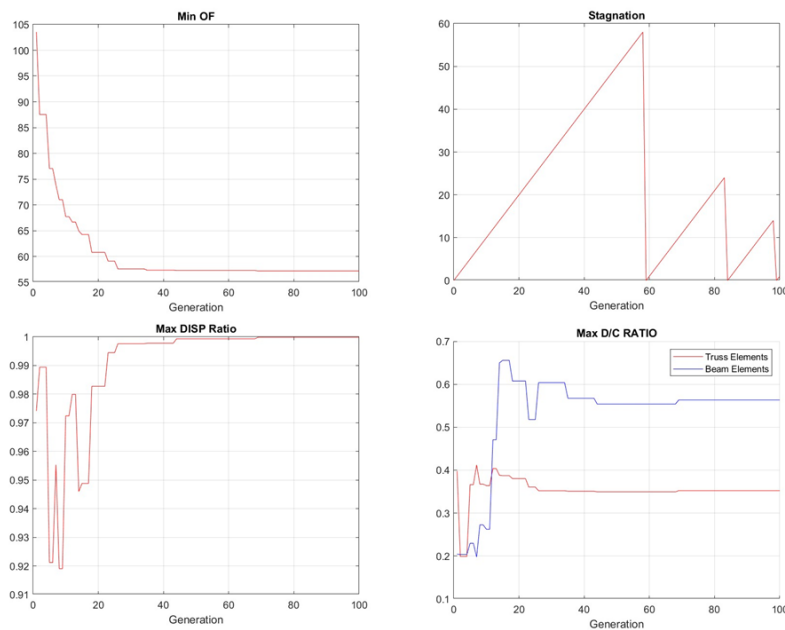


Figure 5.12: (1) Evolution of the Objective Function (2) Stagnation of the solution (3) Inter-Storey Drift Ratio (4) Maximum Demand-Capacity Ratio of the Exoskeletons

5.3.3 Structural Interpretation of Results

Exoskeleton's Design

The resulting solution presents the exoskeletons placed according to the scheme of Figure 5.14. The rectangular timber cross-sections of the typical exoskeleton are the ones shown in Table 5.14.

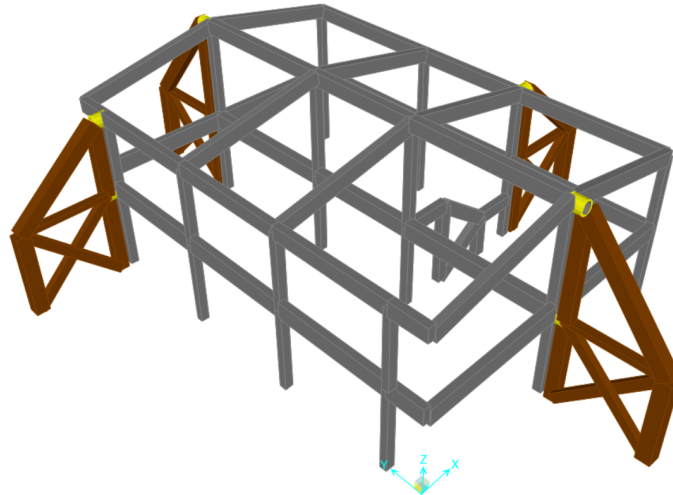


Figure 5.13: Axonometric View of the Timber Exoskeleton Intervention

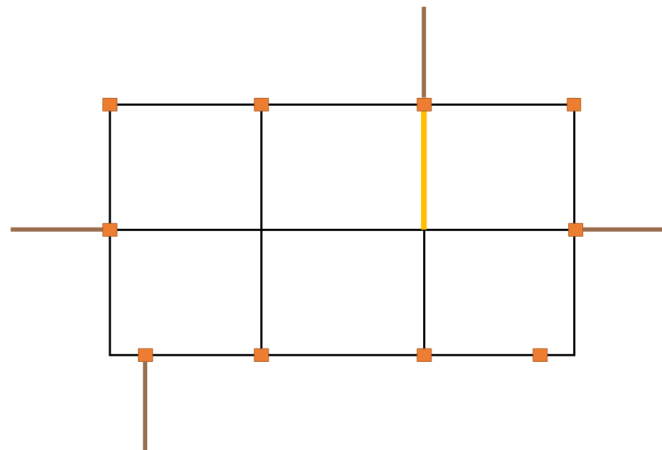


Figure 5.14: Schematic Top View of the Timber Exoskeleton's Positioning

| Element | b | h |
|----------------|-------------|-------------|
| | <i>[mm]</i> | <i>[mm]</i> |
| C1 | 0.35 | 0.42 |
| C2 | 0.45 | 0.48 |
| B | 0.30 | 0.20 |
| D1 | 0.22 | 0.34 |
| D2 | 0.40 | 0.48 |

Table 5.14: Timber Exoskeleton's Cross-sections

The optimal positioning of the timber exoskeletons was found to be identical to that obtained with steel members. This demonstrates that the use of a different material does not affect the optimal placement of these structures in the assessed case study. Furthermore, the fact that the same positioning was obtained after several runs of the algorithm with two different materials indicates that this is a robust solution which constitutes, in terms of exoskeleton's positioning, the global optimal solution of the problem.

The robustness of this configuration is primarily attributable to the capacity to shift the centre of stiffness to a position that is more proximate to the centre of mass. This enables the structural behaviour of the structure subjected to seismic loads to become more regular, while also allowing for the efficient control of lateral displacement.

Structural Effects of the Intervention: Base Shear

The load carried by the non-retrofitted existing structure and by the system structure and timber, exoskeleton is evaluated through the inspection of the base shear carried by them, considering the seismic combinations employed. Figure 5.15 illustrates the base shear experienced by these systems, whereas Table 5.15 presents the structure unloading ratio and the percentage of load carried by the existing structure per the two main directions of the building. To facilitate a comparison between the two different exoskeleton interventions, the steel results are also presented.

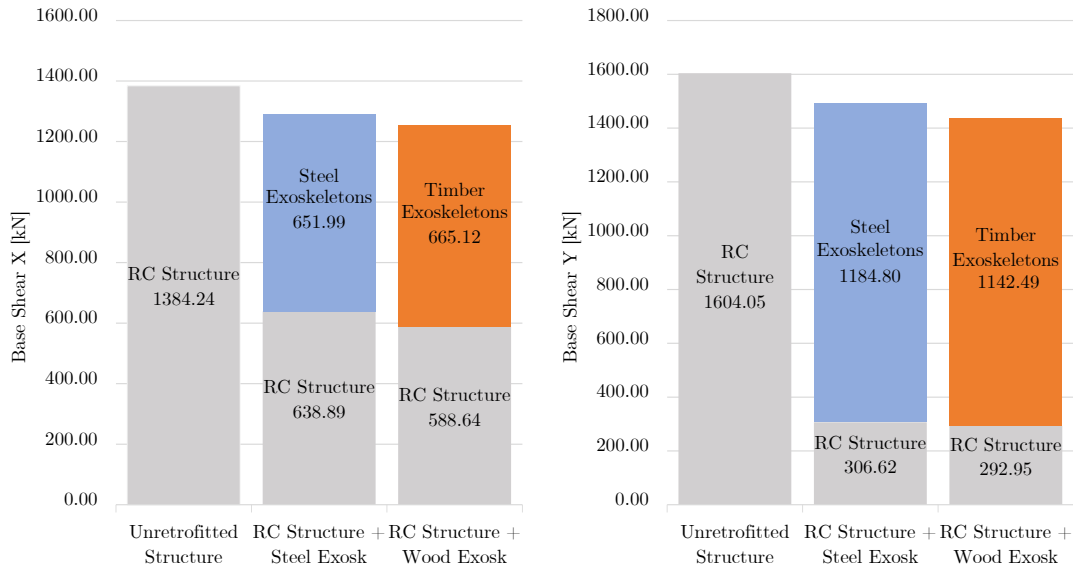


Figure 5.15: Base shear of the Systems

| Base Shear | Unloading Ratio [%] | Carrying Load [%] |
|---------------------|---------------------|-------------------|
| $V_{r,x}$ steel ex | -53.85 | 49.49 |
| $V_{r,y}$ steel ex | -80.88 | 20.56 |
| $V_{r,x}$ timber ex | -57.48 | 46.95 |
| $V_{r,y}$ timber ex | -81.74 | 20.41 |

Table 5.15: Existing Structure Unloading Ratio & Carrying Load

Figure 5.15 and Table 5.15, demonstrate that the improvement of the structural performance in terms of unloading of the existing structure is practically equal for both interventions with steel and timber exoskeletons. This can be attributed to the fact that the same placement of exoskeletons is proposed. Notably, the same degree of improvement is achieved with two solutions in timber and steel materials, despite the lower timber stiffness compared to steel. This implies that the timber exoskeleton intervention requires the same weight of material to ensure an identical structural response, despite its poorer mechanical properties. In this way, it demonstrates the high strength-to-weight ratio that timber material presents.

Regarding the efficiency of unloading the structure in both directions, the same

conclusions drawn for the steel solution also apply to the timber exoskeleton intervention, given that both the unloading ratio and the existing structure's carrying load are practically identical.

It is once again possible to demonstrate how a feasible exoskeleton intervention can be proposed, where the existing structure bears more than 15% of the seismic load.

Structural Effects of the Intervention: Modal Analysis

Table 5.16 presents the software output in terms of modal period and modal mass ratio for the two translational degrees of freedom (x and y), as well as the rotational degree of freedom. The main contributor modes, fundamental modes, are reported since the total dynamic response of the structure is highly dependent on them.

The interpretation of the modal analysis of the not retrofitted structure is identical to that performed for Section 5.2, as it refers to the same structure.

In this case, the installation of exoskeletons improves the seismic response of the building slightly in comparison to the steel solution. Two pure rotational and translational modes, which account for approximately 80% of the participating modal mass, can be identified: these are designated as modes 1 and 2, respectively. Mode 3 is primarily a translational mode in the x direction, accounting for the majority of the required participating mass in that direction and exhibiting a minor contribution also in the torsional component. However, this is not sufficient for accurately representing the dynamic response of the structure, as it is necessary to include at least 80% of the participating modal mass in each degree of freedom. In this context, modes 9 and 10, which are both translational in nature, must be included. The first mode is related to the y direction, while the second to the x direction. Furthermore, it is important to note that the building dynamic response also includes contributions from local modes that are pertinent to the exoskeletons. However, these contributions are relatively minor and can be considered negligible. The introduction of the timber exoskeletons has resulted in a shift in the centre of stiffness, which is now positioned close to the centre of mass of the structure on each floor. This has led to the appearance of practically uncoupled fundamental modes.

| Unretrofitted Structure | | | | | | | |
|--------------------------------|---------------|-----------------------|-----------------------|-----------------------|------------------------------|------------------------------|------------------------------|
| MODE | Period [s] | U _x [%] | U _y [%] | R _z [%] | \sum U _x [%] | \sum U _y [%] | \sum R _z [%] |
| 1 | 0.44 | 0.03 | 0.76 | 0.15 | 0.03 | 0.76 | 0.15 |
| 2 | 0.43 | 0.13 | 0.16 | 0.62 | 0.16 | 0.93 | 0.77 |
| 3 | 0.30 | 0.42 | 0.00 | 0.14 | 0.58 | 0.93 | 0.91 |
| 6 | 0.11 | 0.39 | 0.00 | 0.04 | 0.97 | 0.93 | 0.95 |
| Retrofitted System | | | | | | | |
| MODE | Period [s] | U _x [%] | U _y [%] | R _z [%] | \sum U _x [%] | \sum U _y [%] | \sum R _z [%] |
| 1 | 0.24 | 0.01 | 0.00 | 0.82 | 0.01 | 0.00 | 0.82 |
| 2 | 0.22 | 0.00 | 0.78 | 0.00 | 0.01 | 0.78 | 0.82 |
| 7 | 0.17 | 0.67 | 0.00 | 0.06 | 0.69 | 0.78 | 0.88 |
| 9 | 0.10 | 0.00 | 0.14 | 0.00 | 0.69 | 0.92 | 0.88 |
| 10 | 0.08 | 0.19 | 0.00 | 0.00 | 0.88 | 0.92 | 0.88 |

Table 5.16: Fundamental Vibration Modes

Structural Effects of the Intervention: Demand Capacity Ratios

Figure 5.16 presents the notable improvement in the most compromised DCR of each element of the RC structure. Table 5.17 presents the maximum and average values of DCR for each group of elements of the existing structure considered under seismic loads.

As it is appreciated in the aforementioned results, most of the elements pass the structural safety checks. Again, some of the elements present in the stairs do not pass these safety checks, however, as indicated in Section 5.2, these last are neglected.

Regarding the rest of the elements, a concentration of forces is identified in the columns attached to the exoskeletons. In particular, the column in which the stairs and one exoskeleton meet again presents a shear over-stress. However, as explained in Section 5.2, this condition can be improved with the reconstruction of the staircase.

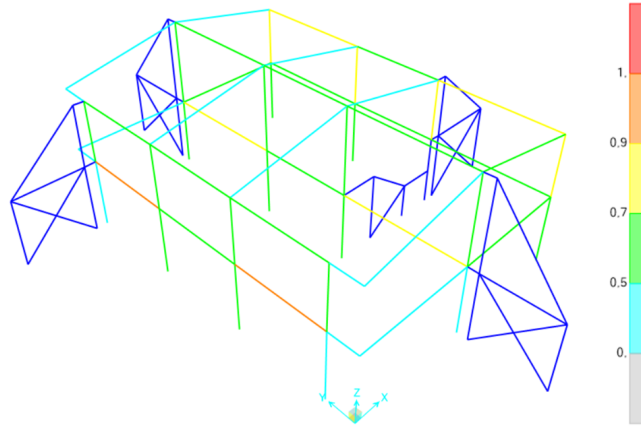


Figure 5.16: DCR of RC Elements Post-intervention

| Elements | DCR_{AVG} | DCR_{MAX} |
|-------------------------------|-------------|-------------|
| GF Columns | 0.50 | 0.59 |
| 1 ST Floor Columns | 0.56 | 0.87 |
| GF Beams | 0.33 | 0.93 |
| Roof Columns | 0.30 | 0.73 |

Table 5.17: Average and Maximum DCR Post-intervention

| | | % Non-verif. elements | Max DCR col | Max DCR beam |
|----------------------------|------------------------------|--------------------------|----------------|-----------------|
| Timber Exoskeletons | Before retrofitting | 82.76 | 2.98 | 2.89 |
| | Orthogonal exosk.: S2 | 0.00 | 0.87 | 0.93 |

Table 5.18: Results of the structural verifications of the existing buildings, in terms of percentage of non-verified elements and Demand-Capacity ratios of the most critical column and beam, before and after the retrofit, for each Scenario (S#)

Proposed Foundation System

In the same way, as done for steel exoskeletons, it is proposed a new foundation system for the timber exoskeleton solution.

Considering the exoskeleton connection type with the existing structure and, after the evaluation of the effects resulting from the design load combinations employed,

the most compromising situation is identified. The exoskeleton foundation should be capable of bearing a tensile load of **886.29** kN for the internal column, while simultaneously a compression load of **-877.11** kN for the external column.

In the most critical scenario, in which both timber and steel solutions are considered, the vertical forces acting on the columns of the exoskeletons are found to be similar. Consequently, the same foundation system, comprising a system of four micro-piles with a diameter of $\text{Ø}200$ mm and a length of 11 m per exoskeleton's column, is also proposed for the timber intervention.

Consequently, the foundation will not be an incident factor in the decision-making process for the selection of one or another exoskeleton solution. However, it should be considered in both cases to compare these solutions with the CFRP intervention and to identify the incidence of foundations on the economic and environmental cost of the exoskeleton solutions.

5.4 Economic and Environmental Comparison of the Scenarios

This section presents an economic and environmental comparison of the evaluated alternatives for the seismic upgrading of the existing building.

The aim of these comparisons is to assess the economic feasibility of each alternative and their environmental performance. This allows to identify the option with higher environmental and economic quality, which will be ultimately the most sustainable retrofit intervention.

It is important to note that these comparisons are made at the same design stage for all the alternatives. In other words, a preliminary design of the intervention has been proposed and therefore a preliminary assessment of the economic and environmental costs is also provided in this section.

5.4.1 Environmental Evaluation of the Alternatives

The environmental evaluation of the different solutions is carried out according to the guidelines of a Life Cycle Assessment (LCA) applied to a building structure, as indicated in the European standards EN 15804 and EN 15978. Concerning the general steps to be followed, the LCA framework can be seen in Figure 2.2.

To start the analysis, some definitions need to be made. First of all, it is essential to clearly define the *Goal & Scope* of the analysis. With the first definition, the objective of the study and its intended application are set, while the second definition shows the depth of the analysis in relation to the proposed objective by clearly defining the product system, the functional unit and the system boundaries.

The goal of the analysis is to assess the environmental impact of three different interventions proposed for the seismic retrofitting of the same existing structure. This is evaluated by calculating the Global Warming Potential total (GWP_{tot}) as an environmental indicator.

With regard to the scope of the analysis, the product system must be defined. In this particular case, this refers to the various refurbishment measures proposed for

the seismic upgrading of the existing structures, as well as all the related activities for their installation.

The *functional unit* is selected to permit a feasible comparison between the various alternatives. Thus, a quantity that remains constant before and after the intervention is preferable. The net floor area of the (existing) building (NFA) [m^2] fulfils these requirements. After obtaining the final environmental impacts, the results are divided by the NFA to work with values that can be used for benchmark and comparative analysis.

As outlined in Section 2.3, the boundaries of the system can be defined in terms of the goal and scope of the analysis. In this context, the phases from the production of the employed materials (A1-A3) to the final disposal of them (C1-C4) define the boundary of the analysis. This approach, known as a cradle-to-gate assessment, is chosen with particular considerations. The construction stage (A4-A5) and the use phase (B1-B3 and B5-B7) are excluded from the analysis, as the highest impacts are related to the production phase. B4 is considered to account for the substitution of elements. Furthermore, the lack of information regarding these phases a priori makes it inadvisable to consider them. With regard to the end-of-life stage, the waste processing (C3) or disposal of material (C4) module is considered depending on the alternative. Finally, as a building LCA has been performed, the beyond-life-cycle module (D) should be declared but not considered in the analysis.

All the aforementioned definitions are summarized in Table 5.19.

The GWP_{total} for each material employed in each alternative, is obtained by summing each module's GWP_k as indicated in Equation 5.3.

$$GWP_{total} = GWP_{A1-A3} + GWP_C + GWP_D \quad [kgCO_2 - eq.] \quad (5.3)$$

The subsequent stage in the LCA evaluation is the definition of the Life Cycle Inventory (LCI). This is achieved through a comprehensive study of various environmental impact databases and environmental product declarations (EPDs).

| | |
|----------------------|-----------------------------------------------------------------------------------------------------------------------------------------------------------------------------------------------------------------------------------------------------------------|
| Goal | Perform and environmental impact comparison among three proposed seismic interventions (CFRP, steel exoskeletons, timber exoskeletons) from the production of the materials to their end of life, in order to evaluate which is the less polluting alternative. |
| Scope | The product considered is just each retrofitting intervention proposed for the seismic upgrading of the building and, the related activities for their installation and dismantling. |
| Functional Unit (FU) | Net Floor Area (NFA) [m^2] |
| System Boundary | Cradle-to-gate. Considered modules: (A1-A3) + (C3 or C4). Declared modules: (A1-A3) + (B4) + (C3 or C4) + (D) |
| Impact Categories | Global Warming Potential total ($GW P_{tot}$) |

Table 5.19: LCA Goal & Scope definition

Production stage: A1 - A3

In this phase, the environmental impacts associated with the raw material supply, manufacturing and transport of materials between these phases are considered.

The data employed in this study is obtained from Ökobaudat for the concrete, steel, and glulam materials used in exoskeleton solutions. For the CFRP solution, the EPDs provided by the enterprise Mapei are used to evaluate the impact of the resin [45]. However, since no information is provided regarding the fibres employed by Mapei, data obtained from [46] is used instead.

The aforementioned database provides information on the environmental impacts of each building LCA phase according to a specified reference unit (RU). The results are presented in Table 5.20.

| Materials (A1-A3) | RU | GWP_{A1-A3} [$kgCO_2 - eq./RU$] |
|---------------------------|------------|-------------------------------------|
| CFRP - Fiber [46] | <i>kg</i> | 31.00 |
| CFRP - Resin [42] | <i>kg</i> | 5.20 |
| CFRP - Resin [47] | <i>kg</i> | 5.20 |
| CFRP - Resin [43] | <i>kg</i> | 10.60 |
| Steel exoskeleton profile | <i>ton</i> | 560.30 |
| Reinforced concrete piles | m^3 | 160.60 |
| Timber exosk. member | m^3 | -608.40 |
| Reinforced concrete piles | m^3 | 160.60 |

Table 5.20: LCA data for Production Stage

Replacement stage: B4

In addition, the expected lifespan of each solution must be evaluated. The exoskeletons are designed according to a seismic reference period, V_R , of 75 years. In contrast, the CFRP solutions have a considerably shorter lifespan, as they are designed to provide the required performance for approximately 15 years. Consequently, in the lifetime of the exoskeleton solutions, the entire life cycle process of a CFRP intervention is completed five times. This last, includes one production stage, four replacement stages and a final last end-of-life stage, to be included into the environmental impact assessment of the CFRP alternative.

Consequently, this final phase is exclusively associated with the CFRP intervention. Accordingly, after the production phase and before the end-of-life stage of this alternative, four complete replacements are hypothesised. In accordance with the specifications indicated in EN 15978, this stage encompasses the production, transportation, replacement process, waste management, and the end-of-life stage of the replaced building component. The employed values consist on the summation of the A1-A3 and C3/C4 modules corresponding to this alternative and, the results are presented in Table 5.21.

| Materials (B4) | RU | $GW P_{B4}$ [$kgCO_2 - eq./RU$] |
|---------------------------|------------|-----------------------------------|
| CFRP - Fiber [46] | <i>kg</i> | 31.00 |
| CFRP - Resin [42] | <i>kg</i> | 6.07 |
| CFRP - Resin [47] | <i>kg</i> | 6.07 |
| CFRP - Resin [43] | <i>kg</i> | 11.55 |
| Steel exoskeleton profile | <i>ton</i> | 0 |
| Reinforced concrete piles | m^3 | 0 |
| Timber exosk. member | m^3 | 0 |
| Reinforced concrete piles | m^3 | 0 |

Table 5.21: LCA data for Replacement Stage

End-of-life stage: C3 or C4

This phase corresponds to the end of life expected for the materials according to the database employed. In case that waste processing is intended, module C3 is considered; if only the disposal of the material is planned, then module C4 is reported. The employed values are listed in Table 5.22.

| Materials (C3 or C4) | RU | $GW P_{C3/C4}$ [$kgCO_2 - eq./RU$] |
|--------------------------------|------------|--------------------------------------|
| CFRP - Fiber [46] | <i>kg</i> | 0.00 |
| CFRP - Resin [47] | <i>kg</i> | 0.87 |
| CFRP - Resin [47] (C3) | <i>kg</i> | 0.87 |
| CFRP - Resin [43] (C3) | <i>kg</i> | 0.95 |
| Steel exosk. profile (C3) | <i>ton</i> | 0.15 |
| Reinforced concrete (C3) | m^3 | 3.45 |
| Timber exosk. member (C3) | m^3 | 753.40 |
| Reinforced concrete piles (C3) | m^3 | 3.45 |

Table 5.22: LCA data for End-of-life Stage

Reuse/Recovery/Recycling stage: D

This phase corresponds to a post-life cycle stage, which, according to EN 15978, should be declared for a complete LCA assessment but not considered in the analysis. In this stage, the possibility of material reuse, recovery or even recycling is evaluated. The employed values are reported in Table 5.23.

| Materials (D) | RU | $GW P_D$ [$kgCO_2 - eq./RU$] |
|---------------------------|-------|--------------------------------|
| CFRP - Fiber [46] | kg | 0 |
| CFRP - Resin [42] | kg | -0.35 |
| CFRP - Resin [47] | kg | -0.35 |
| CFRP - Resin [43] | kg | -0.38 |
| Steel exosk. profile | ton | 209.60 |
| Reinforced concrete | m^3 | -8.12 |
| Timber exosk. member | m^3 | -409.90 |
| Reinforced concrete piles | m^3 | -8.12 |

Table 5.23: LCA data for D Module

Once the environmental impact of the materials employed at each stage for each solution is identified, it is possible to pass the Life Cycle Impact Assessment (LCIA). The total impact of the solution is calculated as a function of the quantity of materials required. The bill of materials (B.O.M.) obtained from the analysis presented in Sections 5.1, 5.2 and 5.3 is transformed to be congruent to the specified RU and to allow the proper calculation of the global warming potential (total) for each alternative.

The total environmental impact of each scenario proposed is calculated according to Equation 5.4. According to the data presented in Table 5.24, the results obtained are shown in Table 5.25. It is important to note that, the number of substitutions n for the CFRP intervention include the emissions regarding to the modules A1-A3, B4 and C3/C4.

$$GW P_{total,int} = \frac{\sum_i (GW P_{total} \cdot B.O.M \cdot n)}{NFA} \quad [kgCO_2 - eq.] \quad (5.4)$$

where:

- $GW P_{total,int}$: Global Warming Potential total of the proposed intervention;
- i : material employed in the evaluated intervention;
- $GW P_{total}$: Global Warming Potential total according to Equation 5.3;
- n : number of substitutions with respect to the expected lifetime of the exoskele-

ton solution (75 years).

- B.O.M: bill of material according to a congruent reference unit (RU);
- NFA: Net floor area as a functional unit [m^2].

| Material (i) | RU | GWP_{total} [$kgCO_2 - eq./RU$] | B.O.M [RU] | n |
|---------------------------|-------|----------------------------------------|---------------|---|
| CFRP - Fiber [46] | kg | 31.00 | 15.52 | 5 |
| CFRP - Resin [42] | kg | 6.07 | 11.23 | 5 |
| CFRP - Resin [47] | kg | 6.07 | 63.29 | 5 |
| CFRP - Resin [43] | kg | 11.55 | 83.71 | 5 |
| Steel exosk. profile | ton | 560.45 | 5.86 | 1 |
| Reinforced concrete | m^3 | 164.05 | 11.06 | 1 |
| Timber exosk. member | m^3 | 145.00 | 12.40 | 1 |
| Reinforced concrete piles | m^3 | 164.05 | 11.06 | 1 |

Table 5.24: LCIA employed data

| Scenario | $GWP_{total,int}$ [$kgCO_2 - eq.$] | $GWP_{total,int}/NFA$ [$kgCO_2 - eq./m^2$] |
|---------------------------------|-----------------------------------------|-------------------------------------------------|
| Scenario 1: CFRP | 9498.36 | 27.45 |
| Scenario 2: Steel Exoskeletons | 5098.57 | 14.74 |
| Scenario 3: Timber Exoskeletons | 3612.98 | 10.44 |

Table 5.25: LCIA Results

The final step in the LCA framework is the interpretation of the results obtained. This enables the identification of the most environmentally impactful intervention, in this case, the use of CFRP and, in particular, composed of carbon fibres. Regarding scenario 2, despite their high performance, the use of steel exoskeletons is the solution with higher environmental impacts, and, more specifically, higher GWP_{total} . The results of scenario 3, which involves the installation of timber exoskeletons, indicate that this is the solution with lower GHG emissions. Furthermore, the potential for reuse, recovery or recycling in the post-life phase (declared module D) is also high, thereby demonstrating the solution's high sustainable potential.

5.4.2 Cost Evaluation of the Alternatives

In this section it is performed the cost evaluation of the preliminary alternatives proposed for the seismic retrofitting of the existing structure.

Regarding to the intervention proposed by the enterprise, described in Section 5.1, the description of cost provided by them is reported in this analysis.

Following the same cost analysis, the total cost of the steel and timber exoskeleton is calculated according to the bill of materials obtained in Sections 5.2 and 5.3 respectively.

The costs considered for each item of the analysis are obtained from the price list of the Campania region published in the year 2024. It refers to the official price list adopted by the Campania Region for public works and supplies throughout the year 2024. This list includes standardized unit costs for various materials, services, and specific works, used as a reference for cost estimation and the preparation of bids in public tenders within the region.

Furthermore, some costs are identified on the price list of DEI, the Typographic Department of Civil Engineering. DEI has been operational in the civil engineering and architecture sector since 1869. Its activities include the development, creation, and commercialisation of different documentation and software for construction industry professionals, which includes national, regional, and thematic price lists.

The Total Cost, **TC**, of each intervention is determined according to Equation 5.5.

$$TC = A + B + C \quad (5.5)$$

where:

- A : Direct Prime Cost or Technical Cost;
- B : Indirect Cost;
- C : Safety Cost;

Direct Prime Cost

The term "prime costs" is defined as all costs directly attributed to the production of each product. These costs are direct and include both the cost of materials and the labour required to its manufacturing.

In particular, inside this item it is considered cost per unit of time of labor (RU), the cost per unit of measure of construction materials (MT) and the cost per unit of time of equipment (AT).

The term RU is used to denote the productive factor of labour, which can be defined as the physical or intellectual activity of humans, commonly referred to as the workforce.

The term MT is employed to describe the results of a human productive activity, which is technically and economically defined. This also encompasses any raw materials that are directly utilised in the construction process.

Finally, AT considers the productive factor capital, which includes instrumental goods, machinery, means of production, rentals, transport, etc. (commonly referred to as rentals and transport).

Indirect Cost

For the purposes of this analysis, indirect costs are defined as comprising mainly *general expenses* and also plant operations that interfere with structural interventions. In particular, the general expenses correspond to the following items:

- Contractual expenses, registration tax.
- Financial charges, including security deposits, performance guarantees, and insurance.
- Organisational and administrative expenses at the contractor's headquarters.
- Administrative management of site personnel and technical oversight.
- Site-related costs for installation, maintenance, lighting, and final site disman-

ting.

- Transport expenses for materials and equipment to the site.
- Provisional works and tools necessary for project execution.
- Survey, layout, exploration, and testing expenses until project certification.
- Access road construction and operational equipment installation.
- Office space and necessary equipment for site management.
- Costs for temporary occupations, damage compensation, and material extraction.
- Custody and maintenance of works until project certification.
- Site adaptation costs, business risk management measures, and additional statutory obligations.
- Extra specific charges outlined in the contract specifications.

Safety Cost

This item concerns the use of safety equipment, such as scaffolding systems. It encompasses the supply and installation of the complete scaffolding, including tarpaulins, base plates, attachment supports, decking, foot guards, screens, and staircase modules. The scaffolding is constructed using tubes and joints and/or pinned sleeves.

Furthermore, extra business safety charges obtained as a 5% of the indirect costs is considered.

Cost Analysis

A detailed analysis of the costs of the three interventions will now be presented. Table 5.26 presents the costs associated with each item included in the analysis for the CFRP intervention, as indicated by the enterprise. The cost analysis of the proposed steel exoskeletons intervention is presented in Table 5.27, while the respective analysis for the timber exoskeletons solution is shown in Table 5.28. In the aforementioned tables, the cost regarding each component (A, B and C) of the total cost of the intervention is described.

Finally, the total cost TC of the intervention as well as its incidence per unit of surface and volume of the existing building is shown in Table 5.29.

| Description | Unitary Cost (€) | Unit of Measurement | Quantity | Cost (€) |
|----------------------------------|-------------------------|----------------------------|-----------------|-----------------|
| Node's retrofitting w/ CFRP | 3000.0 | <i>each</i> | 8 | 24000.0 |
| Column's retrofitting w/ CFRP | 5000.0 | <i>each</i> | 8 | 40000.0 |
| Total Direct Cost (A) | | | | 64000.0 |
| Interferences (25% of A) | | % | 25 | 16000.0 |
| Total Indirect Cost (B) | | | | 16000.0 |
| Scaffolding | 50.0 | m^2 | 495 | 24750.0 |
| Extra safety charges (5% of A+B) | | % | 5 | 4000.0 |
| Total Safety Cost (C) | | | | 28750.0 |

Table 5.26: Cost Analysis of the CFRP Intervention

| Description | Unitary Cost (€) | Unit of Measurement | Quantity | Cost (€) |
|--------------------------------------------------|------------------|---------------------|--------------------------------|----------------|
| Steel Exoskeleton's (S355) | 7.4 | kg | 5860 | 43305.4 |
| Protective Painting | 0.9 | kg | 5860 | 5391.2 |
| RC micro-piles | 100.0 | m | 352 | 35200.0 |
| | | | Total Direct Cost (A) | 83896.6 |
| General Expenses for steel members (17% of A) | | % | 17 | 8278.4 |
| General Expenses for micro-piles (17% of A) | | % | 17 | 5984.0 |
| | | | Total Indirect Cost (B) | 14262.4 |
| Scaffolding | 27.0 | m ² | 185 | 4995.0 |
| Extra safety charges for steel members (5% of B) | | % | 5 | 413.9 |
| Extra safety charges for micro-piles (5% of B) | | % | 5 | 299.2 |
| | | | Total Safety Cost (C) | 5708.1 |

Table 5.27: Cost Analysis of the Steel Exoskeleton's Intervention

The presented analysis and results indicate that the timber exoskeleton solution is highly convenient. This solution is not only the most sustainable, but also the most economically feasible of the three evaluated scenarios, with a total cost that is approximately 30% lower than the other alternatives.

| Description | Unitary Cost (€) | Unit of Measurement | Quantity | Cost (€) |
|---------------------------------------------------|------------------|---------------------|----------|----------------|
| Timber Exoskeleton's (GL28h) | 1934.0 | m^3 | 12.4 | 23981.6 |
| RC micro-piles | 100.0 | m | 352 | 35200.0 |
| Total Direct Cost (A) | | | | 59181.6 |
| General Expenses for timber members (17% of A) | | % | 17 | 4076.9 |
| General Expenses for micro-piles (17% of A) | | % | 17 | 5984.0 |
| Total Indirect Cost (B) | | | | 10060.9 |
| Scaffolding | 27.0 | m^2 | 185 | 4995.0 |
| Extra safety charges for timber members (5% of B) | | % | 5 | 203.8 |
| Extra safety charges for micro-piles (5% of B) | | % | 5 | 299.2 |
| Total Safety Cost (C) | | | | 5498.0 |

Table 5.28: Cost Analysis of the Timber Exoskeleton's Intervention

| Intervention | Total Cost (TC) € | Incidence €/ m^2 | Incidence €/ m^3 |
|---------------------|----------------------|-----------------------|-----------------------|
| CFRP | 108750.1 | 209.5 | 66.8 |
| Steel Exoskeletons | 108750.1 | 200.1 | 63.8 |
| Timber Exoskeletons | 74740.5 | 144.0 | 45.9 |

Table 5.29: Total Cost of the Proposed Interventions

Chapter 6

2nd Stage: Stress-based

Connection Design Framework

In this thesis, the design of the connections is the second stage of a complete preliminary design methodology proposed. Since the connections are mainly dependent on the forces acting on each node, a stress based design is adopted.

Once it has been demonstrated that the intervention by means of timber exoskeletons is the most sustainable and convenient from an environmental and economic point of view, the design of the connections is held for the nodes of the elements which describe this solution. Consequently, on the basis of the results obtained from the 1st stage of the global exoskeleton intervention, it is proposed to design the connection layouts for the timber elements by means of a real-coded automatic routine.

In order to design a connection typology congruent with the behaviour hipotetised in the model of the exoskeleton structure, a pinned joint is designed. In particular, a double shear steel-timber connection is proposed. The automatic routine proposed in this thesis is based on the equations describing the capacity of the typology of connection evaluated.

The automatic routine phylosophy consists of proposing designs of connections in which it is increased its standardisation while at the same time, their total weight remains controlled.

Once a grouping of the connections to be designed has been created, the routine algorithm ensures that the designs proposed for each group represent connection layouts that can be replicated between different groups.

From the other side, all the proposed layouts are introduced as input to an optimisation algorithm that helps to find the most optimal solution. The optimisation function is designed to minimise the total weight of connections, penalising those solutions that present multiple different layouts.

At the end of the chapter, the calibration of the penalty function for the aforementioned objective function is presented, as well as the final design obtained for the connections.

6.1 Pinned Connection for Timber Elements

The optimal timber exoskeleton solution has to be designed with joints that accurately replicate the structural behaviour intended in the model. The structural model uses pinned connections for the nodes of the exoskeleton elements, allowing them to transmit only axial loads and emulate a truss-like structural behaviour. Therefore, the joints in the design must also be pinned or hinged to ensure that they do not provide rotational stiffness. This congruence between the model and the actual structure is crucial to achieving the desired performance.

In the literature, several different types of connections for timber elements are studied to evaluate their ability to transmit bending moments between the members they connect. In particular, [48] proposes a procedure for the classification in terms of strength and stiffness of beam-column connections in timber structures, similar to what currently exists for steel connections. This paper proposes three types of connection models: simple supports, continuous supports and semi-continuous supports, which can be classified respectively as nominal pinned, rigid and semi-rigid in function of the rotational stiffness of the connection and the bending stiffness of the connected beam.

After examining various connection designs, the results show that it is practically impossible to provide a rigid connection for timber elements that provide significant rotational stiffness. Consequently, they demonstrate that the majority of the connections studied are in the field of pinned or semi-rigid connections.

In addition, according to this study, it was possible to classify as a pinned joint a design consisting of a central steel plate (rectangular or T-shaped) with transverse connectors (generally bolts, screws or pins). Motivated by the results of this research, and to propose a joint typology congruent with the model, this last configuration is chosen for this work.

As a final remark, this work focuses only on the connections between the elements of the timber exoskeleton. The connections between the existing structure and the new timber intervention will be the subject of further studies.

6.1.1 Double Shear Steel-to-timber Connection

A *slotted-in steel plate* connection is chosen for the timber element's joints according to what was introduced in the previous section. This type of connection is one of the most commonly employed structural joints for timber structures and consists of a central steel plate slotted into the end of the timber element and fastened with transverse bolts, as shown in Figure 6.1. As previously mentioned, this typology accurately reproduces a pinned connection ensuring the modelled structural behaviour of the exoskeleton. The use of a steel plate in a timber connection is a common practice that generally increases the capacity of the connection compared to a timber-to-timber connection.

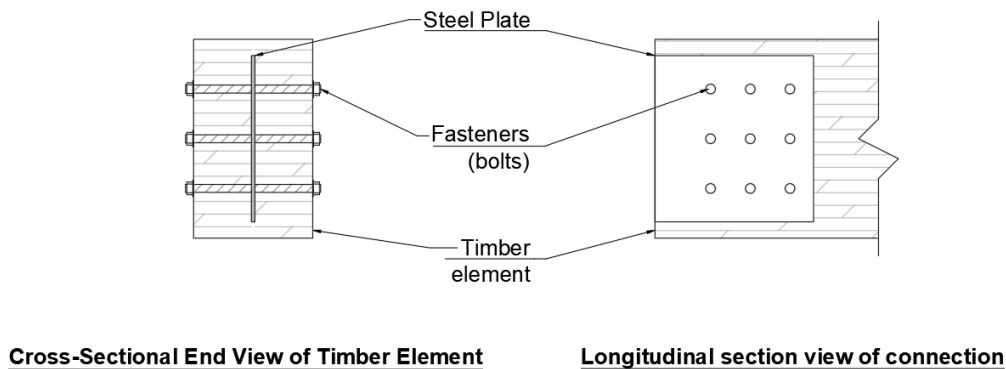


Figure 6.1: Double Shear Steel-to-timber Connection

As the timber members are only axially loaded, the fasteners used in the connection (in this case bolts) receive forces perpendicular to their axes, resulting in shear forces on them. When loaded, the dowel presses against the surrounding timber and steel members, creating an embedding pressure against the dowel. Consequently, the fastener acts as a beam with a distributed load from this embedding pressure. The failure mechanisms for these types of connections are described in detail by the Johansen's theory, which determines the position of the plastic hinges created and the joint's characteristic resistance. In addition, the use of a central steel plate creates two shear planes on each side of the plate, resulting in greater connection strength.

From the previous theory, the expressions for the characteristic resistance of a single

dowel and a single shear plane can be derived, which are those given in Equation 6.1, corresponding to the failure modes shown in Figure 6.2. As there are two shear planes in this case, the characteristic resistances calculated by the previous equations are multiplied by 2.

$$F_{v,Rk} = \min \begin{cases} f_{h,k} \cdot t_1 \cdot d & \text{(g)} \\ f_{h,k} \cdot t_1 \cdot d \left(\sqrt{2 + \frac{4 \cdot M_{y,Rk}}{f_{h,k} \cdot d \cdot t_1^2}} - 1 \right) + \frac{F_{ax,Rk}}{4} & \text{(f)} \\ 2.3 \sqrt{M_{y,Rk} \cdot f_{h,k} \cdot d} + \frac{F_{ax,Rk}}{4} & \text{(h)} \end{cases} \quad (6.1)$$

where:

- $F_{v,Rk}$ characteristic capacity per shear plane, per fastener;
- t_i timber or board thickness;
- $f_{h,k}$ characteristic embedment strength in wood member;
- d fastener diameter;
- $M_{y,Rk}$ characteristic yield moment in fastener,
- $F_{ax,Rk}$ characteristic withdrawal capacity of the fastener;

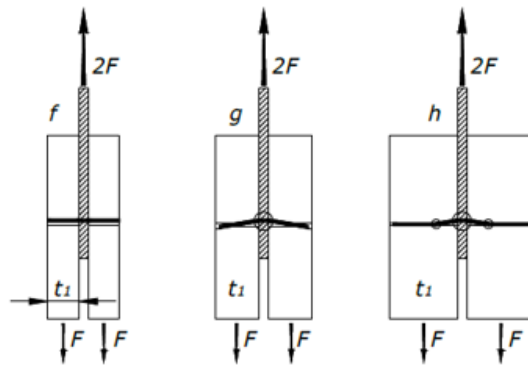


Figure 6.2: Johansen Failure Modes for Steel-to-timber Connection (taken from [49])

The minimum value of the three previous equations determines the characteristic capacity of the connection per shear plane and fastener. Due to the safety margin, the term related to the withdrawal capacity of the fastener is neglected in equations (g) and (h). The previous equations can be found in Section 8.2.3 of EUROCODE 5, while expressions for $f_{h,k}$ as well as for $M_{y,Rk}$ can be found in Section 8.5.1 of the same code, which applies to laterally loaded bolts.

Apart from the failure modes according to Johansen's theory, brittle failure modes can also occur in dowelled joints. However, if the minimum distances between the fasteners and between the fasteners and the edges of the timber elements are respected, it is possible to avoid the verification of these latter failure modes. For this type of connection, the *minimum values of spacing and edge and end distances for bolts* are given in Table 8.4 of EUROCODE 5.

Furthermore, it is important to consider that the load-carrying capacity of a multiple fastener connection (consisting of the same type and dimension) may be lower than the summation of the individual capacity of each fastener. This phenomenon, also known as the "group effect," is due to local variations in timber strength, hole sizes, misalignment of holes, and irregular load transfer among the connection members. In general, when a row of fasteners is loaded in tension, the first and last fasteners receive the highest load level, and consequently, they will fail first. According to the EUROCODE 5, the load carrying capacity of one row of bolts parallel to grain should be calculated using an effective number of fasteners, n_{ef} , and is calculated according to Equation 6.2.

$$F_{v,ef,Rk} = n_{ef} \cdot F_{v,Rk} \quad (6.2)$$

where:

- $F_{v,ef,Rk}$: load carrying capacity of one row of bolts parallel to grain calculated with n_{ef} ;
- n_{ef} : effective number of fasteners **n** in line parallel to the grain;

Particularly, for a bolted connection, n_{ef} is calculated according to Equation 6.3.

$$n_{ef} = \min \left\{ \begin{array}{l} n \\ n^{0.9} \sqrt[4]{\frac{a_1}{13d}} \end{array} \right. \quad (6.3)$$

Finally, given that the connection is designed for timber elements and as already explained in Section 5.3, the effect of moisture strongly affects the mechanical properties of the timber elements, the factor k_{mod} of **0.9** has to be employed. Moreover, the design capacity is obtained by dividing the characteristic capacity by γ_m , which, for the design of a connection is equal to **1.5**. Finally, from the wood side safety checks, the shear design capacity of the connection is given by Equation 6.4.

$$F_{v,ef,Rd} = \frac{k_{mod} \cdot F_{v,Rk}}{\gamma_m} \cdot n_{ef} \cdot s_r \cdot n_r \quad (6.4)$$

where:

- $s_r = 2$: number of shear planes in the connection;
- n_r : number of rows of bolts;

Design of the connection layout

According to Equation 6.4, the resistance of the connection depends on all the variables inside it. In design books, such as [50], the proposed general pre-dimensioning process for these types of connections when the members are subjected to only axial loads, takes into account the most critical variables to propose a connection layout. These sequential steps are listed below.

- 1) Identify the *global design inputs*: maximum axial acting force in the members N , cross-section dimension b and h ; timber resistance class;
- 2) Propose the *connection design inputs*: the thickness of the steel plate t , bolt diameter d , the tensile strength of bolt $f_{u,b}$ and steel plate $f_{u,p}$ and, inter-axis distances among bolts and bolts and borders according to Table 8.4 of EUROCODE 5;

- 3) Evaluate the connection characteristic strength parameters $M_{y,Rk}$ and $f_{h,k}$;
- 4) Evaluate the design shear resistance for a single bolt $F_{v,Rd,1}$ according to Equations 6.1 by multiplying for k_{mod} and dividing by γ_m ;
- 5) Adjust the transverse distance among bolts a_2 according to the available spacing in the height h of the member and the proposed transverse distance to the borders a_4 . Determine the required number of rows of bolts n_r as shown in Equation 6.5;

$$n_r = \frac{h - 2 \cdot a_4}{a_2} + 1 \quad (6.5)$$

- 6) For the required number of rows, propose a longitudinal inter-axis distance a_1 between fasteners and evaluate the group effect. Solve for n in Equation 6.6;

$$n^{0.9} \sqrt[4]{\frac{a_1}{13d}} = \frac{N}{n \cdot F_{v,Rd,1}} \quad (6.6)$$

After this procedure, it is possible to determine the required number of rows n_r of bolts and number of bolts per row n in a *double shear steel-to-timber connection*.

6.2 Automatic Routine for the Preliminary Design of Connections

6.2.1 Automation of Connection's Design

In the previous section, a conventional procedure for the design of the layout of a double-shear steel-to-timber connection was presented. These steps may be performed several times according to the global design inputs coming from the structural analysis. In other words, as the cross-sections of the timber elements and the acting force on them are different, it is expected that different layouts have to be designed.

The connection layout is essentially determined by the steel plate thickness, t_p , and dimensions, the number of bolts per row, n or n_b , and the number of rows of bolts, n_r . Consequently, two connections are considered to be identical provided that the aforementioned variables are the same.

In general, it is a common practice of engineers to perform a "grouping" for the connections to be designed. This grouping consists of classifying all the nodes which present similar global design parameters and, consequently, will require the same connection layout, into the same unique group. For this type of connection (double-shear steel-to-timber), the different groups can be created in function of the cross-section's dimensions and a certain established force range. In this manner, all nodes in which the timber element has the same cross-section and the acting force falls within the pre-established force range will be included in the same group and designed according to the same parameters. These parameters are the dimensions of the group's cross-sections and the maximum force acting on the elements belonging to that group.

It is evident that the method of creating the grouping and designing the connections is not absolute and is contingent upon the designer's choices. Moreover, this process is iterative in nature. This is because, although the cross-sections of two different groups are different, the values of the maximum acting forces may result in the design of the same connection layout. Consequently, the force range can be re-adjusted.

As a consequence of the preceding discussion, several issues and deficiencies emerge in the preliminary design phase of connections. Initially, if the global structural problem involves a very heterogeneous situation, a significant number of different connection layouts must be designed, which requires an important amount of time.

Furthermore, it is of interest to propose a grouping technique which allows for the reduction of the number of different connection layouts while simultaneously controlling the total weight of connections which is directly related to their cost. It is evident that during the assembly phase, it is preferable to install as few different typologies of connections as possible. This approach enhances constructability by minimising the potential for errors during installation.

This thesis proposes an automatic routine through the creation of an algorithm which attempts to follow the previous design philosophy and address the identified step-backs. Initially, the algorithm automatically generates a grouping of the connections to be designed based on the aforementioned global design parameters (N and cross-section dimensions). Subsequently, the code can automatically propose

several layouts for each group in accordance with previously proposed connection design inputs (t, d, a_1) . Following the evaluation of all proposed alternatives, the code performs a filtering process, selecting those with the minimum weight (weight of the single connection) and which are repeated among the different design groups. This option filtering allows for the identification of potential solutions that can be employed in more than one group. Finally, the processed information is then introduced in an optimization algorithm, which is able to find an optimal solution that reduces the number of different connections while controlling the total weight of connections.

The underlying philosophy of this code is to arrive at a final design in which the trade-off between total connection weight and complexity of design (number of different typologies) is assessed. This is achieved by the successive phases of the algorithm in the proposed automatic routine, which mainly consists of refining the preliminary grouping in the first phase and selecting the best solution with the help of an optimization algorithm. It should be noted, however, that if the global analysis of the solution reveals significant heterogeneity in the connection design parameters (i.e., very different cross-sections and acting forces), the number of final different layouts is highly dependent on the structural global analysis output.

The implementation of an automatic routine through an algorithm with these characteristics can exponentially reduce the time required for the design of connections in the preliminary design phase. It is highlighted that the created algorithm is compatible only with the double-shear steel-to-timber connection studied in this thesis; however, in future works, it can be extended to allow an automatic design of different typologies.

6.2.2 Routine Algorithm

The automatic routine is set in an algorithm written in MATLAB. Initially, with the OAPI tools, the global design parameters are extracted from the structural model of the most optimal solution found according to Section 5.3. Figure 6.3 illustrates the systematic phases followed by the automatic routine algorithm.

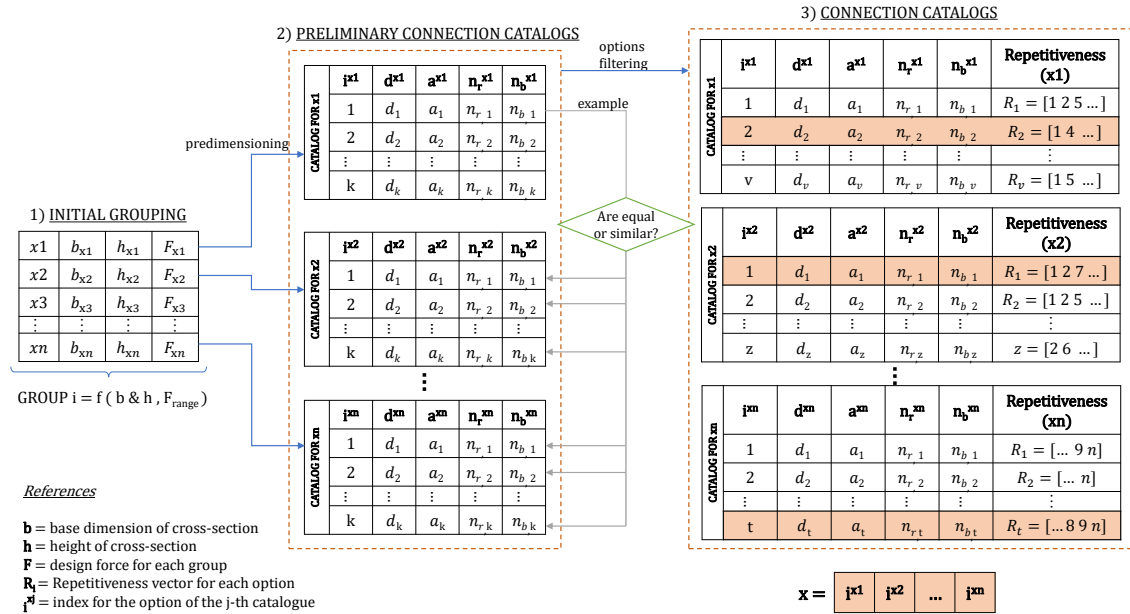


Figure 6.3: Flowchart of Automatic Routine Algorithm

The code begins with the initial creation of a grouping of connections to be designed until the creation of final catalogues, which are introduced later in an optimization framework. The final catalogue contains the different layouts which have passed some filtering phases and which constitute potential solutions for each group of connections. Given the numerous connections to be designed, with each connection comprising multiple proposed layouts, the resulting catalogues are later introduced as input in a genetic optimization algorithm. This last automatically defines the chromosome length and identifies the optimal solution that respects the imposed conditions.

Moreover, to facilitate the comprehension of the macro-processes conducted within the routine and their interrelationships, an entity-relationship (ER) diagram is presented in Figure 6.4. This diagram describes the organisational structure of the information within the proposed framework. As previously stated, the process begins with the obtaining of the axial force for each element of the structural model. A number of these elements are grouped together into a single entity, which is defined in terms of the variables b , h and F . From these initial groups, it is possible to define one preliminary catalogue for each of them. A single catalogue contains

several options derived from the preliminary design of the connection. These options are defined in accordance with the proposed variables d and a_1 , which together with the group's variables determine n_r and n_b . Subsequently, each preliminary catalogue is subjected to filtration and processing, resulting in the creation of a final catalogue for each group of connections. Additionally, each final catalogue comprises numerous options, identical to some of those present in the preliminary catalogue. However, due to the filtration process and the enhanced repetitiveness of connections, an option from the preliminary catalogue may be present in one or more final catalogues, or not present at all.

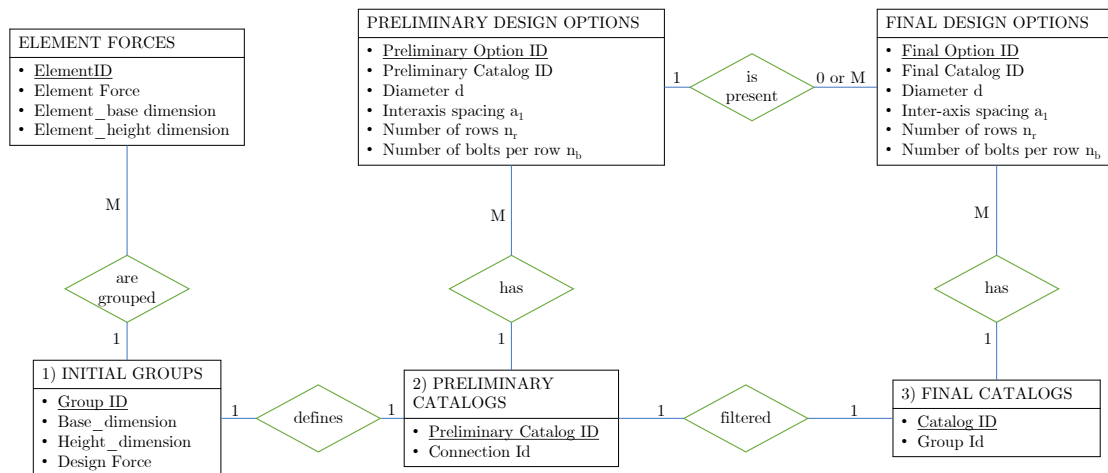


Figure 6.4: Entity-relationship Diagram for the information inside the Automatic Routine

Initial Grouping

The initial stage of the automatic routine involves the formation of groups of connections to be designed. From the structural model of the optimal solution, derived from the global optimisation of the exoskeleton's positioning and sizing, as shown in Section 5.3, the maximum axial forces in each element are identified.

Given that each member of the exoskeleton is subjected to an axial force that is constant along its axis, it can be assumed that the two extreme nodes of the members

must transmit the same force (neglecting small differences due to their own-weight). To simplify the problem, it is assumed that both nodes of each member be designed with the same connection layout.

The grouping of the different connections to be designed is performed in accordance with the member's cross-sectional dimension and a previously set force range. In other words, those nodes in which the cross-section of the element is identical and the acting force on them is within the fixed force interval are grouped.

In order to provide a wide number of groups for the analysis and ensure a good exploration of the domain, it is preferable to adopt small force ranges. In this case, the force range has been set to 50 kN. Consequently, all nodes with the same cross-section have been classified into force ranges of 50 kN each, thereby enabling the definition of each group.

At the end of this phase, a total of n connections must be designed in function of the specified group cross-section dimensions (b and h) and maximum axial force (F). Each group is identified with a unique id.

Preliminary Connection Catalogs

In this phase, the algorithm performs the classical pre-dimensioning procedure for a double-shear steel-to-timber connection presented in Section 6.1.1, but in this case, it is done for several proposed design inputs. These inputs are the diameter of bolts (d) and the longitudinal inter-axis spacing among them (a_1), while the rest of the variables incident on the connection resistance are fixed.

The reason behind fixing the remaining variables while allowing for different values for the aforementioned two is that, following an exhaustive analysis of the equations that describe the capacity of timber connections from the wood side safety checks, it has been determined that the most influential variables are d and a_1 . In addition, the remaining fixed variables can be determined primarily as a function of the bolt diameter.

Concerning the type of bolt employed, bolts of the resistance class 10.9 are selected. In particular, the types M16, M18, M20 and M24, which are the most commonly

employed in practice are proposed.

As previously stated, the longitudinal inter-axis spacing among bolts a_1 has a great influence on the *group effect* in timber connections. As demonstrated by Equation 6.3, this effect influences up to a maximum distance of 13 times the bolt's diameter. Given that the minimum possible distance for a_1 is $5d$, three inter-axis spacings are proposed: $5d$, $7d$ and $12d$. This approach allows for the evaluation of the trade-off between connections with greater spacing between bolts and larger plates, while simultaneously reducing the total number of bolts required.

Regarding the connection layout, the inter-axis spacing among bolts as well as the distance between the perimetral bolts and the edges of the members have been chosen as the minimum possible values indicated in Table 8.4 of EUROCODE 5. This ensures that the connection will have the minimum possible bulk for each proposed value of d . The imposed dimensions are illustrated in Figure 6.5, where the adopted values are presented in Table 6.1.

The variables e_1 and e_2 correspond to the minimum distances required for the perimetral bolts and the sides of the steel plates, which are taken from Table 4.2.XVIII of [4] regarding the steel-side safety checks. In the same way, p_1 and p_2 are the minimum inter-axis distances taken from the steel recommendations but in this case, are considered equal to the ones imposed from the wood side since these are more restrictive.

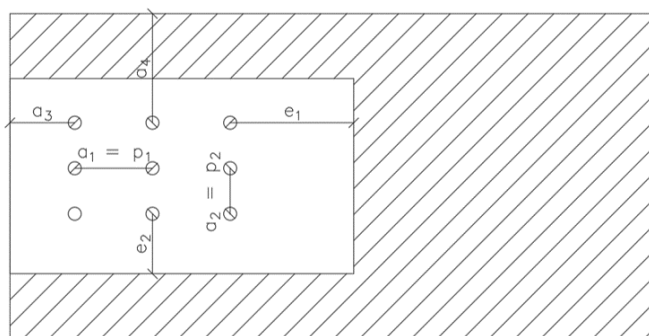


Figure 6.5: Inter-axis and Border Distances to Respect

Another design assumption is considered for the connection layouts. The number of bolts per row denoted as n_r , is maximised according to the Equation 6.5 by adopting

| Distance | Adopted Value |
|----------|-------------------------|
| a_1 | $[5d - 13d]$ |
| a_2 | $4d$ |
| a_3 | $\max(7d, 80\text{mm})$ |
| a_4 | $3d$ |
| p_1 | a_1 |
| p_2 | a_2 |
| e_1 | $1.2 d_0$ |
| e_2 | $1.2 d_0$ |

Table 6.1: Inter-axis and Border Distances Adopted Values

the minimum possible transverse spacing. Consequently, a greater number of bolts are positioned transversely, resulting in shorter plates for which the centre of stiffness is situated closer to the end of the element. This ensures that the expected pinned or hinged behaviour of the connection is achieved. Moreover, this consideration also allows for the design of smaller steel plates with reduced weight.

Once the aforementioned assumptions have been established, the algorithm proceeds to perform a preliminary dimensioning of the connection for each proposed pair of bolt diameter, d , and inter-axis spacing, a_1 . This preliminary dimensioning is carried out in relation to the global design parameters of the groups, specifically the cross-section dimensions and the maximum axial force, F . The number of rows of bolts, n_r , and the number of bolts per row, n_b , are determined for each case.

The resulting layouts for each group are collected into independent *Preliminary Connection Catalogs*. Given that four values of d and three of a_1 are submitted, a total of 12 different layouts are obtained for each group's catalogue.

About the thickness of the steel plate, t , it is assumed for constructability reasons that this is maintained constant in all the designs. Initially, in this phase, the algorithm proposes a thickness of 6 mm for the steel plate. After all the designs have been obtained, the steel-side safety checks of the different layouts are performed.

The verifications can be found in the [4] regulation and include the evaluation of the plastic resistance of the gross section as well as the ultimate strength of the net section, both of the steel plate. Moreover, the shear ultimate strength of the bolts

and the embedment resistance of the steel plate are evaluated.

The algorithm identifies which are the options which do not pass the steel-side safety checks and eliminates them from the corresponding catalogue. If, at the end of the process, the number of options in the catalogues is reduced by more than 70% of their initial quantity, the pre-dimensioning process is restarted with a steel plate 1 mm thicker. This ensures that the Preliminary Catalogues present a sufficiently wide range of options to be assessed in the subsequent stages.

Options Filtering

In the preliminary catalogue for each group, it is trivial to identify which option is the best in terms of its weight. The weight of the connection is obtained by adding the weight of the steel plate to that of the required bolts. Consequently, the option with the lowest weight is the most feasible. However, the goal of the 2nd design stage methodology presented in this thesis, is not to identify the configuration of connections with the lowest weight. Instead, the aim is to develop a design of connection layouts that increases their standardisation (enhancing constructability) while controlling the total weight. Consequently, all options that do not present the lowest weight can still be potential solutions, as they may be present in other catalogues, enabling the design of connections of different catalogues with the same layout.

In the third phase, a filtering process is applied to the catalogue options. The objective of this filtering is to compare each option i in the current catalogue with all other options j in the remaining catalogues.

In this comparison, the following conditional equations are evaluated:

$$(d_i = d_j) \wedge (a_{1,i} = a_{1,j}) \wedge (n_{r,i} = n_{r,j}) \wedge (n_{b,i} = n_{b,j})$$

$$(d_i = d_j) \wedge (a_{1,i} = a_{1,j}) \wedge (n_{r,i} = n_{r,j} - 1) \wedge (n_{r,i} \cdot n_{b,i} \geq n_{r,j} \cdot n_{b,j}) \wedge (n_{b,j} - n_{b,i} = \delta n_b)$$

If the upper conditional is verified, then the two compared options are **equal**. Conversely, if the conditional equation of the bottom is true, then the two options are

similar.

Equal options are defined as those that have the same diameter of bolt, longitudinal inter-axis spacing, and the same number of rows of bolts and bolts per row. In the case that it is determined the aforementioned options are equal and are present in different catalogues, a *Repetitiveness* index is added to the option, which allows for the identification of the catalogues in which the evaluated option appears. This index is included in a vector \vec{R} as exemplified below:

$$\vec{R} = [1 , 3 , 5]$$

In this example, if the option is characterised by the shown *Repetitiveness* vector \vec{R} , implies that this option can be found in the catalogues of connection groups 1, 3 and 5.

On the other side, similar options are those which have the same d and a_1 , but they present a different total number of bolts. These are defined in order to enhance the standardisation of connections even more. Consequently, if an option i has the same d and a_1 as another j , but it is slightly weaker (has fewer bolts per row) in relation to a limit δ_{nb} , then the option j (which has a higher capacity) is added to the catalogue of the option i , and the repetitiveness index identifies the added option in both catalogues. The limit, designated as δ_{nb} , is set at five additional bolts. This value, according to the case study, corresponds to a higher resistance of a maximum of 15%. Consequently, it is reasonable to introduce the stronger option in the catalogue of the weaker one.

Once this phase is complete, the *Preliminary Catalogues* are populated with additional similar options, thereby exceeding the initial 12 layouts. In addition, each alternative is assigned a repetitiveness index, indicating its presence in the different catalogues.

Final Connection Catalogs

The final catalogues for each group of connections to be designed are obtained by filtering the solutions present from the previous phase even more deeply. This

process is done independently for the catalogue of each group, with the aim of identifying the most suitable solutions.

Initially, in each catalogue, options with an equal Repetitiveness vector are identified. Consequently, if two options are present in the same catalogues but one has a lower weight, the heavier option is discarded.

The resulting options are evaluated to determine whether the Repetitiveness vector of one option, designated as "a," is contained in the vector of another option, designated as "b." If this is verified and it is also proved that "a" has a higher weight than "b," the first option must be eliminated. This process ensures that if there is another option that can be replicated in the same or more quantity of connection groups, only the lighter option is retained.

On the basis of the previous reasoning, it is possible to obtain the final catalogue for each group of connections to be designed. In the end, the resulting catalogues comprise only those options that are present in other catalogues (enhancing the standardisation of designs) and, at the same time, have the minimum possible weight for that particular Repetitiveness vector.

At this point, the automatic generation of catalogues and intelligent filtering is concluded. The final catalogues, the different group's ID, and the identification of the nodes of the structural elements belonging to each group are introduced as input in the optimisation framework.

Optimization Framework

The optimization algorithm employed follows the same framework as that used for the obtention of the global solution of exoskeletons, as described in Section 3.2.2. However, it presents some particularities.

Initially, it is important to note that the chromosome is not fixed in variables, as it will have as many variables as connection groups defined. Consequently, each variable represents the ID of the connection layout chosen in the final catalogue of the corresponding group. These catalogues are introduced as an input into the optimisation algorithm at the final step of the automatic routine. They contain the

potential connection layouts derived from the aforementioned filtering process.

The mathematical formulation of the optimization problem is described as follows.

$$\mathbf{min} f(\mathbf{x}) = \left[\sum_{i=1}^n w_i \cdot j_i \right] \cdot \phi_1(N_{dif}) \quad (6.7)$$

$$\mathbf{x} = [x_1 , \dots , x_i , \dots , x_n]$$

subjected to :

$$x_i^{lower} < x_i < x_i^{upper}$$

where

- \mathbf{x} : chromosome with design variables
- x_i : index of selected layout in catalogue of group i ;
- n : number of groups defined in the first phase of automatic routine;
- N_{dif} : number of different layouts present in the solution;
- ϕ_1 : penalty function;

The term within brackets of the OF represents the weight of all the connections present in all the nodes the exoskeletons installed. Accordingly, w_i is the weight of the selected layout for the group i , and j_i is the number of nodes which are inside that group.

The penalty function, denoted by ϕ_1 , is a function of the number of different layouts present in an individual's chromosome. This penalty is described by the rectilinear mathematical function shown in Figure 6.6, whose independent variable is N_{dif} . The sensitivity analysis presented in the following section allows for the calibration of the slope of the penalty function.

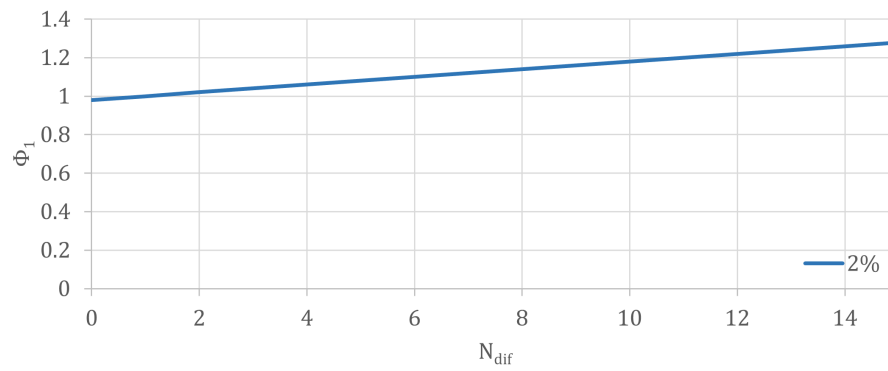


Figure 6.6: Penalty Function ϕ_1 for Optimization Algorithm

Furthermore, x_i^{lower} and x_i^{upper} represent, respectively, the lower and upper bound indexes of the options present in the catalogue of group i .

6.3 Analysis and Interpretation of Results

This section presents the analysis conducted using the created automatic routine and the optimisation algorithm for the connection design. Initially, the calibration of the penalty function employed is discussed to calibrate the optimal slope for the function, which aligns with the analysis goals. Once the penalty function is properly tuned, the optimal solution of ten complete runs is identified and described at the end of this section.

6.3.1 Calibration of Penalty Function

It is important to note that the importance of the weight of connections is evident. The minor is the weight of the connections, and then the minor is the economic cost and environmental impact of the solutions according to the approach adopted for their evaluation. Furthermore, the standardisation of connections (or reduction of the number of connection layouts) is a straightforward approach that offers significant benefits during the assembly phase since it enhances constructability and simplifies the design phase of the connections, as fewer options need to be evaluated.

Nevertheless, it is not entirely clear how to quantify the importance of standardising the connection designs. In fact, when the production and assembly phases are carefully considered, even the influence of the total weight of the connection can be discussed. In other words, these two variables are strongly dependent on the enterprise in charge of the connection production and/or their assembly, as well as on the site in which the project is located. It is possible to identify solutions in previously executed projects that do not minimise the total weight of connections and do not prioritise standardisation, however, these solutions are economically viable. This is because production enterprises can offer discounts based on their manufacturing process and available stock.

Consequently, it can be asserted that there is a high degree of variability and a lack of information regarding the actual influence of the addressed design variables. Consequently, the approach proposed in this thesis does not lead to a globally optimal solution, since different optimal solutions can be proposed.

However, a methodology is proposed to simplify the decision-making process in the design of connections. This approach aims to achieve two main objectives: quantitatively, it seeks to reduce the total weight of the connections; qualitatively, it focuses on standardizing the connections.

In order to achieve this goal, it is necessary to calibrate the penalty function imposed in the optimization framework described in Section 6.2.2. This parameter tuning must be carried out to successfully allow the obtaining of a solution in which the standardization of connections is maximized at the expense of a minimum increase in the total weight of connections.

It is therefore proposed that a linear penalty function be applied which accounts for the standardisation of connections. For N_{dif} equal to 1, the penalty function is fixed to be 1. In other words, solutions with 1 typology of connections are not going to be penalised. As shown in Figure 6.7, nine different slopes are subjected to a tuning process in which the one which better adjusts to the foreseen goal will be chosen.

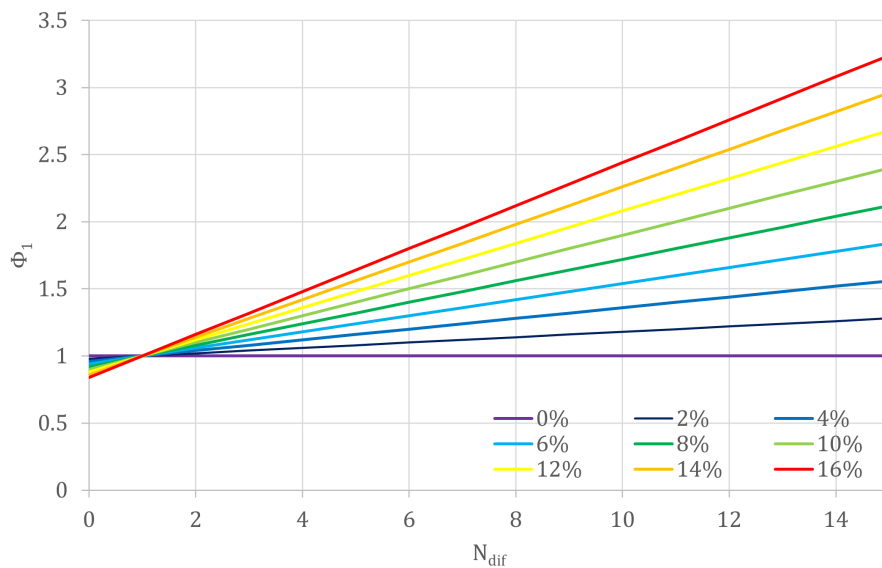


Figure 6.7: Penalty Functions ϕ_1 Assessed

For each penalty function, ten complete runs of the automatic routine algorithm are performed, followed by the optimisation of the solutions. From each analysis, the number of different connections, N_{dif} , and the total weight of the optimal solution for the connection, $W_{c,tot}$, are obtained. Additionally, a penalty function with a

slope of 0% is proposed as the reference scenario for the analysis. Since this slope does not penalize low standardization and focuses solely on finding solutions with the lowest possible weight, the remaining penalty functions are compared against this reference. This comparison allows for the identification of the trade-off between the reduction of the number of connection typologies versus the increase in their total weight, relative to the reference situation.

The configuration of the optimization process employed for each run is detailed in Table 6.2.

| Parameter | Value |
|-------------------------------|--------------|
| Number of runs | 10 |
| Number of individuals per run | 100 |
| Number of iterations | 100 |
| Stagnation check iteration | 15 |

Table 6.2: Optimization Algorithm Parameters

Interpretation of Results

The results of the penalty function's slope tuning are presented in Figure 6.8. From this figure, it can be observed that there is a clear trade-off between the total weight of the connections adopted and the number of different layouts of connections. Consequently, the optimal solutions, which present higher standardisation, are also those which present higher values of total weight.

Furthermore, it is possible to identify a rapid reduction in the number of connections with a minimal increase in weight from a slope of 0% to a slope of 2%, while a further slight improvement is also appreciated until a slope of 4%.

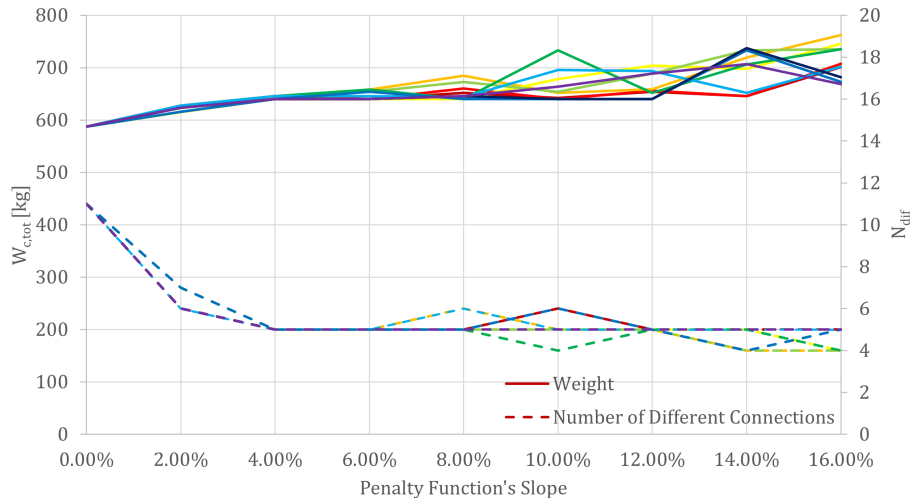


Figure 6.8: Results Penalty Function's Slope Calibration

In order to identify the most representative trend for the different penalty functions assessed, the average and standard deviation of the obtained results after the ten iterations were calculated. These statistical parameters for the studied slopes are presented in Table 6.3.

| Penalty Slope % | $\bar{X} = W_{c,tot}$ [kg] | $\sigma(\bar{X})$ [kg] | $N_{dif}(\bar{X})$ [-] |
|--------------------|-------------------------------|---------------------------|---------------------------|
| 0 | 587.3 | 0.00 | 11 |
| 2 | 622.3 | 4.98 | 6 |
| 4 | 641.6 | 2.93 | 5 |
| 6 | 646.8 | 8.12 | 5 |
| 8 | 652.4 | 15.45 | 5 |
| 10 | 663.8 | 30.63 | 5 |
| 12 | 667.5 | 23.82 | 5 |
| 14 | 697.7 | 36.76 | 5 |
| 16 | 711.3 | 32.12 | 5 |

Table 6.3: Average Results per each Slope

The preceding results demonstrate the appearance of a noising effect, particularly after a slope of 8%, which is characterised by a marked variability in the optimal results. This effect disturbs the optimal solution research for high slopes since the high penalisation of the individuals with high numbers of connections (which, at

the same time, have the lowest weight) guides the algorithm to rapidly discard the solutions with potential configurations in terms of minimal weight. This effect can be mitigated by increasing the exploration and exploitation of the optimization algorithm for runs involving high slopes of the penalty function.

Furthermore, the average trend represented in Figure 6.9, can be analysed. This figure illustrates a clear improvement in standardisation for a penalty function with a slope of 2% at the expense of a low increase in total weight. Moreover, once the plateau at a slope of 4% is reached, there is no improvement in the reduction of connections, while the optimal solutions found present a successive increase in weight. These results reflect the noising effect that appears for high slopes of the penalty function, which it would have been expected to find unless the same solution was already found at slope 4%. However, despite the described variability of the data, there are no significant gains in standardisation for that region. Consequently, it is not necessary to increase the exploration and exploitation of the optimization research in order to find more accurate solutions, as it has been demonstrated that no interesting results can be found.

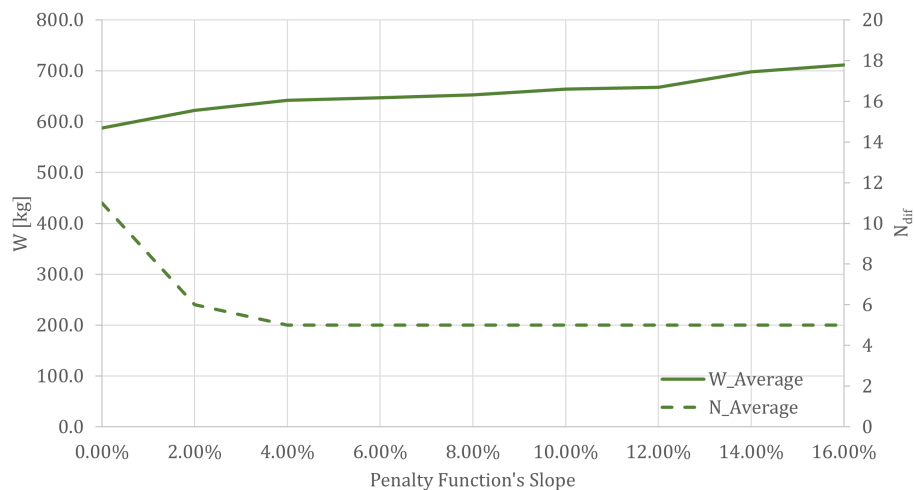


Figure 6.9: Average Trend of Penalty Function's Slope Calibration

In order to quantify the enhancement of the standardisation of connections at the expense of an increase in their total weight for the different functions assessed, a new index is introduced. Once the percentual increase in weight and reduction in the number of different connections with respect to the reference situation (slope of

0%) have been calculated, this index represents the ratio between the two previous quantities. This approach enables a clear quantification of the gain in standardisation of connections, normalised by the increase in their total weight. The results are presented in Table 6.4.

| Penalty Slope % | $\bar{X} = W_{c,tot}$ [kg] | $N_{dif}(\bar{X})$ [-] | $\Delta W_{c,tot}$ % | ΔN_{dif} % | $\Delta N_{dif}/\Delta W_{c,tot}$ % |
|---------------------------|-------------------------------|---------------------------|-------------------------|-----------------------|----------------------------------------|
| 0 | 587.32 | 11 | - | - | - |
| 2 | 622.32 | 6 | 5.96 | -45.45 | -7.63 |
| 4 | 641.63 | 5 | 9.25 | -54.55 | -5.90 |
| 6 | 646.84 | 5 | 10.13 | -54.55 | -5.38 |
| 8 | 652.40 | 5 | 11.08 | -54.55 | -4.92 |
| 10 | 663.82 | 5 | 13.02 | -54.55 | -4.19 |
| 12 | 667.50 | 5 | 13.65 | -54.55 | -4.00 |
| 14 | 697.73 | 5 | 18.80 | -54.55 | -2.90 |
| 16 | 711.32 | 5 | 21.11 | -54.55 | -2.58 |

Table 6.4: Connection's Standardization versus Increase on Total Weight

As can be seen from Table 6.4, the slope of 2% maximises the ratio described previously and therefore falls within the scope of the connections design. Consequently, this slope is sufficiently calibrated for the type of penalty function employed and the case of study under evaluation.

6.3.2 Connections Layout Design

From the ten analyses performed employing the penalty function with a slope of 2%, the solution presenting the highest standardisation and the minimum weight is selected.

The optimal solution for the connections typologies is presented in Table 6.5. Furthermore, the number of required connections per typology is also provided.

The final solution comprises six distinct connection layouts, each identified with a unique ID. Each connection is characterised by a specific bolt diameter employed \varnothing , inter-axis spacing of bolts a_1 , number of rows of bolts n_r , and number of bolts per row n_b .

| Typology ID | t_p [mm] | \varnothing [mm] | a_1 [mm] | n_r | n_b |
|-------------|---------------|-----------------------|---------------|-------|-------|
| 1 | 14 | 16 | 80 | 4 | 4 |
| 2 | 14 | 16 | 80 | 4 | 2 |
| 3 | 14 | 16 | 80 | 2 | 3 |
| 4 | 14 | 20 | 100 | 4 | 2 |
| 5 | 14 | 16 | 80 | 7 | 3 |
| 6 | 14 | 16 | 80 | 7 | 2 |

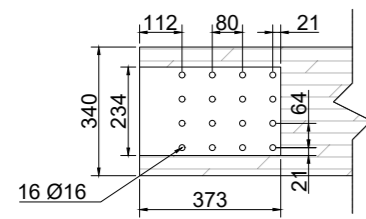
Table 6.5: Design of the Connections Layout

The location of each connection typology, along with their geometric details, is presented in the technical drawings, *Plan 3*.

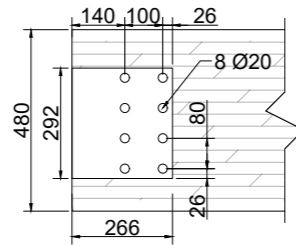
The following sections present the economic and environmental impact of the connections previously designed for the timber exoskeletons intervention. Consequently, it is necessary to calculate the precise weight of the connections, disaggregating it among the bolts and steel plates. In order to facilitate the management of data within the algorithmic routine, the weight considered within the framework is based on a unitary length of bolts. However, to accurately calculate the weight of bolts, which is a function of the width of the cross-sections, the total weight of the solution chosen is recalculated based on the actual required length of bolts. The results are presented in Table 6.6.

| Member | W [kg] |
|--------------|-------------|
| Steel Plates | 626.00 |
| Bolts | 269.19 |
| Total | 895.19 |

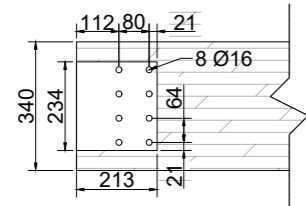
Table 6.6: Weight of Connections



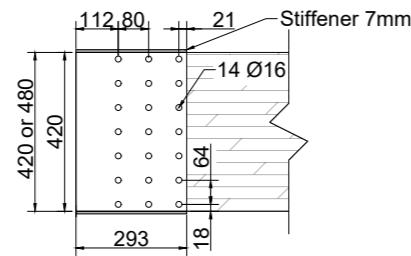
CONNECTION 1
SCALE: 1/20



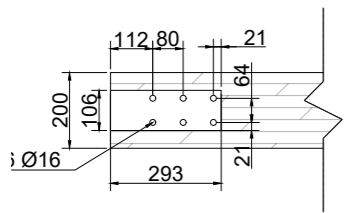
CONNECTION 4
SCALE: 1/20



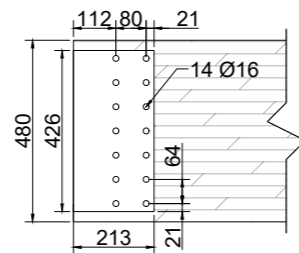
CONNECTION 2
SCALE: 1/20



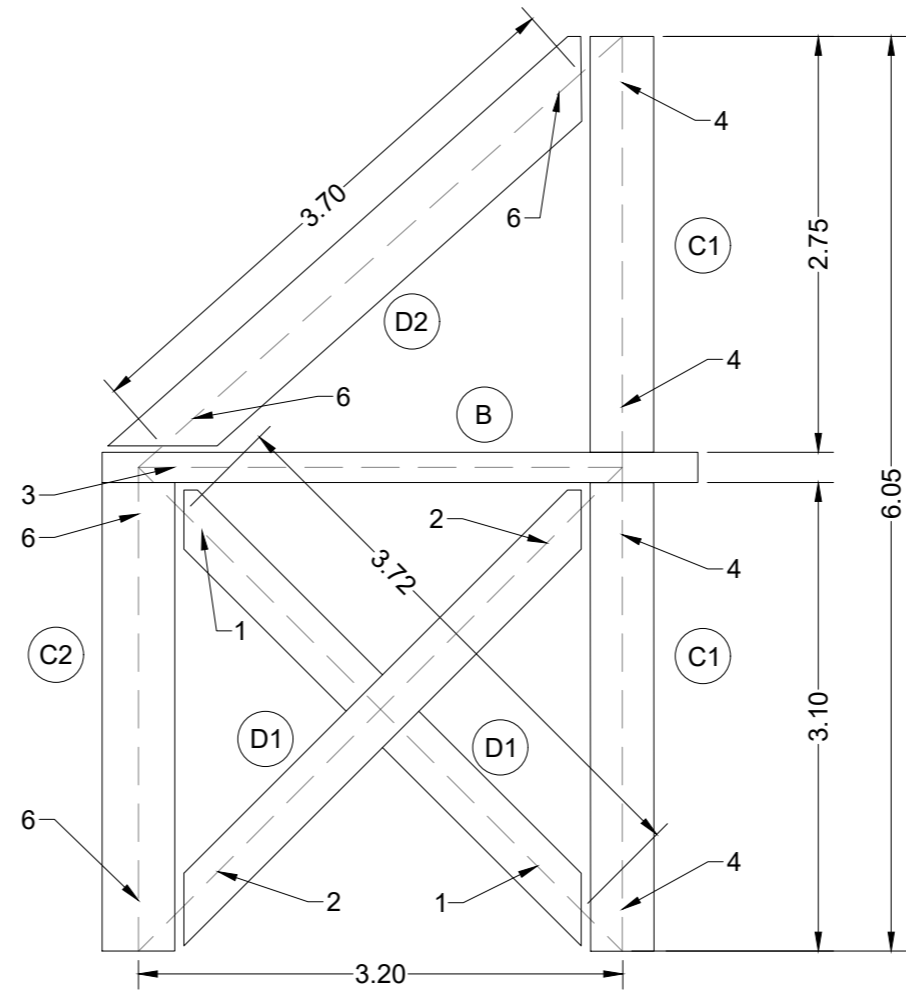
CONNECTION 5
SCALE: 1/20



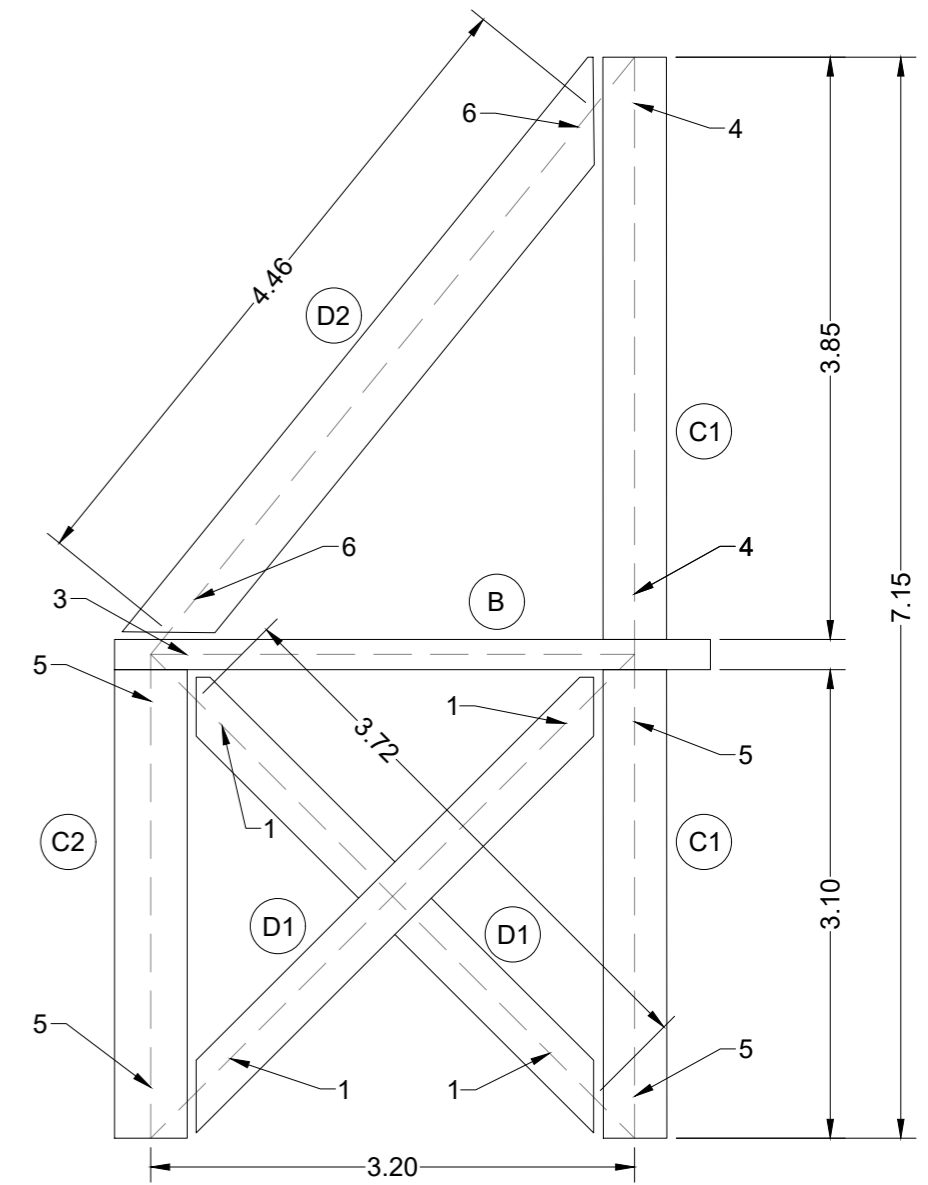
CONNECTION 3
SCALE: 1/20



CONNECTION 6
SCALE: 1/20



EXOSKELETON TYPE 1 - X DIRECTION
SCALE: 1/50



EXOSKELETON TYPE 2 - Y DIRECTION
SCALE: 1/50

DIMENSIONS

| ELEMENT | ID | b [m] | h [m] |
|------------|----|-------|-------|
| COLUMN 1 | C1 | 0,35 | 0,42 |
| COLUMN 2 | C2 | 0,45 | 0,48 |
| BEAM | B | 0,30 | 0,20 |
| DIAGONAL 1 | D1 | 0,22 | 0,34 |
| DIAGONAL 2 | D2 | 0,40 | 0,48 |

EXOSKELETON ELEMENTS DIMENSIONS
SCALE: ~

NOTE 1:

In the present view it is possible to identify the **height h** of the exoskeleton's elements, as specified in the corresponding table.

NOTE 2:

Connection 5 is installed in members with a cross-section height of 420 mm and 480 mm. For the members with height of 420 mm, it is also projected a stiffener welded transversally to the steel plate in order to increase the transverse resistance of it. The stiffener dimensions are 293x180x7 mm



MASTER'S DEGREE THESIS

PLAN: 3 - EXOSKELETON'S CONNECTIONS

INSTITUTION: POLITECNICO DI TORINO

AUTHOR: TOMÁS LAZZURI

SCALE: SPECIFIED DATE: 19/07/2024 VERSION: V.1

PLAN: CONNECTIONS POSITIONING & DETAILS N°: 001

6.4 Economic Cost and Environmental Impact of the Connections

The results obtained for the timber solution in Section 5.4 do not consider the contribution of the connections among the elements. Once the best solution for the design of connections of the optimal timber exoskeleton intervention has been identified, the contribution of these connections to the environmental impact and economic cost of the overall intervention (exoskeletons and connections) will be evaluated.

Environmental Impact of Connections

Similarly to the approach taken in Section 5.4.1 for the assessment of the environmental impact of the proposed global interventions, the emissions associated with the connections are evaluated through an LCA analysis. Table 6.7 provides a summary of the main definitions used in the goal & scope phase.

| | |
|----------------------|---------------------------------------------------------------------------------------------------------------------------------------------------------------------------------------------------------------------------------------------------------------------------------------------------------------|
| Goal | Evaluate and quantify the environmental impact of the connections proposed for the members of the optimal timber exoskeletons solution, from the production of materials to their end of life, in order to understand the impact of the connections on the overall intervention (exoskeletons & connections). |
| Scope | The product under consideration encompasses all the connections designed, taking into account the elements that comprise them, bolts and steel plates. |
| Functional Unit (FU) | Net Floor Area (NFA) [m^2] |
| System Boundary | Cradle-to-gate. Considered modules: (A1-A3) + (C3 or C4). Declared modules: (A1-A3) + (C3 or C4) + (D) |
| Impact Categories | Global Warming Potential total ($GW P_{tot}$) |

Table 6.7: Connections LCA Goal & Scope definition

The datasets employed for the *Production*, *End-of-life* and *Beyond Life's Cycle* stages are obtained from the available EPDs regarding the members which comprise the connection. In particular, the data provided by Ökobaumat is employed for the steel plates, while the EPD published by BUMAX® in The International

EPD® System are utilised for the bolts. The results for all aforementioned stages are presented in Table 6.8.

| Materials | RU | $GWP [kgCO_2 - eq./RU]$ |
|-------------------|------------|-------------------------|
| GWP_{A1-A3} | | |
| Steel Plates | <i>ton</i> | 2529.00 |
| Bolts | <i>kg</i> | 1.21 |
| $GWP_{C3/C4}$ | | |
| Steel Plates (C4) | <i>ton</i> | 0.15 |
| Bolts (C3) | <i>kg</i> | 0.08 |
| GWP_D | | |
| Steel Plates | <i>ton</i> | -1467 |
| Bolts | <i>kg</i> | 0.09 |

Table 6.8: LCA Data for each Stage

Regarding the expected lifespan of the connections, the same 75 years considered for the timber exoskeletons is also employed for this analysis. Finally, the total environmental impact regarding exclusively the connections is calculated according to Equation 5.4. Considering the data presented in Table 6.9, the obtained results are shown in Table 6.10.

| Material (i) | RU | GWP_{total} [$kgCO_2 - eq./RU$] | B.O.M | n |
|--------------|------------|----------------------------------------|--------|---|
| | | | [RU] | |
| Steel Plates | <i>ton</i> | 2529.15 | 0.63 | 1 |
| Bolts | <i>kg</i> | 1.29 | 269.19 | 1 |

Table 6.9: LCIA employed data for Connections

| Scenario | GWP_{total} [$kgCO_2 - eq.$] | GWP_{total}/NFA [$kgCO_2 - eq./m^2$] |
|------------------------------------|-------------------------------------|---------------------------------------------|
| Connections of timber exoskeletons | 1929.31 | 5.58 |

Table 6.10: LCIA Results for Connections

It is imperative to recall that the LCA is conducted on the connections of a retrofitting intervention proposed for building construction. Consequently, as indicated in EN

15978, the beyond-life cycle module D is reported but not considered in the previously shown results.

The final step in the LCA methodology is the interpretation of the obtained results. For this purpose, it is helpful to recall the results obtained for the environmental impact of timber exoskeletons, which are described in Section 5.4.1. From these results, it was determined that the impact of exoskeletons installed comprising their foundation system was **10.44** $kgCO_2eq/m^2$. Conversely, the connections designed for the optimal solution present an impact of **5.58** $kgCO_2eq/m^2$. Consequently, the overall intervention comprising timber exoskeletons, foundation system and connections between the members presents an environmental impact of **16.02** $kgCO_2eq/m^2$. It is thus demonstrated that in the case study analysed, despite the proposed connection design methodology accounting for the reduction of total weight, their impact accounts for the **35%** of the global system impact.

Economic Cost of Connections

Finally, the influence of the connections on the total cost of the timber exoskeletons intervention is evaluated. The same cost analysis held in Section 5.4.2 is now presented, but in this case, it also includes the items regarding the production and assembly of the steel connections of the elements.

In general, for preliminary projects, the cost of the connections is calculated as a percentage, which may vary between 15% and 30% depending on the type of project. However, a different approach is proposed in this section. Since it is possible to know the weight of the steel required for the connections of the timber elements, a new reference price is introduced which accounts for their production and assembly. Consequently, the unitary cost of the connections was obtained from a leader enterprise in timber constructions, Holzbau Sud, and was subsequently included in the cost analysis.

The aforementioned cost item is included in the direct prime cost. Furthermore, the indirect cost, as well as the associated safety cost for connections, are calculated with the respective percentile considered for the rest of the items.

The cost analysis of the complete timber exoskeletons intervention, comprising timber elements, their connection and the foundation system, is described in Table 6.11.

| Description | Unitary Cost (€) | Unit of Measurement | Quantity | Cost (€) |
|---------------------------------------------------|-------------------------|----------------------------|-----------------|-----------------|
| Timber Exoskeleton's (GL28h) | 1934.0 | m^3 | 12.4 | 23981.6 |
| Steel Connections | 7.0 | kg | 895.19 | 6266.3 |
| RC micro-piles | 100.0 | m | 352 | 35200.0 |
| Total Direct Cost (A) | | | | 65447.9 |
| General Expenses for timber members (17% of A) | | % | 17 | 4076.9 |
| General Expenses for connections (17% of A) | | % | 17 | 1065.3 |
| General Expenses for micro-piles (17% of A) | | % | 17 | 5984.0 |
| Total Indirect Cost (B) | | | | 11126.1 |
| Scaffolding | 27.0 | m^2 | 185 | 4995.0 |
| Extra safety charges for timber members (5% of B) | | % | 5 | 203.8 |
| Extra safety charges for connections (5% of B) | | % | 5 | 53.3 |
| Extra safety charges for micro-piles (5% of B) | | % | 5 | 299.2 |
| Total Safety Cost (C) | | | | 5551.3 |
| Total Cost (A+B+C) | | | | 82125.4 |

Table 6.11: Cost Analysis of the Complete Timber Exoskeleton's Intervention

The results of the cost analysis presented in Table 6.11 indicate that connections account for 8.99% of the total cost of the intervention. The values obtained are slightly below the typical range, as the connections were designed according to a

methodology that prioritises control of the total weight. Consequently, given that the cost is proportional to the mass of the connections, they have a moderate impact on the total cost.

Connections Impact

The results obtained regarding the contribution of connections in the environmental and total cost impact of the overall intervention demonstrate that they constitute **35%** of the $GW P_{total}$, while they have a modest total cost contribution of **9%**.

Figure 6.10 illustrates the contribution of connections to the overall environmental impact and total cost of the intervention, expressed as a percentage. It can be observed that connections represent a considerable proportion of the environmental impact. This is due to the selection of steel-to-timber connections for the joint between timber members. However, it is not possible to propose a more sustainable design for connections due to the performance required for transmitting the loads among the exoskeletons members. Consequently, this contribution should be considered when proposing this type of intervention, and the obtained results motivate further research into new materials which can ensure proper performance at a low environmental impact.

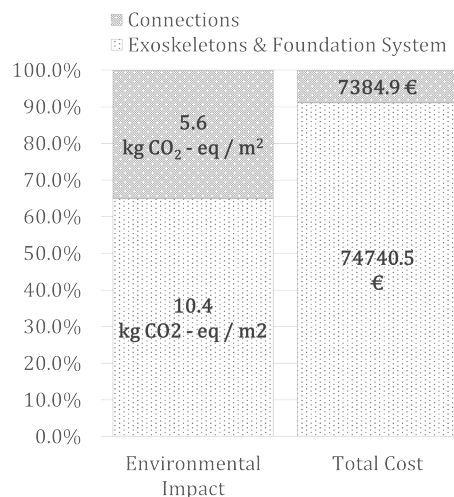


Figure 6.10: Environmental and Cost Impact of Connections

Chapter 7

Conclusions and Future Developments

At the beginning of the thesis, the three main objectives have been defined. Firstly, an innovative pre-dimensioning technique for exoskeletons has been presented employing a displacement-based approach incorporated into an optimisation framework. This allows the seismic performance of an existing structure to be improved by a system of exoskeletons designed to control the lateral displacements of the structure and, consequently, the associated damage to its structural elements.

The second goal was to carry out an environmental and economic comparison between three proposed interventions for an existing structure belonging to a school complex located in Naples. The three alternatives under comparison consist of the intervention with a classical CFRP system proposed by the company in charge of the real project and two exoskeleton alternatives designed according to the aforementioned strategy. In order to evaluate the feasibility of introducing more sustainable materials in the proposed interventions, the members of the exoskeletons solutions are made of high-performance steel and glued laminated timber.

Finally, the third objective of the thesis was to propose an automatic routine for the design of exoskeleton joints, which can be further extended to other types of structures. Furthermore, it was intended to evaluate the impact of the optimal design of the joints in the exoskeletons solution.

Consequently, in order to fulfil the aforementioned objectives, this thesis proposes a two-stage optimisation framework for the design of sustainable exoskeletons and their connections. The first stage consists of the global design of the positioning and sizing of the exoskeleton members, in which it has been possible to determine the potential of these interventions from an economic and environmental point of view. The design of these retrofitted structures is carried out according to a displacement-based criteria, mainly focused on controlling the structural damage of the existing structure's elements. In addition, once the best solution has been identified, a second stage stress-based design of the connections is conducted. The connections are designed in such a way as to maximise their standardisation at the expense of a minimum increase in their total weight. In this way, it was possible to determine the environmental impact and the economic cost of the joints, as well as their incidence in the solution adopted.

The analysis conducted across the two stages of the proposed methodology permits the drawing of several conclusions, which are presented below.

- Firstly, the capacity of exoskeleton systems to unload the existing structure has been demonstrated. These retrofit interventions, designed according to the displacement-based approach proposed, can safely unload the structure in a significant way, while still taking advantage of the lateral strength of the existing structure. This demonstrates how exoskeleton interventions can be designed to allow the existing structure to take more than 15% of lateral loads and still provide a safe retrofit intervention, as shown by the evaluation of the DCR of the existing structure's members;
- Furthermore, with regard to the methodology proposed for the design of exoskeletons, it has been demonstrated the efficiency of the optimization algorithm provides finding an optimal solution that accounts for the control of the damage of structural elements as well as the safety checks of the new members of the exoskeleton. It was demonstrated that an optimal timber solution could be identified, whereby the percentage of non-verified elements was reduced significantly after the interventions. For the structural members of the existing structure, this percentage changed from 82.76% to 0%.
- The displacement-based approach adopted can be easily introduced in the optimisation framework since a straightforward dynamic linear analysis is performed. Moreover, the fact that the positioning and sizing of the exoskeleton structures is evident for each individual evaluated, allows a complete understanding of the solutions as well as a simpler interpretation of their effects on the existing structure. In this way, the classical methodology proposed by several authors in the literature, in which the MDoF system is transformed into an equivalent SDoF and its design variables are optimised, is successfully improved in the approach proposed in this thesis, since the effects on the distribution of loads and errors associated with the simplification of the SDoF system are directly considered, since at each moment the coupled MDoF system is analysed.
- In addition, from the comparison of the three scenarios proposed for the seismic upgrading of the existing structure, it is possible to see how the exoskeleton

interventions constitute a solution that has a significantly lower environmental impact and at the same time is economically convenient, respecting the classical application of CFRP systems. In particular, the timber exoskeletons were adopted as the final intervention to propose from the systems evaluated in the first stage, as they present an environmental impact that is 29% lower than that of steel exoskeletons and 62% lower than that of the CFRP solution. Furthermore, the economical analysis demonstrated that the timber exoskeletons were 28% cheaper than the steel exoskeletons solution and 31% cheaper than CFRP.

- Regarding the second stage of the proposed design methodology, has to be considered that the optimal designs correspond exclusively to a double-shear steel-to-timber connection typology used for the optimal timber exoskeleton solution obtained in the first stage. It has been possible to create an automatic routine coupled with an optimisation algorithm, which together are capable of efficiently obtaining optimal connections layouts designs with a minimum required time. This optimal design is mainly aimed at maximising the standardisation of the joints with a minimum increase in their total weight. As a result, it was possible to find a solution aimed at minimising the weight of the connections, and it was also possible to evaluate their environmental and economic impact in the global solution proposed. Finally, it was identified that connections represent an important 35% of the environmental impact of the overall solution, while they represent only a modest 9% of the total economic cost. Consequently, it can be concluded that for the case study considered, where there is no significant number of connections to be designed, a pinned double-shear steel-to-timber connection has a much greater incidence on the environmental impact of the solution than on the economic one.

It is important to emphasise the limitations that outline the analyses and conclusions made. Firstly, as regards the first stage of the design methodology, the inter-storey limit imposed to control the structural damage of the structure is derived from literature research and demonstrated to efficiently achieve the design objectives. However, this limit can be further calibrated according to the different case studies. The consideration of a single variable that accounts for the total damage of the

structure tends to oversimplify the problem but still provides strong support for the proposed optimisation framework.

Furthermore, regarding to the second stage, the work is limited to only one proposed typology of connection, since it is demonstrated in research its feasibility of reproducing a pinned connection behaviour. However, the main limitation of the proposed approach is the lack of information on the importance of the standardisation of the joints, especially in the production and assembly phases. Since there is a high variability in this information depending on the company and the location of the project, a large database would be required to consider the impact on the standardisation and even the different typologies of connections in the above-mentioned phases. In addition, it would be possible to individualise other variables that may have a strong impact on the cost of joints or on their environmental impact, making it possible to better calibrate the proposed methodology for the design of connections and to arrive at other meaningful optimal solutions.

The work presented in this thesis motivates the development of future research. Studies can be carried out to improve the calibration of the inter-storey drift or to use more design variables that take into account the damage to the structural elements of the existing structure. Accordingly, it can be very helpful for the design of exoskeletons, through the methodology already presented, to propose certain ranges for the damage threshold as a function of the type of building to be retrofitted and its height, which is directly related to the lateral stiffness of the existing structure.

Regarding the automatic stress-based routine for designing the connections of the timber exoskeletons, the methodology already presented can be easily extended for further applications in different types of structures. In addition, it is possible to introduce other typologies of connections, which can even impart a certain rotational stiffness to the joint, and in this way, their design can be included in the first stage of this methodology and make a significant contribution to the control of the lateral displacements of the exoskeletons.

Last but not least, it would be interesting to obtain information from different production and assembly companies regarding the criteria they follow for the production of elements and their installation. In this way, it will be possible to develop a data

set that takes into account the most incident variables in the production and assembly phases of civil engineering projects, and in this way propose more feasible designs in the future.

Chapter 8

Bibliography

- [1] Marina Economidou, Bogdan Atanasiu, Chantal Despret, Joana Maio, Ingerborg Nolte, Oliver Rapf, Jens Laustsen, Paul Ruyssevelt, D Staniaszek, D Strong, et al. Europe’s buildings under the microscope. a country-by-country review of the energy performance of buildings. 2011.
- [2] PD Gkournelos, TC Triantafillou, and DA Bournas. Seismic upgrading of existing reinforced concrete buildings: A state-of-the-art review. *Engineering Structures*, 240:112273, 2021.
- [3] Laure Itard and Gerda Klunder. Comparing environmental impacts of renovated housing stock with new construction. *Building Research & Information*, 35(3):252–267, 2007.
- [4] DM17/01/2018. *Aggiornamento delle “Norme tecniche per le costruzioni”*. Italian Ministry of Infrastructures and Transportation, Rome, Italy, 2018. in Italian.
- [5] Janine M Benyus et al. *Biomimicry: Innovation inspired by nature*, 1997.
- [6] Göran Pohl and Werner Nachtigall. *Biomimetics for Architecture & Design: Nature-Analogies-Technology*. Springer, 2015.
- [7] Gianmaria Di Lorenzo, Eleonora Colacurcio, Agustina Di Filippo, Antonio Formisano, Alfredo Massimilla, and Raffaele Landolfo. State-of-the-art on steel exoskeletons for seismic retrofit of existing rc buildings. *Int. J.*, 37(1), 2020.

-
- [8] Federal Emergency Management Agency (FEMA). Techniques for the seismic rehabilitation of existing buildings. Technical Report FEMA 547/2006, 2006.
- [9] Vivian WY Tam, Chi Ming Tam, SX Zeng, and William CY Ng. Towards adoption of prefabrication in construction. *Building and environment*, 42(10):3642–3654, 2007.
- [10] Anna Reggio, Rita Greco, Giuseppe Carlo Marano, and Giuseppe Andrea Ferro. Stochastic multi-objective optimisation of exoskeleton structures. *Journal of Optimization Theory and Applications*, 187(3):822–841, 2020.
- [11] Anna Reggio, Luciana Restuccia, and Giuseppe Andrea Ferro. Feasibility and effectiveness of exoskeleton structures for seismic protection. *Procedia Structural Integrity*, 9:303–310, 2018.
- [12] Giacomo Iovane, Antonio Sandoli, Dante Marranzini, Raffaele Landolfo, Andrea Prota, and Beatrice Faggiano. Timber based systems for the seismic and energetic retrofit of existing structures. *Procedia Structural Integrity*, 44:1870–1876, 2023.
- [13] Fabio Mazza. Dissipative steel exoskeletons for the seismic control of reinforced concrete framed buildings. *Structural Control and Health Monitoring*, 28(3):e2683, 2021.
- [14] Jana Candelaria Olivo Garcia. *Optimization of Steel Exoskeletons for the Seismic Retrofit of Reinforced Concrete Structures via Genetic Programming*. PhD thesis, Politecnico di Torino, 2023.
- [15] DA Pohoryles, DA Bournas, F Da Porto, Amedeo Caprino, Giuseppe Santarsiero, and Thanasis Triantafillou. Integrated seismic and energy retrofitting of existing buildings: A state-of-the-art review. *Journal of Building Engineering*, 61:105274, 2022.
- [16] Lorenzo Badini, Stephan Ott, Patrik Aondio, and Stefan Winter. A new integrated approach on the seismic strengthening of existing rc buildings with external cross-laminated timber panels. In *World Conference on Timber Engineering 2021*, 2021.

-
- [17] Costantino Menna, Ciro Del Vecchio, Marco Di Ludovico, Gerardo Maria Mauro, Fabrizio Ascione, and Andrea Prota. Conceptual design of integrated seismic and energy retrofit interventions. *Journal of building engineering*, 38:102190, 2021.
- [18] Chiara Passoni, Jack Guo, Constantin Christopoulos, Alessandra Marini, and Paolo Riva. Design of dissipative and elastic high-strength exoskeleton solutions for sustainable seismic upgrades of existing rc buildings. *Engineering Structures*, 221:111057, 2020.
- [19] C Christopoulos and A Filiatrault. *Principles of passive supplemental damping and seismic*. IUSS Press, Pavia, Italy, 2006.
- [20] Jana Olivo, Raffaele Cucuzza, Gabriele Bertagnoli, and Marco Domaneschi. Optimal design of steel exoskeleton for the retrofitting of rc buildings via genetic algorithm. *Computers & Structures*, 299:107396, 2024.
- [21] L Martelli, L Restuccia, and GA Ferro. The exoskeleton: a solution for seismic retrofitting of existing buildings. *Procedia Structural Integrity*, 25:294–304, 2020.
- [22] Anna Reggio, Luciana Restuccia, Lucrezia Martelli, and Giuseppe Andrea Ferro. Seismic performance of exoskeleton structures. *Engineering Structures*, 198:109459, 2019.
- [23] Huanjun Jiang, Bo Fu, and Linzhi Chen. Damage-control seismic design of moment-resisting rc frame buildings. *Journal of Asian Architecture and Building Engineering*, 12(1):49–56, 2013.
- [24] Xiaoxuan Qi and Jack P Moehle. *Displacement design approach for reinforced concrete structures subjected to earthquakes*. Earthquake Engineering Research Center, College of Engineering/University of . . . , 1991.
- [25] Ahmed Ghobarah. On drift limits associated with different damage levels. In *International workshop on performance-based seismic design*, volume 28. Department of Civil Engineering, McMaster University Ontario, Canada, 2004.
- [26] Huanjun Jiang, Xilin Lu, and Linzhi Chen. Seismic fragility assessment of rc moment-resisting frames designed according to the current chinese seismic de-

-
- sign code. *Journal of Asian Architecture and Building Engineering*, 11(1):153–160, 2012.
- [27] Gianmaria Di Lorenzo, Roberto Tartaglia, Alessandro Prota, and Raffaele Landolfo. Design procedure for orthogonal steel exoskeleton structures for seismic strengthening. *Engineering Structures*, 275:115252, 2023.
- [28] Vincenzo Ciampi, Maurizio De Angelis, and F Paolacci. Design of yielding or friction-based dissipative bracings for seismic protection of buildings. *Engineering Structures*, 17(5):381–391, 1995.
- [29] Alessandra Marini, Chiara Passoni, and Andrea Belleri. Life cycle perspective in rc building integrated renovation. *Procedia Structural Integrity*, 11:28–35, 2018.
- [30] Jeffrey S Russell, Kevin E Swiggum, Jeffrey M Shapiro, and Achmad F Alaydrus. Constructability related to tqm, value engineering, and cost/benefits. *Journal of performance of constructed facilities*, 8(1):31–45, 1994.
- [31] James T O’Connor, Stephen E Rusch, and Martin J Schulz. Constructability concepts for engineering and procurement. *Journal of Construction Engineering and Management*, 113(2):235–248, 1987.
- [32] Tolga Çelik, Saeed Kamali, and Yusuf Arayici. Social cost in construction projects. *Environmental impact assessment review*, 64:77–86, 2017.
- [33] Andrew Gilchrist and Erez N Allouche. Quantification of social costs associated with construction projects: state-of-the-art review. *Tunnelling and underground space technology*, 20(1):89–104, 2005.
- [34] Brian R Keeble. The brundtland report: ‘our common future’. *Medicine and war*, 4(1):17–25, 1988.
- [35] ISO. Iso 14040: Environmental management — life cycle assessment — principles and framework. *Int. Organ. Stand. Geneva, Switz*, 2006.
- [36] ISO. Iso 14044: Environmental management — life cycle assessment — requirements and guidelines. *Int. Organ. Stand. Geneva, Switz*, 2006.

-
- [37] EN. 15804:2012 + a1:2013, sustainability of construction works - environmental product declarations - core rules for the product category of construction products. *CEN: Brussels, Belgium*, 2012.
- [38] EN. 15978, sustainability of construction works - assessment of environmental performance of buildings - calculation method. *CEN: Brussels, Belgium*, 2011.
- [39] Rafael Mart, Panos M Pardalos, and Mauricio GC Resende. *Handbook of heuristics*. Springer Publishing Company, Incorporated, 2018.
- [40] John H Holland. *Adaptation in natural and artificial systems: an introductory analysis with applications to biology, control, and artificial intelligence*. MIT press, 1992.
- [41] Ministero delle Infrastrutture e dei Trasporti. Allegato a alle norme tecniche per le costruzioni: Pericolosità sismica. *DM 17 gennaio*, 2018.
- [42] Mapei S.p.A. Epd - mapewrap primer 1.
- [43] Mapei S.p.A. Epd - mapewrap 31.
- [44] Guillermo Xabier Bustamante. *Influence of pile shape on resistance to lateral loading*. Brigham Young University, 2014.
- [45] Mapei S.p.A. Epd - mapei.
- [46] Sujit Das. Life cycle assessment of carbon fiber-reinforced polymer composites. *The International Journal of Life Cycle Assessment*, 16:268–282, 2011.
- [47] Mapei S.p.A. Epd - mapewrap 11.
- [48] Giacomo Iovane, Celeste Noviello, Federico M Mazzolani, Raffaele Landolfo, and Beatrice Faggiano. A proposal for the mechanical classification of beam-to-column joints for timber structures.
- [49] Directive 2004/18/EC Directive 98/34/EC. *EN 1995-1-1 (2004) (English): Eurocode 5: Design of timber structures - Part 1-1: General - Common rules and rules for buildings*. The European Union Per Regulation 305/2011, 2011.
- [50] Annika Mårtensson Roberto Crocetti, Helena Lidelöw and Bert Norlin. *Design of timber structures. Volume 3*. Swedish Wood, 2022.